

UCLA

UCLA Electronic Theses and Dissertations

Title

Computational Exploration of Reactivities and Catalysis of Pericyclic Reactions

Permalink

<https://escholarship.org/uc/item/6st5r669>

Author

Fell, Jason Scott

Publication Date

2018

Peer reviewed|Thesis/dissertation

UNIVERSITY OF CALIFORNIA

Los Angeles

Computational Exploration of Reactivities and Catalysis of Pericyclic Reactions

A dissertation submitted in partial satisfaction of the requirements for the degree Doctor of
Philosophy in Chemistry

by

Jason Scott Fell

2018

© Copyright by

Jason Scott Fell

2018

ABSTRACT OF THE DISSERTATION

Computational Explorations of Reactivities and Catalysis of Pericyclic Reactions

By

Jason Scott Fell

Doctor of Philosophy in Chemistry

University of California, Los Angeles, 2018

Professor Kendall N. Houk, Chair

This dissertation describes research that delves into exploring puzzling chemical phenomena utilizing modern computational chemistry methods. Theoretical chemical models that are coupled with quantum mechanical (QM) calculations can dissect complex chemical reactions into many components that influence chemical reactivity and selectivity. Each chapter of this dissertation demonstrates that QM calculations can help predict and explain the complexities of chemical phenomena involving reaction mechanisms.

The first section (hapters 1 thru 4) details computational explorations of reactivities and selectivities of pericyclic reactions. Pericyclic reactions are an important class of chemical reactions wherein the reacting species form a cyclic transition state with aromatic delocalization.

Often these reactions occur with high degrees of regio- and stereoselectivity. Chapter 1 explores the large differences in reactivity between cyclic 1- and 2-azadienes in Diels-Alder reactions. Chapter 2 investigates how thiol addition to substituted oxanorbornadienes promotes a retro-Diels-Alder reaction, as well as how the substitution pattern on the norbornadiene affects the rates of fragmentation. Chapter 3 probes how an anion-accelerated Cope rearrangement is inherently stereoselective. Chapter 4 explores if the enzyme iridoid synthase is a natural Diels-Alderase by modeling the uncatalyzed Diels-Alder reaction and determining if the background reaction is achievable and inherently stereoselective.

The second section, Chapter 5, delves into utilizing QM calculations to predict the potential reactivity of a proposed catalyst to selectively perform anti-Markovnikov hydrations of olefins. Our calculations predict that the proposed di-manganese catalyst would produce the anti-Markovnikov product preferentially to the Markovnikov product at a ratio as low as 12:1 and as high as 100:1 depending on the catalyst ligands.

The third section (Chapters 6 and 7) tackle the stereoselectivity of chemical reactions involving nucleophilic additions to aldehydes and imines. Chapter 6 explores the mechanism and origins of the diastereoselectivity of cross-benzoin reactions of furfural and α -amino aldehydes catalyzed by a triazolium-based NHC. Chapter 7 the polar-Felkin-Anh stereoselectivity of nucleophilic addition to α -chiral imines in the presence of Lewis acid catalysts.

The dissertation of Jason Scott Fell is approved.

Jennifer M. Murphy

Yi Tang

Alexander Michael Spokoyny

Kendall N. Houk, Committee Chair

University of California, Los Angeles

2018

DEDICATION

I dedicate my thesis to my friends, family, colleagues and mentors.

TABLE OF CONTENTS

ABSTRACT OF THE DISSERTATION	ii
DEDICATION	v
TABLE OF CONTENTS	vi
ACKNOWLEDGEMENTS	viii
VITA	xiii
 CHAPTER 1. Origins of the Unfavorable Activation and Reaction Energies of 1-Azadiene Heterocycles Compared to 2-Azadiene Heterocycles in Diels-Alder Reactions	 1
ABSTRACT	2
INTRODUCTION	2
COMPUTATIONAL METHODS	7
RESULTS	7
DISCUSSION	13
CONCLUSIONS	22
ACKNOWLEDGEMENTS	23
REFERENCES	23
 CHAPTER 2. Theoretical analysis of the retro-Diels-Alder reactivity of oxanorbornadiene thiol and amine adducts	 26
ACKNOWLEDGEMENTS	34
REFERENCES	34
 CHAPTER 3. New Class of Anion-Accelerated Amino-Cope Rearrangements as Gateway to Diverse Chiral Structures	 36
ABSTRACT	37
INTRODUCTION	37
RESULTS AND DISCUSSION	41
CONCLUSIONS	48
ACKNOWLEDGEMENTS	49
REFERENCES	49

CHAPTER 4. Computational Evaluation of the Mechanism of the Intramolecular Cyclization of 8-Oxogeranial	51
REFERENCES	57
CHAPTER 5. Computational investigation of anti-Markovnikov hydration of olefins by a di-manganese catalyst	59
ACKNOWLEDGEMENTS	65
REFERENCES	66
CHAPTER 6.	
ABSTRACT	68
INTRODUCTION	68
COMPUTATIONAL METHODS	72
RESULTS AND DISCUSSION	73
CONCLUSIONS	79
ACKNOWLEDGEMENTS	80
REFERENCES	80

ACKNOWLEDGEMENTS

First and foremost, I would like to acknowledge my doctoral advisor, Kendall N. Houk. Ken has an amazingly sharp wit that is coupled with an encyclopedic knowledge of organic chemistry, and he is incredibly patient with an excellent sense of humor. Through his mentorship I have transformed to be a better scientist. I am most thankful for having the privilege to be apart of his lab and to help push back the frontiers of science.

I would be remiss if I did not acknowledge my advisors and teachers from Sacramento State University. When I first began my chemistry career I was advised by a classmate of mine, Lindsey Noriega, to get involved in undergraduate research. She convinced me to join a research lab, and I quickly joined the lab of Dr. Brad Baker. I worked under Brad for 2 years, where I learned that in research for every successful experiment there are many more failures that precede. I am very grateful for the patience Brad had with me and for the many lessons he gave me on the meaning of primary research.

While in undergrad I had the privilege of being mentored by excellent faculty, namely Dr. Cynthia Kellen-Yuen (Dr. K), Dr. Susan Crawford and Dr. James Miranda. Dr. K was one of the faculty advisors for the chemistry club, and I had the pleasure to work with her to making the club successful as well as to have her give great advice on graduate school and much needed encouragement. Susan was my physical chemistry lab instructor, and she always pushed her students to think critically into every project and experiment we performed. James is credited for teaching me organic chemistry, as well as getting me involved with Filipino Martial Arts.

While in college I made great friends with my chemistry cohort. Jacob, Lindsay, Wayne, Anthony, Megan, Layla, Monique and Vi made quantitative analysis just bearable. During the last

two years of undergrad if it wasn't for the friendships of Victor, Nick, Kris, Joel, Tracy, Nadia, Mike C., Mike V., Angela, Nikki, Corri, Maddy, Komal, and Calvin I would have never finished college. I will always remember the late nights spent writing lab reports, studying for exams, and celebrating our successes. It was also during this time I made friends at UC Davis; Jason Harrison, Osvaldo Gutierrez and Hoby Wedler, who showed me how amazing and powerful computational chemistry was. They got me fascinated in using theory to understand chemical reactions and that computations could be used to model enzymes.

After graduating with my bachelor's degree, I stayed at Sacramento State and joined the lab of Dr. Ben Gherman. Ben is incredibly insightful, and he taught me how to do chemical calculations. I had the fortunate opportunity to pursue an amalgam of different projects that were both assigned as well as self-generated. Ben was always open to new ideas and very supportive of all my endeavors, and he encouraged pursuing any new knowledge.

I am incredibly thankful for all the support of my family. My grandfather, Adolf, always encouraged me to continue learning and to further my education. I wish Adolf could have lived just a little longer to hear that I was accepted to graduate school. My parents, Leo and Laraine, have been incredibly supportive through all my years of education, and now they are ecstatic that they will no longer have to go to any more graduations. My Aunt Angie and Uncle John have also been highly supportive of me throughout my life, as well as my sister, Sherrie, who has always been incredibly supportive of my work.

At the beginning of my second year I had the fortunate experience of finding my biological father, Vincent. For most of my life I never thought I would never find any of my biological family, and now I have two brothers, Vincent and Gabriel and a second mother, Vicki. I have worked extra

hard to make a great example for my brothers to learn from, and to show them that having perseverance and willpower can make them accomplish anything.

I am thankful for the friends that have kept me grounded through my studies. I have been able to count on James, Steve, Andrew “Del,” Andrew “Drew,” Scott and TJ to always be ready to tell a story and go to a new world. Wallace, Byron, Kevin, Chris, Katie, Siobhan, Sam, Michelle, Ann, Matt, Becky and Jessie have been able to keep me sane. All my friends have been with me through the worst and best parts of my life, and without them I am doubtful I would have been successful at anything in life.

Before my studies at the university, I had two amazing teachers that saw I had great potential when I was younger. Mrs. Rey was my third-grade teacher and she saw that I had great potential for learning. Before the third grade my teachers thought I was lazy and not interested in learning, however Mrs. Rey thought that I wasn’t being challenged. She let me explore the books in the school’s library and she encouraged me to read literature that I found interesting. This led me to reading books at a higher-grade level and sparked an early interest in science. My high school physics teacher, Mr. Keith, was instrumental in guiding me to continue my scientific studies. Mr. Keith made physics fun and interesting, but most importantly he always pushed me to stay curious.

My time at UCLA was made a little more facile and entertaining from the friendships I made both in and out of the lab. Upon arriving at UCLA I made many friendships with my chemistry cohort, notably Steven Sasaki for connecting all 80 of us 1st years together. Of most importance I should mention Orin, Nathan M., Nathan G., and Brian for being excellent friends during the toughest parts of graduate school. Outside of the lab I found much solace at the

Wellesbourne and Upper West. Lastly, my neighbors Mimi and Daphne have been great friends that have listened to me vent (or complain) and celebrate success.

Within the Houk lab there were many people who had a significant impact on my growth and success. In my earlier years I was mentored by Blanton, Steven, Ashay, Colin, Jessie, Mareike, Marc, Pia, Jacob, Buck and Peng, these people have been incredibly helpful and be able to dish out much needed advice when needed. I would be remiss if I did not mention the younger group members Adam, Janice, Katherine, Kersti, Melissa, Gina and Declan for wanting to learn and having a great attitude.

Lastly, and certainly not the least, I am so thankful for my girlfriend Sara. As of this writing Sara and I have been together for nearly 8 and a half years. We have shared many high and low points, yet through each passing day we grow stronger together. Sara has been so supportive and encouraging of me to keep working hard. She has also shared her family with me, who I love dearly as much as my own, and I am incredibly thankful for. Lily, Sara's mother, has become another mom to me. The rest of Sara's cousins, aunts and uncles are all incredibly supportive of my work. Words cannot express how much Sara means to me.

To everyone mentioned herein: thank you.

Chapter 1 is a modified version of the publication, “Origins of the Unfavorable Activation and Reaction Energies of 1-Azadiene Heterocycles Compared to 2-Azadiene Heterocycles in Diels-Alder Reactions”. (Fell, J. S.; Martin, B. M.; Houk, K. N. *J. Org. Chem.* **2017**, 82, 1912.)

Chapter 2 is a modified version of the publication, “Theoretical analysis of the retro-Diels-Alder reactivity of oxanorbornadiene thiol and amine adducts”. (Fell, J. S.; Lopez, S. A.; Higginson, C. J.; Finn, M. G.; Houk, K. N. *Org. Lett.* **2017**, 19, 4504.)

Chapter 3 is a modified version of the publication, “New Class of Anion-Accelerated Amino-Cope Rearrangements as Gateway to Diverse Chiral Structures”. (Chogii, I.; Das, P.; Fell, J. S.; Scott, K. A.; Crawford, M. N.; Houk, K. N.; Njardarson, J. T. *J Am. Chem. Soc.* **2017**, 139, 13141.)

VITA

Education

- California State University, Sacramento* 2010-2013
M.S. Department of Chemistry. Thesis: Computational Study of Inorganic, Bioinorganic, and Bioorganic Systems
- California State University, Sacramento* 2006-2010
B.S. Chemistry, minor in English.
- Sierra College* 2003-2006
A.S. Natural Sciences. A.A. Liberal Arts.

Publications

1. Yates, J. M.; Fell, J. F.; Miranda, J. M.; Gherman, B. F. "Metal-Salens As Catalysts In Electroreductive Cyclization and Electrohydrocyclization: Computational and Experimental Studies," *Electrochem. Soc. Trans.* **2013**, I, 12.
2. Yates, J. M.; Fell, J. F.; Miranda, J. M.; Gherman, B. F. "Metal-Salens As Catalysts In Electroreductive Cyclization and Electrohydrocyclization: Computational and Experimental Studies," *J. Electrochem. Soc.* **2013**, 160, G3080.
3. Fell, J. S.; Steele, D. M.; Hatcher III, T. C.; Gherman, B. F. "Electronic effects on the reaction mechanism of the metalloenzyme peptide deformylase," *Theor. Chem. Acc.* **2015**, 134, 1.
4. Fell, J. S.; Martin, B. N.; Houk, K. N. "Origins of the Unfavorable Activation and Reaction Energies of 1-Azadiene Heterocycles Compared to 2-Azadiene Heterocycles in Diels-Alder Reactions," *J. Org. Chem.* **2017**, 82, 1912.
5. Fell, J. S.; Lopez, S. A.; Higginson, C. J.; Finn, M. G.; Houk, K. N. "Theoretical analysis of the retro-Diels-Alder reactivity of oxanorbornadiene thiol and amine adducts," *Org. Lett.* **2017**, 19, 4504.
6. Chogii, I.; Das, P.; Fell, J. S.; Scott, K. A.; Crawford, M. N.; Houk, K. N.; Njardarson, J. T. "New Class of Anion-Accelerated Amino-Cope Rearrangements as Gateway to Diverse Chiral Structures," *J Am. Chem. Soc.* **2017**, 139, 13141.

Presentations

1. 239th American Chemical Society National Meeting, San Francisco, California. Jason S. Fell, Niria Arellano, Brad Baker. "Calculated emission rates and analysis of biogenic volatile

organic compounds, monoterpenes, and sesquiterpenes from common tree species indigenous to the Sierra Nevada foothills region of Northern California.” (Poster) March 2010.

2. 22nd Annual Undergraduate American Chemical Society Research Conference for Northern California, Sacramento, California. J. S. Fell, B. Baker. “Analysis of Sample Lifetimes on Solid Phase Extraction Cartridges.” (Poster) May 2010.

3. 23rd California State University Biotechnology Symposium, Anaheim, California. J. S. Fell, D. M. Steele, B. F. Gherman, “Electronic Effects on the Reaction Mechanism of the Metalloenzyme peptide Deformylase.” (Poster) January 2011.

4. 43rd Western Regional American Chemical Society Meeting, Pasadena, California. J. S. Fell, D. M. Steele, B. F. Gherman. “Electronic Effects on the Reaction Mechanism of the Metalloenzyme peptide Deformylase.” (Poster) November 2011.

5. 25th California State University Biotechnology Symposium, Anaheim, California. J. S. Fell, B. F. Gherman. "Computational Analysis of Metal-Salen Mediated Electroreductive Cyclizations." (Poster) January 2013.

6. 2013 Seaborg Symposium, University of California, Los Angeles. J. S. Fell, B. N. Martin, K. N. Houk. "Why 1-aza-substituted pentaheterocycles are generally less reactive than 2-aza-substituted pentaheterocycles in Diels-Alder cycloadditions." (Poster) October 2013.

7. 35th Reaction Mechanisms Conference, University of California, Davis. J. S. Fell, B. N. Martin, K. N. Houk. "Why oxazole is a good diene in Diels-Alder reactions: a theoretical study." (Poster) June 2014.

8. 248th American Chemical Society National Meeting, San Francisco, California. J. S. Fell, B. N. Martin, K. N. Houk. "Why oxazole is reactive and isoxazole is not: a theoretical study of these Diels-Alder dienes and broad applicability to other systems." (Poster) August 2014.

9. 2017 Seaborg Symposium, University of California, Los Angeles. Jason S. Fell, Isaac Chogii, Pradipta Das, Kevin A. Scott, Mark N. Crawford, Jon T. Njardarson and Kendall N. Houk. "Computational Investigation of the Mechanism of an Anion Accelerated Amino-Cope Rearrangement." (Poster) November 18, 2017.

10. 37th Reaction Mechanisms Conference, University of British Columbia, Vancouver, Canada. J. S. Fell, L. Moore, A. Lo, J. T. Shaw, K. N. Houk. "Origins of Anti Felkin-Anh Selectivity of Nucleophilic Additions to α -Chiral Imines." (Poster) June 2018.

11. Gordon Research Conference: Stereochemistry, Salve Regina University, Newport, Rhode Island. J. S. Fell, A. Duan, P. Yu, Y. H. Lam, M. Gravel, K. N. Houk. "Computational Investigation of the Diastereoselective NHC-Catalyzed Cross-Benzoin Reactions between Furfural and *N*-Boc Protected α -Amino Aldehydes." (Poster) July 2018.

Chapter 1

Origins of the Unfavorable Activation and Reaction Energies of 1-Azadiene Heterocycles Compared to 2-Azadiene Heterocycles in Diels-Alder Reactions

Fell, J. S.; Martin, B. N.; Houk, K. N. *J. Org. Chem.* **2017**, 82, 1912.

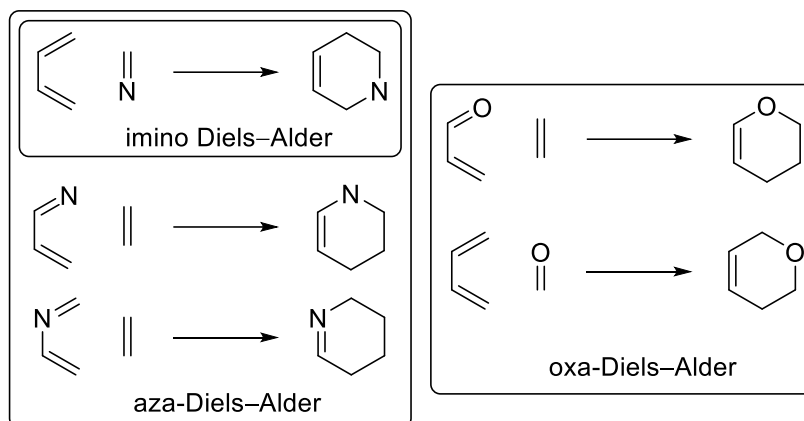
Abstract

The reactivities of butadiene, cyclopentadiene, furan, thiophene, pyrrole, and their 1-aza- and 2-azaderivatives in Diels–Alder reactions with ethylene and fumaronitrile were investigated with density functional theory (M06-2X/6-311G(d,p)). The activation free energies for the Diels-Alder reactions of cyclic 1-azadienes are 10-14 kcal mol⁻¹ higher than those of cyclic 2-azadienes, and the reaction free energies are 17-20 kcal mol⁻¹ more endergonic. The distortion/interaction model shows that the increased activation energies of cyclic 1-azadienes originate from increased transition state distortion energies and unfavorable interaction energies, arising from addition to the nitrogen terminus of the C=N bond.

Introduction

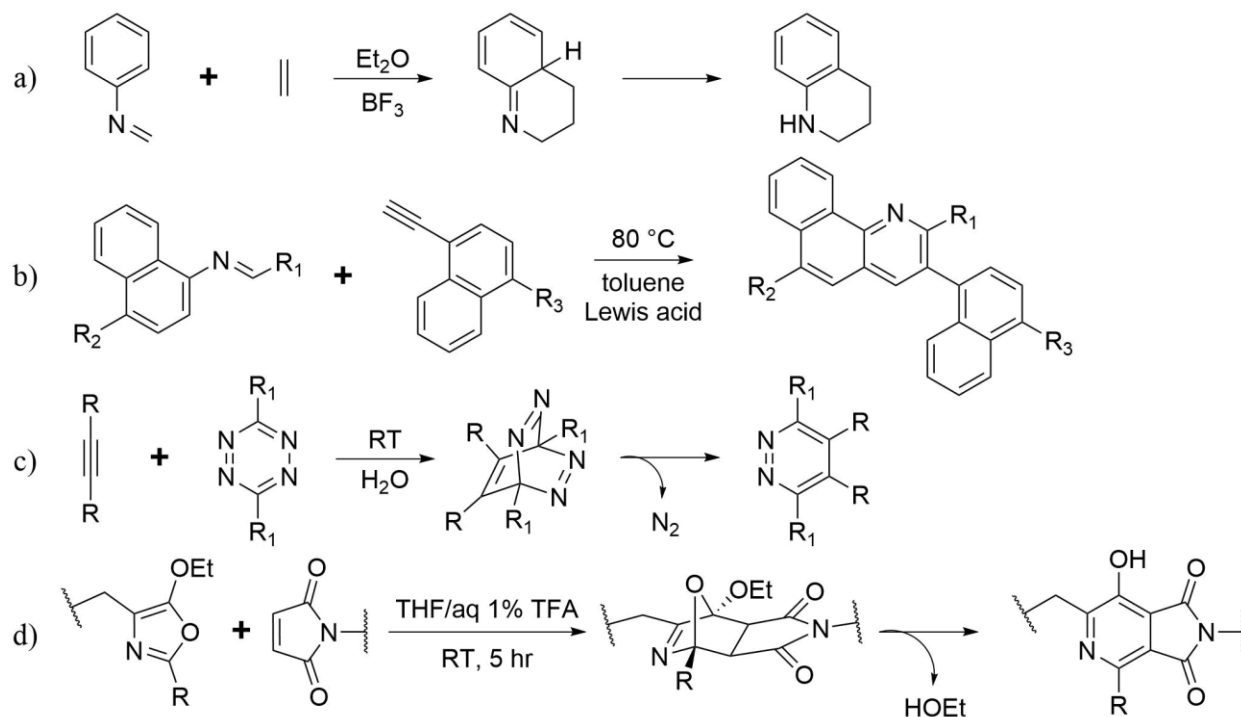
The hetero-Diels–Alder (DA) reaction is a [4 + 2] cycloaddition in which one or more heteroatoms are integrated into the diene or dienophile. These reactions are efficient methods for the synthesis of functionalized heterocycles. Common subclasses of the hetero-DA reaction are the imino-DA involving an aza-dienophile, oxa-DA and aza-DA reactions, which are shown in Scheme 1.1.¹

Scheme 1.1. The common subclasses of the hetero-DA reactions: the aza-DA, imino-DA and the oxa-DA reactions.



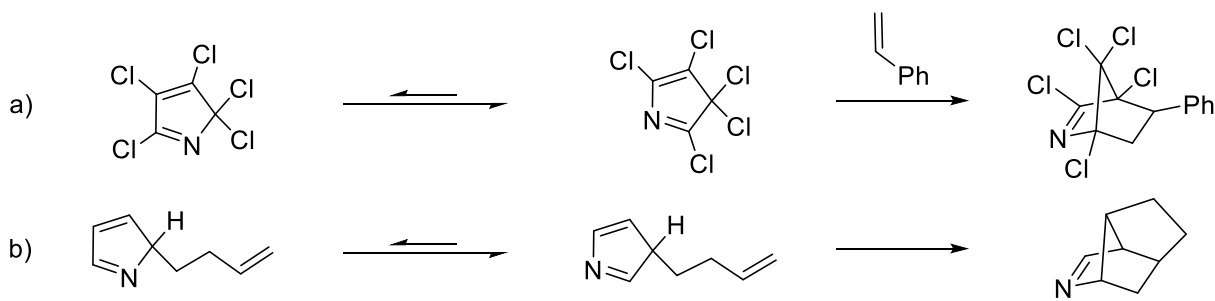
The aza-DA reaction has significant synthetic utility in producing nitrogen-containing heterocycles such as piperidines² and tetrahydroquinones,³ which are valuable intermediates for the synthesis of natural products.^{4,5} The Povarov reaction involves reactions of 2-azadienes with electron rich alkenes in the presence of a Lewis acid catalyst (Scheme 1.2a),⁶ and the formation of benzoquinolines (Scheme 1.2b),⁷ tetrahydroquinolines⁸⁻¹⁰ and hexahydropyrroloquinolines.¹¹ The aza-DA reaction has applications in biorthogonal click chemistry such as tetrazine-alkyne¹² cycloadditions (Scheme 1.2c) and the Kondrat'eva ligation^{13,14} (Scheme 1.2d). Several recent examples in the literature highlight 2-azadienes in aza-DA reactions to efficiently produce quinolines.¹⁵⁻²⁰

Scheme 1.2. Examples of azadienes utilized in various cycloaddition reactions.



While 2-azadienes and oxazoles readily react with numerous dienophiles, DA reactions of 1-azadienes and isoxazoles require high temperatures and catalysts.²¹ The 1-aza-DA reactions are much less common than all-carbon DA reactions.^{22,23} Scheme 1.3 highlights earlier experimental aza-DA reactions that attempted to utilize cyclic 1-azadienes but rather isomerized to 2-azadienes before the subsequent cycloaddition reaction could occur.

Scheme 1.3. Two 1-azadienes that rearrange before entering into DA reactions.



Jung and Shapiro attempted the aza-DA reaction of 2,3,4,5,5-pentachloro-1-azacyclopentadiene with styrene (Scheme 1.3a), but discovered that the 1-azadiene rearranged to the 2-azadiene, which then undergoes the cycloaddition.²⁴ They proposed that there is a lower thermodynamic driving force in reactions of 1-azadienes versus 2-azadienes. Vogel *et al.* studied intramolecular DA reactions of the butenyl pyrroles shown in Scheme 1.3b. They were only able to isolate the 2-azadiene product, and computed this to be favored as well.²⁵ A theoretical study from our group showed that the reaction of oxazole with ethylene is exergonic while that of isoxazole is endergonic.²¹ The unfavorable thermodynamics and lower reactivity of isoxazole were thought to involve the loss of conjugation of the enamine in the bicyclic product from the isoxazole reaction.

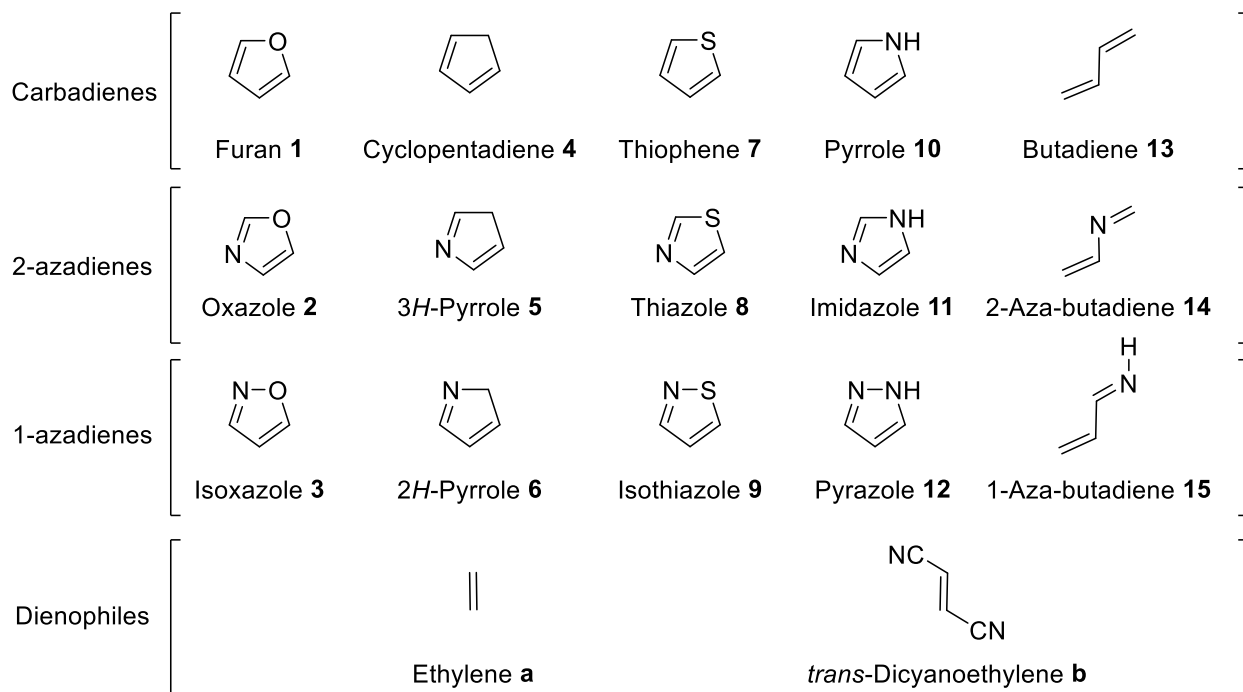
Boger *et al.* reported the first asymmetric aza-DA reaction of N-sulfonyl-1-azabutadiene with enol ethers.²⁶ This reaction of a 1-azadiene occurs at room temperature and without a catalyst, however this DA reaction is made favorable by the diene being activated and acyclic and utilizing electron rich dienophiles. There are recent examples in the literature of unactivated acyclic 1-azadienes that require high temperatures and Lewis acid catalysts to react in cycloaddition reactions.²⁷⁻²⁹

Our group has recently explored the reactivity of benzene and six-membered azabenzenes with ethylene in DA reactions.³⁰ The activation barriers decrease with each replacement of CH with N, and the reaction becomes highly regioselective to form C-C bonds than C-N bonds. The formation of two C-C bonds is favored by 15 kcal mol⁻¹ over reactions where one C-C and one C-N bond are formed, and the formation of two C-N bonds is least favored. The diene becomes less aromatic with each nitrogen replacement, which consequently reduces the energy to distort the diene and increases the interaction energy between the diene and dienophile. Our general interest in

understanding cycloaddition chemistry has prompted us to further investigate the effect of introducing a nitrogen atom within 5-membered heterocycles.

We have employed density functional theory (DFT) calculations to predict the activation and reaction enthalpies and free energies of the DA reactions involving acyclic and heterocyclic dienes shown in Scheme 1.4 with ethylene (**a**) and fumaronitrile (*trans*-1,2-dicyanoethylene (**b**)). We have utilized the distortion/interaction (D/I) or Activation Strain model³¹⁻³⁸ to analyze the differences in activation energies between the 1-aza- and 2-azadiene cycloadditions. We report a detailed analysis of the differences in activation and reaction energies of DA reactions of unactivated cyclic all-carbon containing dienes, 1-aza- and 2-azadienes.

Scheme 1.4. The dienes and dienophiles studied here.



Computational Methods

All calculations were performed with Gaussian 09.³⁹ Gas-phase ground state and transition state geometries were optimized with Truhlar's M06-2X functional⁴⁰ and the 6-311G(d,p) basis set. These have been found by our group to give relatively accurate energies for cycloaddition reactions.^{41,42} Vibrational frequencies were computed to determine if the optimized structures are minima or saddle points on the potential energy surface corresponding to ground state and transition state geometries, respectively. Free energies were calculated for 1 atm at 298.15 K. Truhlar's quasiharmonic correction was applied in order to reduce error in estimation of entropies arising from the treatment of low frequency vibrational modes as harmonic oscillations by setting all frequencies less than 100 cm⁻¹ to 100 cm⁻¹.^{43,44} Molecular structures are displayed with CYLview.⁴⁵

Results

We first compared our calculated M06-2X/6-311G(d,p) enthalpies to measured experimental enthalpies of formation. We compared the differences in experimental and calculated enthalpies of formation ($\Delta\Delta H_f^\circ$) of oxazole (**2**), isoxazole (**3**), imidazole (**11**) and pyrazole (**12**), which are shown in Figure 1.1.

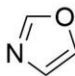
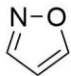
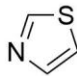
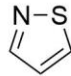
				
2	3	11	12	
$\Delta H_f^\circ(\text{Exp.})$	-3.71 ± 0.13	18.78 ± 0.13	30.6 ± 1.8	40.3 ± 2.1
$\Delta\Delta H_f^\circ(\text{Exp.})$	22.49 ± 0.13		12.7 ± 2.8	
$\Delta\Delta H_f^\circ(\text{Calc.})$	25.6		11.8	

Figure 1.1. Experimental and calculated heats of formation, in units of kcal mol⁻¹.

The calculated $\Delta\Delta H_f^\circ$ for **2** and **3** is 25.6 kcal mol⁻¹, and the calculated $\Delta\Delta H_f^\circ$ for **11** and **12** is 11.8 kcal mol⁻¹. The experimental $\Delta\Delta H_f^\circ$ for **2** and **3** are 22.49 ± 0.13 kcal mol⁻¹,⁴⁶ and the experimental $\Delta\Delta H_f^\circ$ for **11** and **12** are 12.7 ± 1.4 kcal mol⁻¹.⁴⁷ Our M06-2X/6-311G(d,p) calculated enthalpies are in good agreement with the experimentally measured enthalpies. Note the less reactive **3** and **12** are much less stable than the more reactive **2** and **11**!

Figure 1.2 shows the computed transition structures of the DA reaction of ethylene with dienes **1** thru **15**. The activation free energies and enthalpies are provided below the corresponding transition structure. The top, middle, and bottom rows display the carbadienes, 2-azadienes and 1-azadienes, respectively.

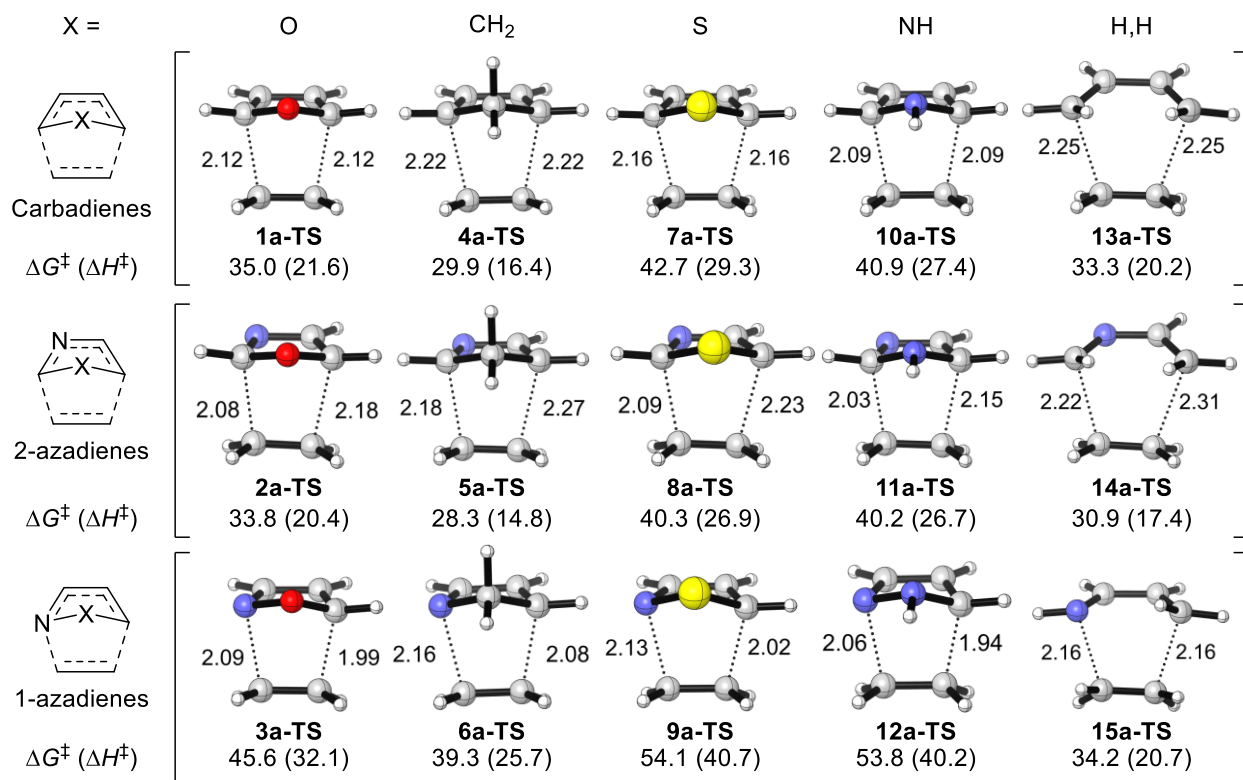


Figure 1.2. The DA transition states of ethylene with each diene in this study displayed with the associated free energies and enthalpies of activation. Energies and distances are in units of kcal mol⁻¹ and Å, respectively.

The activation free energies of the DA reactions of ethylene (**a**) with the carbadienes (**1**, **4**, **7**, **10** and **13**) range from 30 to 43 kcal mol⁻¹. The introduction of a nitrogen atom at the 2-position within the diene (dienes **2**, **5**, **8**, **11** and **14**) decreases the barrier by only 1 to 3 kcal mol⁻¹. However, a nitrogen atom at the 1-position of the diene portion (dienes **3**, **6**, **9**, **12** and **15**) increases the barrier by 9 to 11 kcal mol⁻¹ in all five cases.

The transition structures of the DA reactions of ethylene with the symmetrical carbadienes, (**1**, **4**, **7**, **10** and **13**)a-TS, are all concerted and synchronous. The transition structures of the 1-aza- and 2-azadienes are also concerted but asynchronous. The asynchronicities of bond

formation for **(2, 5, 8, 11 and 14)a-TS** are 0.09 to 0.12 Å, with the shortest forming bond at positions 4 and 5. Transition structures **(3, 6, 9 and 12)a-TS** have an asynchronicity of 0.08 to 0.11 Å, with the shortest forming bond at positions 1 and 6, with the exception of **15a-TS** this is synchronous. The forming bonds in the 1-azadiene transition structures are 0.03 to 0.15 Å shorter compared to forming bonds in the transition structures of the carbadienes, which is an indication of later transition states with increased activation energies for those endothermic reactions, in accord with the Hammond Postulate.⁴⁸

We also investigated the free energies and enthalpies of reaction for the DA reaction of ethylene with the dienes. The cycloadducts for each reaction are displayed in Figure 1.3 with the associated reaction free energy and enthalpy. The top, middle, and bottom rows display the cycloadducts of the DA reaction of ethylene (**a**) with the carbadienes, 2-azadienes and 1-azadienes, respectively.

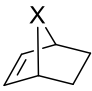
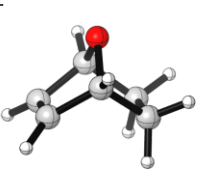
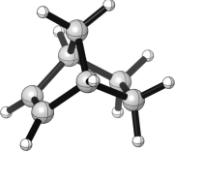
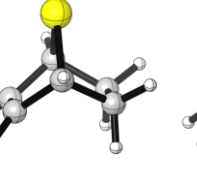
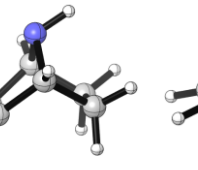
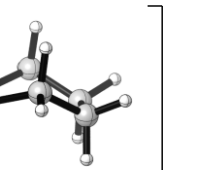
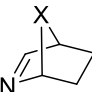
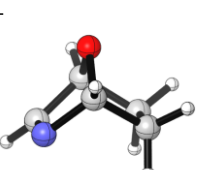
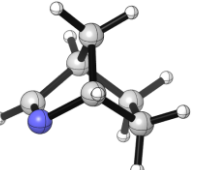
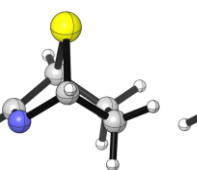
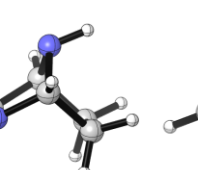
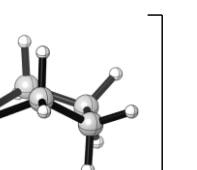
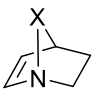
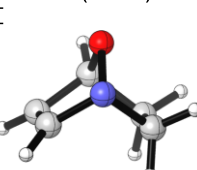
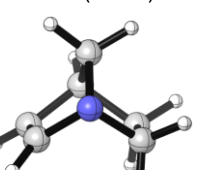
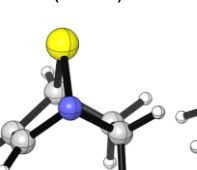
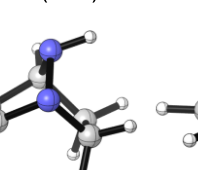
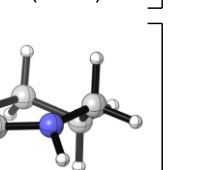
X =	O	CH ₂	S	NH	H,H
					
Carbadienes	1a	4a	7a	10a	13a
$\Delta G_{\text{rxn}} (\Delta H_{\text{rxn}})$	3.1 (-11.1)	-13.0 (-27.5)	4.0 (-10.3)	11.9 (-2.5)	-25.0 (-38.7)
					
2-azadienes	2a	5a	8a	11a	14a
$\Delta G_{\text{rxn}} (\Delta H_{\text{rxn}})$	2.1 (-12.1)	-16.1 (-30.6)	1.2 (-13.0)	10.4 (-3.9)	-31.3 (-45.7)
					
1-azadienes	3a	6a	9a	12a	15a
$\Delta G_{\text{rxn}} (\Delta H_{\text{rxn}})$	19.9 (5.6)	3.4 (-11.2)	21.9 (7.6)	30.9 (16.5)	-24.0 (-38.5)

Figure 1.3. The cycloadducts of the DA reaction of ethylene with each diene in this study displayed with the associated free energies and enthalpies of reaction. Energies and distances are in units of kcal mol⁻¹ and Å, respectively.

Cyclopentadiene (**4**), butadiene (**13**), 2H-pyrrole (**5**), 2-azabutadiene (**14**) and 1-azabutadiene (**15**) are the only dienes in the study with exergonic free energies of reaction. The DA reactions of the 2-azadienes with ethylene have reaction free energies 1 to 3 kcal mol⁻¹ more exergonic than the reactions with the carbadienes, while the DA reactions of the 1-azadienes with ethylene are 16 to 20 kcal mol⁻¹ more endergonic.

We have also calculated the same free energies using the more realistic dienophile, fumaronitrile (**b**). The results of these calculations are tabulated in the SI. With fumaronitrile the activation free energy changes range from +1.6 to -11.8 kcal mol⁻¹, while the reaction free

energy change between -2.0 to $+5.8$ kcal mol $^{-1}$. Although the cyano groups usually increase reactivity as expected, these groups also make the reaction thermodynamics less favorable because the cyanos are removed from conjugation during the reaction.

Nitrogen substitution at either the 1- or 2-position within a diene has a remarkable influence on the activation and reaction free energies for DA reactions. We also studied the influence of multiple nitrogen substitution within a diene. We compared the activation and reaction energies of furan (**1**), oxazole (**2**), isoxazole (**3**) and oxadiazoles (**16**, **17**, **18** and **19**). Figure 1.4 shows the respective transition structures and cycloadducts.

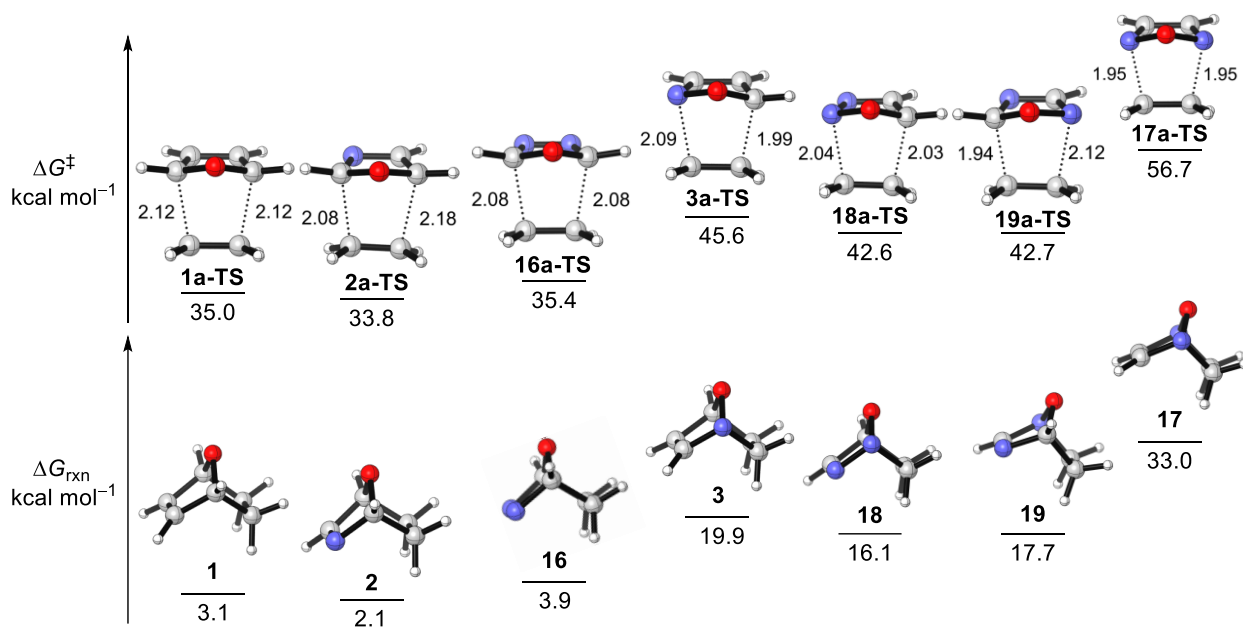


Figure 4. The computed activation and reaction free energies for DA reactions of several N,O-heterocycles with ethylene.

The introduction of a second nitrogen atom at the 3-position of oxazole (corresponding to the 2-position of the diene unit, diene **16**) has only a small influence on the energetics. However, introducing a nitrogen at the 2-position of furan (corresponding to the 1-position of the diene unit,

dienes **18** and **19**) raises the barrier by 9-11 kcal mol⁻¹ and the free energy of reaction by 17-21 kcal mol⁻¹ compared to that of dienes **1**, **2** and **16**. When a second nitrogen is introduced at the 4-position of isoxazole (corresponding to the 1-position of the diene unit, diene **17**), the free energy barrier increase 22 kcal mol⁻¹ and the reaction energy is 30 kcal mol⁻¹ more endergonic than that of furan.

Discussion

To understand these general reactivity trends, we have explored the origins of the low reactivity of 1-azadienes compared to 2-azadienes using the distortion/interaction model.²⁵ We follow this discussion with an explanation of the reactivity trends observed for different heterocycles based upon reaction free energies and diene aromaticities. We first compare the activation free energy with the reaction free energies for the cyclic dienes. The results are given in Figure 1.5.

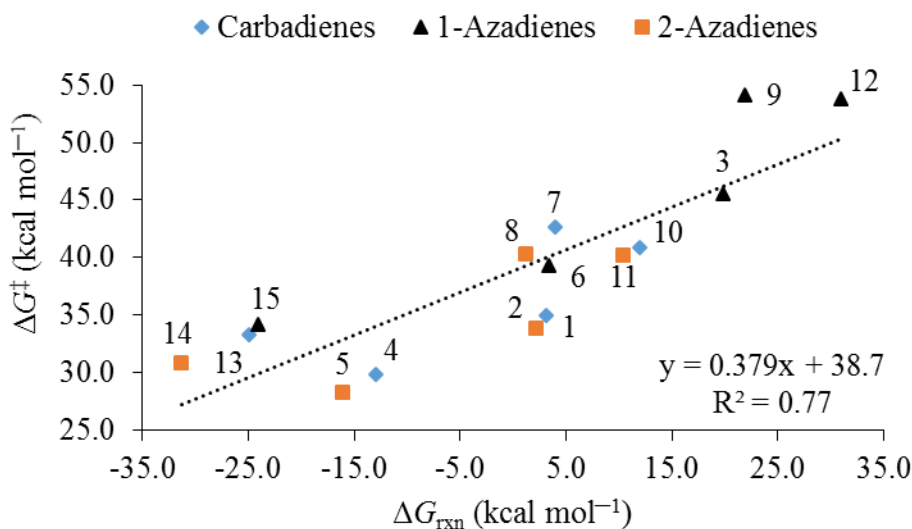


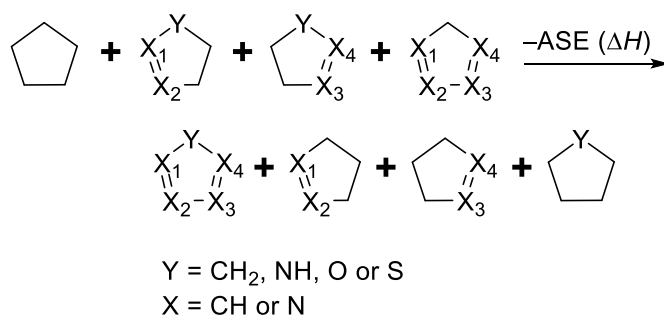
Figure 1.5. Plot of ΔG^\ddagger vs. ΔG_{rxn} for the reaction of ethylene with all of the dienes.

There is a modest correlation ($R^2 = 0.77$) between the activation and reaction free energies. The slope is near 0.5, expected by Dimroth, Evan-Polanyi, Hammond and Marcus models.⁴⁹ The DA

reactions of furan (**1**), oxazole (**2**), cyclopentadiene (**4**) 3H-pyrrole (**5**), butadiene (**13**), 2-azabutadiene (**14**) and 1-azabutadiene (**15**) with ethylene are predicted to have similar reactivity. 2H-pyrrole (**6**), thiophene (**7**), thiazole (**8**), pyrrole (**9**) and imidazole (**11**) are predicted to have DA reactions that are endergonic and reaction rates 3 to 5 orders of magnitude slower than the previous group of dienes. The 1-azadienes isoxazole (**3**), isothiazole (**9**), and pyrazole (**12**) (the three black triangles furthest right in Figure 4) are predicted to have DA reactions that are highly endergonic as well as reaction rates 7 to 13 orders of magnitude slower than the first group.

The reaction free energies for the different heterocycles can be correlated with the heterocycle aromaticity. Aromaticity can be quantified in many ways. The aromatic stabilization energy (ASE) is the energy of stabilization arising from cyclic delocalization of π electrons.^{50,51} For five-membered heterocycles, Schleyer *et al.* devised a homodesmotic scheme for calculating the ASE shown in Scheme 1.5.⁵¹

Scheme 1.5. Schleyer's homodesmotic scheme for calculating the aromatic stabilization energy ASE of heterocycles.



The equation balances the number of single and double bonds on each side of the equation, as well as conjugation, so only the enthalpy (ΔH) gain from cyclic conjugation is measured. The M06-2X/6-311G(d,p) calculated ASE of the cyclic dienes are listed in Table 1.1 as ΔH .

Table 1.1. The calculated ASE (ΔH) of the cyclic dienes using Schleyer's homodesmotic scheme. The method for calculating energies was M06-2X/6-311G(d,p). The bond distances and energies are reported in units of Ångstroms and kcal mol⁻¹, respectively.


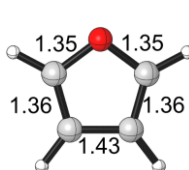
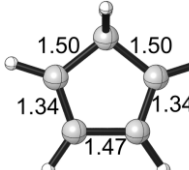
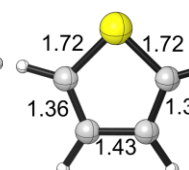
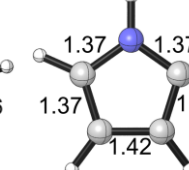
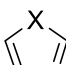
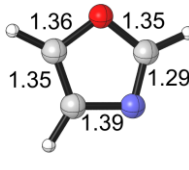
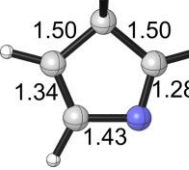
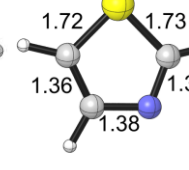
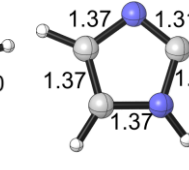
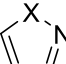
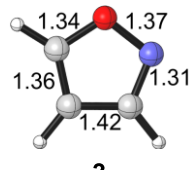
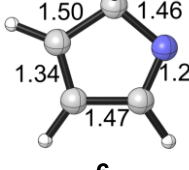
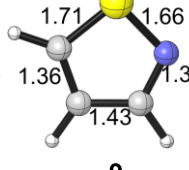
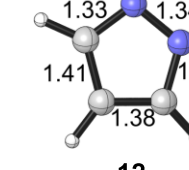
X =	O	CH ₂	S	NH
 Carbadienes	 1 14.3	 4 2.9	 7 16.8	 10 19.9
 2-Azadienes	 2 11.1	 5 1.8	 8 15.8	 11 20.1
 1-Azadienes	 3 15.7	 6 3.0	 9 17.5	 12 23.9

Figure 1.6 shows a plot of the ΔG_{rxn} for the DA reactions of the cyclic dienes (**1-12**) with ethylene versus the aromaticity (ASE) of the diene.

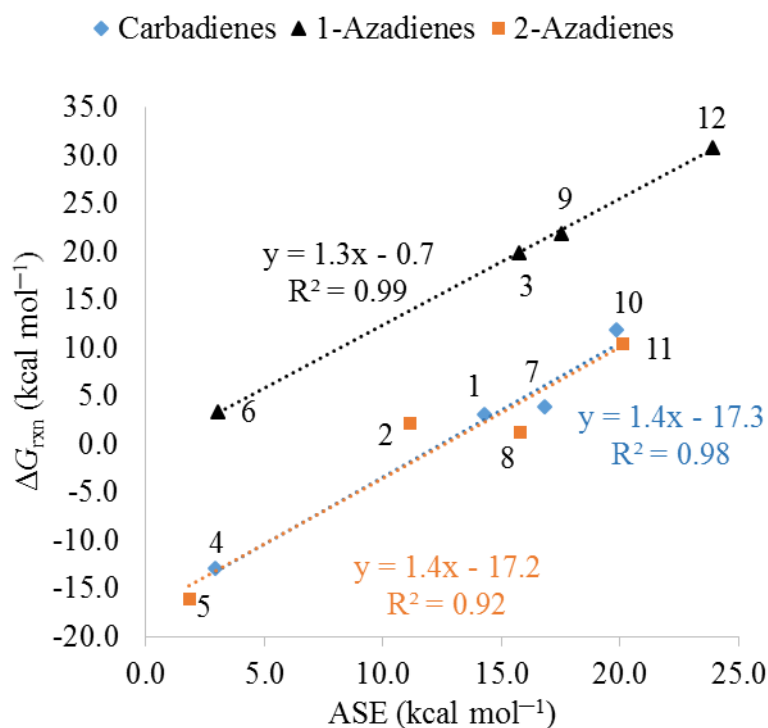


Figure 1.6. The correlations of ΔG_{rxn} versus cyclic diene aromaticity (ASE) of the carbadienes (blue diamonds), 1-azadienes (black triangles) and 2-azadienes (orange squares).

There is a good correlation between diene aromaticities and the free energies of reactions of each set of dienes. The reaction free energies of 1-azadienes (black triangles) are nearly 16 kcal mol⁻¹ higher than the 2-azadienes (orange squares) and the carbadienes (blue diamonds). As each diene becomes more aromatic, the energy of reaction becomes more endergonic.

To understand the origin of the reactivity differences between 1-aza- and 2-azadienes, the activation energies have been analyzed with the D/I (or activation strain^{33,34}) model. The D/I model dissects the activation energy (ΔE^\ddagger) into two components: the distortion (ΔE_d^\ddagger) and interaction (ΔE_i^\ddagger) energies.^{31,32,52} E is the electronic energy. The ΔE_d^\ddagger is the energy required to distort the reactants into their respective TS[‡] geometries. The ΔE_i^\ddagger is a consequence of closed shell repulsions (steric effects), occupied-vacant orbital interactions (charge-transfer), and electrostatic and

polarization effects. The D/I model has been used to explain the reactivity of DA cycloadditions.³⁵⁻

³⁷ Recently we have shown that the poor reactivity of cyclohexadiene and cycloheptadiene relative to that of cyclopentadiene is related to the differences in distortion energies.³⁸

Figure 1.7 shows a plot of the electronic energies of activation versus the distortion energies.

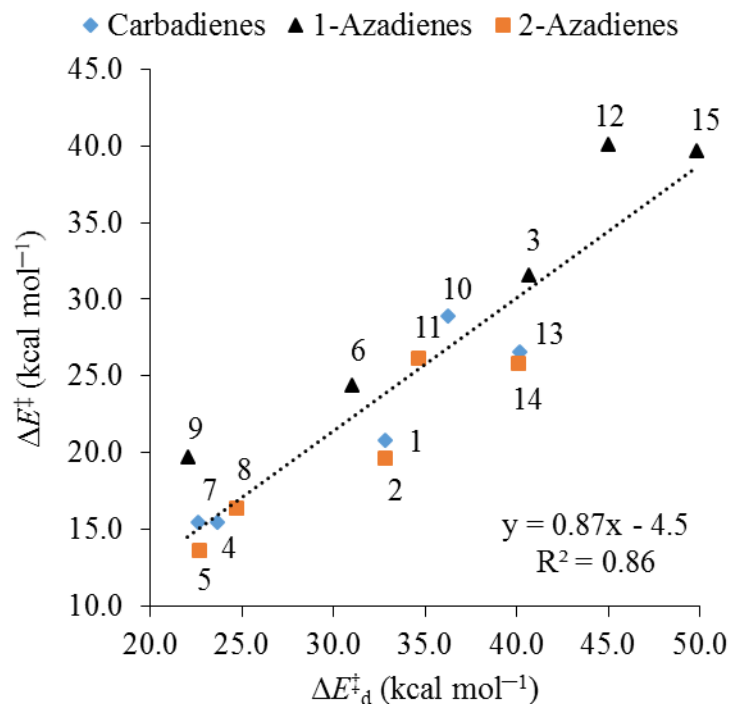


Figure 1.7. ΔE^\ddagger vs. ΔE_d^\ddagger for the DA reaction of ethylene with the dienes.

There is a reasonably good correlation between the activation energies and the distortion energies. It is significantly more difficult to distort 1-azadienes as opposed to 2-azadienes or the carbadienes. This was found in studies of DA reactions of benzene and six-membered poly-aza-heterocycles in previous studies by our group.^{30,35} It is due to the unfavorable energetics of addition to C=N π bonds and the poorer overlap of orbitals involving N and C in forming a new σ bond.³⁵ With the exception of the acyclic dienes (**13**, **14** and **15**), the energy required to distort the cyclic

1-azadienes is 31 to 50 kcal mol⁻¹, while the cyclic 2-azadienes, cyclopentadienes and monoheterocycles require 23 to 40 kcal mol⁻¹ to distort.

In addition to the single point analysis at the transition state, we have also carried out the D/I analysis along the reaction coordinate for oxazole (**2**) and isoxazole (**3**). The total electronic energy (ΔE), distortion energy (ΔE_{dist}) and interaction energy (ΔE_{int}) are plotted versus the average dihedral angle ($\omega_{\text{Ave.}}$) of the bending oxygen atom for oxazole (black) and isoxazole (orange) are displayed in Figure 1.8.

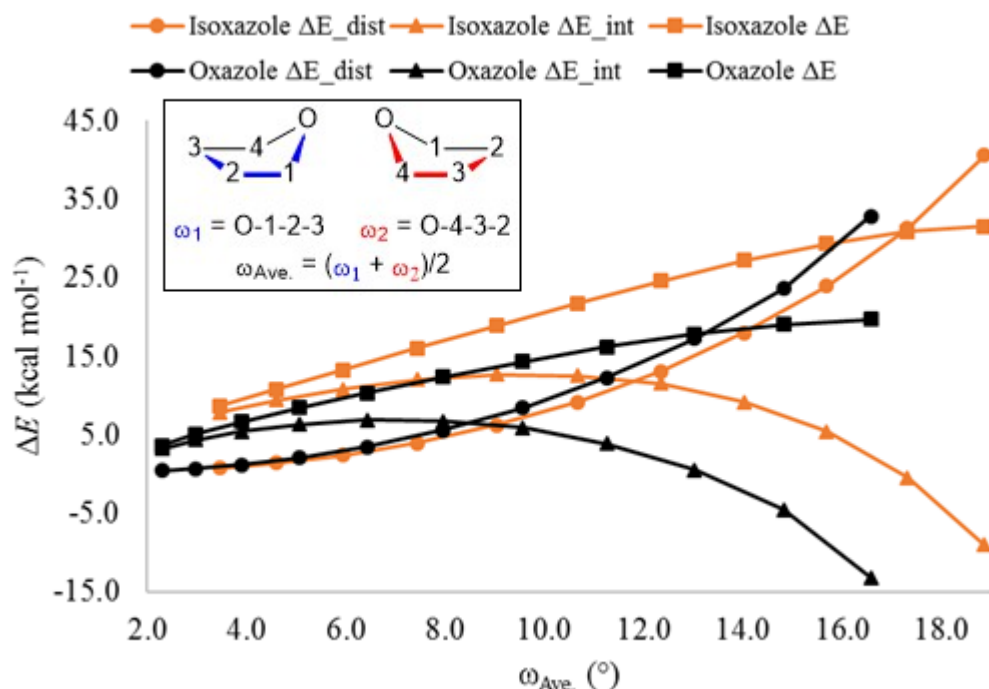


Figure 1.8. Plots of total energy, distortion energy and interaction energy versus the average dihedral angle of the bending oxygen atom of oxazole (black lines) and isoxazole (orange lines) in the DA reaction with ethylene. The last points to the right are the respective transition states.

The transition state of **2** with ethylene occurs earlier than that of **3**, consistent with the greater exothermicity of the reaction of **2**. The total energies for **2** are always lower along the reaction

coordinate than **3**. The change in distortion energy over the reaction coordinate is slightly elevated for **2** compared to **3** until the transition state is reached, where the difference in distortion energies is 7.8 kcal mol⁻¹ in favor of oxazole (**2**). Along the reaction coordinate the interaction energy is always more favorable for **2** due to the greater orbital overlap of carbon than of nitrogen and ethylenes *p*-orbital.⁵³⁻⁵⁵ The interacting *p*-orbital of nitrogen in **3** is more contracted, resulting in less favorable interaction energy. As we have previously reported in the aza-DA reaction of azabenzenes with ethylene, the replacement of CH with N increases the reactivity of the diene primarily due to more favorable interaction energy along the reaction coordinate.³⁰ We showed earlier that reaction barriers correlate very closely with distortion energies, but the calculations in Figure 8 showed that the interaction energies influence the position of the transition state.

Another way to look at this focuses on the thermodynamic contribution to the activation barriers. The difference in reaction energies shifts the transition states to favor the oxazole reaction all along the reaction path. To explain the difference in reaction energies for addition to C=C and C=N bonds, we evaluated what bonds are being broken and formed in each DA reaction. A set of isodesmic reactions for each aza-substituted diene is shown in Figure 1.9.

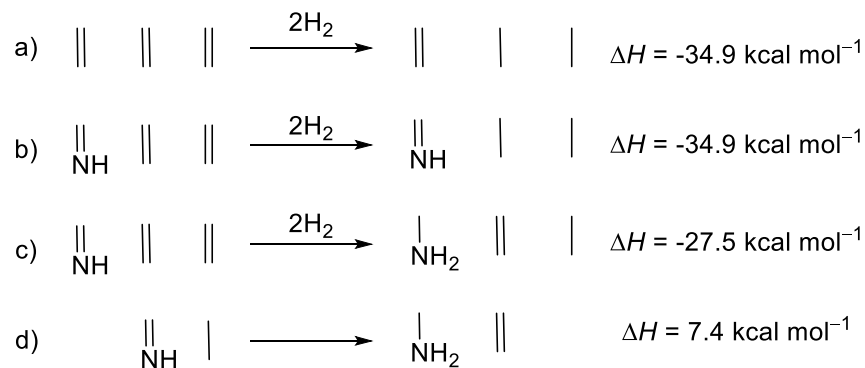


Figure 1.9. a) Expressions for bond changes in the DA reaction of ethylene with furan (**1**) and cyclopentadiene (**4**), b) oxazole (**2**) and 3H-pyrrole (**5**), and c) isoxazole (**3**) and 2H-pyrrole (**6**). d) The energy differences between these reactions can be expressed isodesmically. Computations were performed using M06-2X/6-311G(d,p).

In the DA reactions with carbadienes three double bonds are converted into two single bonds and one double bond (Figure 1.9a), calculations on this transformation gives a calculated enthalpy of $-34.9 \text{ kcal mol}^{-1}$. When 2-azadienes react (i.e.: oxazole, **2**, and 3H-pyrrole, **5**), two C=C and one C=N bonds are converted to two C–C and one C=N (Figure 1.9b), which of course has the same enthalpy as the reaction with carbadienes. The reactions of 1-azadienes (i.e.: isoxazole, **3**, and 2H-pyrrole, **6**) differ in that one C=N and one C=C bonds are converted to one C–N and one C–C (Figure 1.9c); this has an overall reaction enthalpy of $-27.5 \text{ kcal mol}^{-1}$. The difference between these reactions can be written as the conversion of one C=N and one C–C to one C–N and one C=C bonds (Figure 1.9d), which has an enthalpy of $+7.4 \text{ kcal mol}^{-1}$. The experimental enthalpies of hydrogenation of methanimine and ethylene are -32.5 ± 0.1 and $-21.62 \pm 0.1 \text{ kcal mol}^{-1}$ respectively.⁵⁶⁻⁵⁸ The M06-2X energetics (Figure 1.10) are in agreement with experiment. These two measurements indicate that it is thermodynamically more favorable to convert a C=C π bond to a C–C single bond as compared to the C=N to C–N transformation.

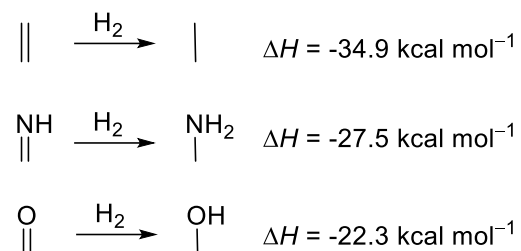


Figure 1.10. Calculated M06-2X/6-311G(d,p) enthalpies of hydrogenation of simple dienes.

Bond strength energy is related to the difference in electronegativity of the two atoms involved. This is the basis of Pauling's definition of electronegativity.⁵⁹ Pauling, Sanderson, and others have shown that bond energy is proportional to the differences in electronegativity between the constituent atoms in the bond.^{59,60} In the cycloadditions, the C(sp²)-X(sp²) double bond is being converted to a C(sp³)-X(sp³) single bond. Conversion to the more saturated system becomes more difficult as X becomes more electronegative, and as two polar bonds (the double bond) are converted to one polar bond.

An additional contributing factor involves the change in hybridization that occurs upon addition to the N of a C=N double bond. In this process, the sp² lone pair on N becomes an sp³ lone pair: the decrease in s-character is destabilizing as well. This has been discussed previously by Borden *et al.* in comparing electronic structures and reactions of nitrenes and carbenes.⁶¹

These energetic trends nicely rationalize why the cyclic 1-azadienes are less reactive than the non-aza- or 2-azadienes. However we find only small differences for the acyclic cases. This intrinsic difference is counteracted by the stabilizing enamine resonance in the product of the DA reactions of 1-azadienes. We have calculated the enthalpic cost of loss of conjugation in an allylic amine, shown in Figure 1.11.

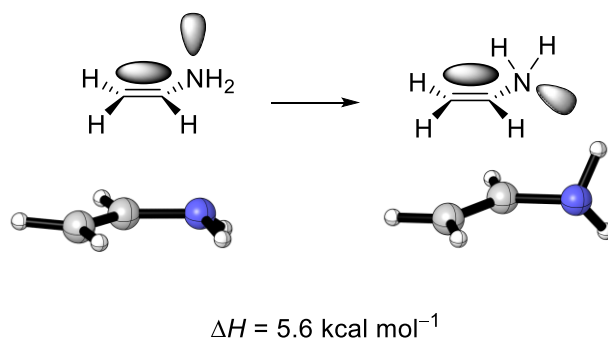


Figure 1.11. Enthalpy of rotation and deconjugation of nitrogen in acetaldehyde enamine, calculated using M06-2X/6-311G(d,p).

We find there is a $5.6 \text{ kcal mol}^{-1}$ enthalpy cost to disrupt the nitrogen conjugation by rotation. This enthalpy cost is present in the product of reaction of all of the cyclic 1-azadienes. In the reaction of **15** and **a**, the enthalpic cost of addition to a C=N bond is mostly counteracted by the nitrogen lone pair conjugation in the non-planar enamine product. We earlier note the importance of this factor in causing isoxazole to be far less reactive than oxazole.²¹

Conclusions

The Diels-Alder reactions of a variety of acyclic and substituted heterocyclic dienes with ethylene and fumaronitrile have been investigated using DFT. Activation and reaction energies increase with respective diene aromaticity. The significant difference between the reactivities of 1-aza- and 2-azadienes is related to the thermodynamics of these reactions. The distortion energies nicely correlate with reactants and the origins of this correlation is shown to be related to the overall thermodynamics of the reaction. Addition to a C=N bond is intrinsically less favorable than addition to a C=C bond, and the former require more energy to distort in the transition states for 1-azadienes in these DA reactions. In acyclic 1-azadienes there is a compensation due to the

conjugation of the developing sp^3 nitrogen lone pair with the double bond, which is not possible in the adducts from cyclic 1-azadienes.

Acknowledgements

We thank the National Science Foundation (CHE-1361104) for financial support of this research. High performance computing resources were provided by the UCLA Hoffman2 cluster and the NSF Extreme Science and Engineering Discovery Environment (TG-CHE040013N). We thank Zili Fan and Fang Liu for helpful discussions.

References

- (1) Eschenbrenner-Lux, V.; Kumar, K.; Waldmann, H. *Angew. Chem., Int. Ed.* **2014**, *53*, 11146.
- (2) Buffat, M. G. P. *Tetrahedron* **2004**, *60*, 1701.
- (3) Sridharan, V.; Suryavanshi, P. A.; Menendez, J. C. *Chem. Rev. (Washington, DC, U. S.)* **2011**, *111*, 7157.
- (4) Girling, P. R.; Kiyoi, T.; Whiting, A. *Org. Biomol. Chem.* **2011**, *9*, 3105.
- (5) Kouznetsov, V. V. *Tetrahedron* **2009**, *65*, 2721.
- (6) Domingo, L. R.; Aurell, M. J.; Saez, J. A.; Mekelleche, S. M. *RSC Adv.* **2014**, *4*, 25268.
- (7) Mazaheripour, A.; Dibble, D. J.; Umerani, M. J.; Park, Y. S.; Lopez, R.; Laidlaw, D.; Vargas, E.; Ziller, J. W.; Gorodetsky, A. A. *Org. Lett.* **2016**, *18*, 156.
- (8) Dagousset, G.; Zhu, J.; Masson, G. *J. Am. Chem. Soc.* **2011**, *133*, 14804.
- (9) Liu, H.; Dagousset, G.; Masson, G.; Retailleau, P.; Zhu, J. *J. Am. Chem. Soc.* **2009**, *131*, 4598.
- (10) Dagousset, G.; Drouet, F.; Masson, G.; Zhu, J. *Org. Lett.* **2009**, *11*, 5546.
- (11) Dagousset, G.; Retailleau, P.; Masson, G.; Zhu, J. *Chem. - Eur. J.* **2012**, *18*, 5869.
- (12) Yang, J.; Seckute, J.; Cole, C. M.; Devaraj, N. K. *Angew. Chem., Int. Ed.* **2012**, *51*, 7476.
- (13) Jouanno, L.-A.; Chevalier, A.; Sekkat, N.; Perzo, N.; Castel, H.; Romieu, A.; Lange, N.; Sabot, C.; Renard, P.-Y. *J. Org. Chem.* **2014**, *79*, 10353.
- (14) Kondrat'eva, G. Y. *Khim. Nauka Prom-st.* **1957**, *2*, 666.
- (15) Yu, X.-L.; Kuang, L.; Chen, S.; Zhu, X.-L.; Li, Z.-L.; Tan, B.; Liu, X.-Y. *ACS Catal.* **2016**, *6*, 6182.
- (16) Almansour, A. I.; Arumugam, N.; Suresh Kumar, R.; Carlos Menendez, J.; Ghabbour, H. A.; Fun, H.-K.; Ranjith Kumar, R. *Tetrahedron Lett.* **2015**, *56*, 6900.
- (17) Dai, W.; Jiang, X.-L.; Tao, J.-Y.; Shi, F. *J. Org. Chem.* **2016**, *81*, 185.
- (18) Min, C.; Seidel, D. *Chem. - Eur. J.* **2016**, *22*, 10817.
- (19) Richmond, E.; Ullah Khan, I.; Moran, J. *Chem. - Eur. J.* **2016**, *22*, 12274.
- (20) Muthukrishnan, I.; Vinoth, P.; Vivekanand, T.; Nagarajan, S.; Maheswari, C. U.; Menendez, J. C.; Sridharan, V. *J. Org. Chem.* **2016**, *81*, 1116.

- (21) Gonzalez, J.; Taylor, E. C.; Houk, K. N. *J. Org. Chem.* **1992**, *57*, 3753.
- (22) Masson, G.; Lalli, C.; Benohoud, M.; Dagousset, G. *Chem. Soc. Rev.* **2013**, *42*, 902.
- (23) Behforouz, M.; Ahmadian, M. *Tetrahedron* **2000**, *56*, 5259.
- (24) Jung, M. E.; Shapiro, J. J. *J. Am. Chem. Soc.* **1980**, *102*, 7862.
- (25) Eddaif, A.; Laurent, A.; Mison, P.; Pellissier, N.; Carrupt, P. A.; Vogel, P. *J. Org. Chem.* **1987**, *52*, 5548.
- (26) Clark, R. C.; Pfeiffer, S. S.; Boger, D. L. *J. Am. Chem. Soc.* **2006**, *128*, 2587.
- (27) Tay, G. C.; Sizemore, N.; Rychnovsky, S. D. *Org. Lett.* **2016**, *18*, 3050.
- (28) Yan, X.; Ling, F.; Zhang, Y.; Ma, C. *Org. Lett.* **2015**, *17*, 3536.
- (29) He, L.; Laurent, G.; Retailleau, P.; Folleas, B.; Brayer, J.-L.; Masson, G. *Angew. Chem., Int. Ed.* **2013**, *52*, 11088.
- (30) Yang, Y.-F.; Liang, Y.; Liu, F.; Houk, K. N. *J. Am. Chem. Soc.* **2016**, *138*, 1660.
- (31) Ess, D. H.; Houk, K. N. *J. Am. Chem. Soc.* **2007**, *129*, 10646.
- (32) Ess, D. H.; Houk, K. N. *J. Am. Chem. Soc.* **2008**, *130*, 10187.
- (33) van Zeist, W.-J.; Bickelhaupt, F. M. *Org. Biomol. Chem.* **2010**, *8*, 3118.
- (34) Bickelhaupt, F. M. *J. Comput. Chem.* **1999**, *20*, 114.
- (35) Liu, F.; Liang, Y.; Houk, K. N. *J. Am. Chem. Soc.* **2014**, *136*, 11483.
- (36) Levandowski, B. J.; Zou, L.; Houk, K. N. *J. Comput. Chem.* **2016**, *37*, 117.
- (37) Fernandez, I.; Bickelhaupt, F. M. *J. Comput. Chem.* **2014**, *35*, 371.
- (38) Levandowski, B. J.; Houk, K. N. *J. Org. Chem.* **2015**, *80*, 3530.
- (39) Frisch, M. J.; Trucks, G. W.; Schlegel, H. B.; Scuseria, G. E.; Robb, M. A.; Cheeseman, J. R.; Scalmani, G.; Barone, V.; Mennucci, B.; Petersson, G. A.; Nakatsuji, H.; Caricato, M.; Li, X.; Hratchian, H. P.; Izmaylov, A. F.; Bloino, J.; Zheng, G.; Sonnenberg, J. L.; Hada, M.; Ehara, M.; Toyota, K.; Fukuda, R.; Hasegawa, J.; Ishida, M.; Nakajima, T.; Honda, Y.; Kitao, O.; Nakai, H.; Vreven, T.; Montgomery, J. A.; Peralta, J. E.; Ogliaro, F.; Bearpark, M.; Heyd, J. J.; Brothers, E.; Kudin, K. N.; Staroverov, V. N.; Kobayashi, R.; Normand, J.; Raghavachari, K.; Rendell, A.; Burant, J. C.; Iyengar, S. S.; Tomasi, J.; Cossi, M.; Rega, N.; Millam, J. M.; Klene, M.; Knox, J. E.; Cross, J. B.; Bakken, V.; Adamo, C.; Jaramillo, J.; Gomperts, R.; Stratmann, R. E.; Yazyev, O.; Austin, A. J.; Cammi, R.; Pomelli, C.; Ochterski, J. W.; Martin, R. L.; Morokuma, K.; Zakrzewski, V. G.; Voth, G. A.; Salvador, P.; Dannenberg, J. J.; Dapprich, S.; Daniels, A. D.; Farkas; Foresman, J. B.; Ortiz, J. V.; Cioslowski, J.; Fox, D. J. Wallingford CT, 2009.
- (40) Zhao, Y.; Truhlar, D. G. *Theor. Chem. Acc.* **2008**, *120*, 215.
- (41) Lan, Y.; Zou, L.; Cao, Y.; Houk, K. N. *J. Phys. Chem. A* **2011**, *115*, 13906.
- (42) Paton, R. S.; Mackey, J. L.; Kim, W. H.; Lee, J. H.; Danishefsky, S. J.; Houk, K. N. *J. Am. Chem. Soc.* **2010**, *132*, 9335.
- (43) Zhao, Y.; Truhlar, D. G. *Phys. Chem. Chem. Phys.* **2008**, *10*, 2813.
- (44) Ribeiro, R. F.; Marenich, A. V.; Cramer, C. J.; Truhlar, D. G. *J. Phys. Chem. B* **2011**, *115*, 14556.
- (45) Legault, C. Y.; 1.0b ed. Université de Sherbrooke, 2009.
- (46) McCormick, D. G.; Hamilton, W. S. *J. Chem. Thermodyn.* **1978**, *10*, 275.
- (47) Bedford, A. F.; Edmondson, P. B.; Mor-timer, C. T. *J. Chem. Soc.* **1962**, 2927.
- (48) Hammond, G. S. *J. Am. Chem. Soc.* **1955**, *77*, 334.
- (49) Jencks, W. P. *Chem. Rev.* **1985**, *85*, 511.
- (50) von Ragué Schleyer, P.; Jiao, H.; Goldfuss, B.; Freeman, P. K. *Angew. Chem., Int. Ed. Engl.* **1995**, *34*, 337.

- (51) Cyranski, M. K.; Krygowski, T. M.; Katritzky, A. R.; Schleyer, P. v. R. *J. Org. Chem.* **2002**, *67*, 1333.
- (52) Fernandez, I.; Bickelhaupt, F. M. *Chem. Soc. Rev.* **2014**, *43*, 4953.
- (53) Houk, K. N. *Acc. Chem. Res.* **1975**, *8*, 361.
- (54) Fleming, I. *Frontier Orbitals and Organic Chemical Reactions*; Wiley: London, 1976.
- (55) Fleming, I.; Michael, J. P.; Overman, L. E.; Taylor, G. F. *Tetrahedron Lett.* **1978**, 1313.
- (56) Manion, J. A. *Journal of Physical and Chemical Reference Data* **2002**, *31*, 123.
- (57) Peerboom, R. A. L.; Ingemann, S.; Nibbering, N. M. M.; Liebman, J. F. *J. Chem. Soc., Perkin Trans. 2* **1990**, 1825.
- (58) Aston, J. G.; Siller, C. W.; Messerly, G. H. *J. Am. Chem. Soc.* **1937**, *59*, 1743.
- (59) Pauling, L. *J. Am. Chem. Soc.* **1932**, *54*, 3570.
- (60) Sanderson, R. T. *J. Am. Chem. Soc.* **1983**, *105*, 2259.
- (61) Kemnitz, C. R.; Karney, W. L.; Borden, W. T. *J. Am. Chem. Soc.* **1998**, *120*, 3499.

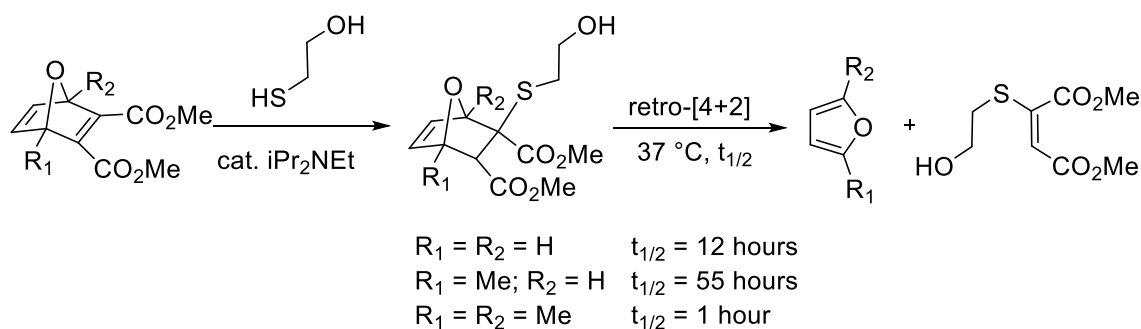
Chapter 2

Theoretical analysis of the retro-Diels-Alder reactivity of oxanorbornadiene thiol and amine adducts

Fell, J. S.; Lopez, S. A.; Higginson, C. J.; Finn, M. G.; Houk, K. N. *Org. Lett.* **2017**, *19*, 4504.

The thiol-promoted retro-[4+2] cycloadditions¹ of 7-oxanorbornadienes have been reported by Finn and coworkers.^{2,3} Oxanorbornadienes bearing electron withdrawing substituents undergo rapid conjugate addition of amines and thiolates,^{4,5} and a subsequent retro-[4+2] cycloaddition (Scheme 2.1). The thiol addition step is fast, while the fragmentation is rate-determining. The nature of the substituents at the oxanorbornadienes affects the rate of fragmentation, with oxanorbornene adduct half-lives ranging from 1 hour to 8 months. The mild conditions of this chemistry make it useful for *in vivo* drug delivery^{6,7} and degradable materials synthesis,⁸ where the thiol is often a cysteine residue.

Scheme 2.1. Conjugate addition of β -mercaptoethanol to oxanorbornadienes, followed by retro-[4+2] cycloaddition to produce substituted furans and thiomaleate.



Finn and coworkers rationalized this range of half-lives by hyperconjugative effects and intramolecular hydrogen bonding, illustrated in Figure 2.1. The transition structures were thought to be stabilized via sulfur lone pair orbital (n) hyperconjugation into the carbon-carbon σ^* orbital of the breaking bond. An intramolecular hydrogen bond is also possible in non-aqueous environments, such as DMSO, in which the kinetics were determined.

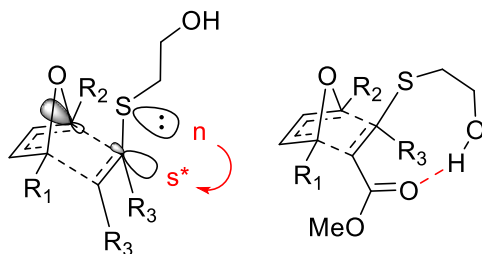


Figure 2.1. $n \rightarrow \sigma^*$ hyperconjugation by sulfur (left) and intramolecular hydrogen bonding (right).

Our general interest in understanding cycloaddition reactivity prompted us to study the origins of substituent effects on retro-[4+2] reactivity of 7-oxanorbornadienes. We have used the M06-2X^{9,10} density functional that has been previously shown to give relatively accurate energies for cycloaddition reactions.^{11,12} We utilized the 6-31+G(d) basis set for geometry optimizations, and DMSO solvation effects were accounted for with single point energy calculations utilizing a polarization continuum model with a 6-311+G(d,p) basis set. Reactions of molecules in Figure 2.2 were studied.

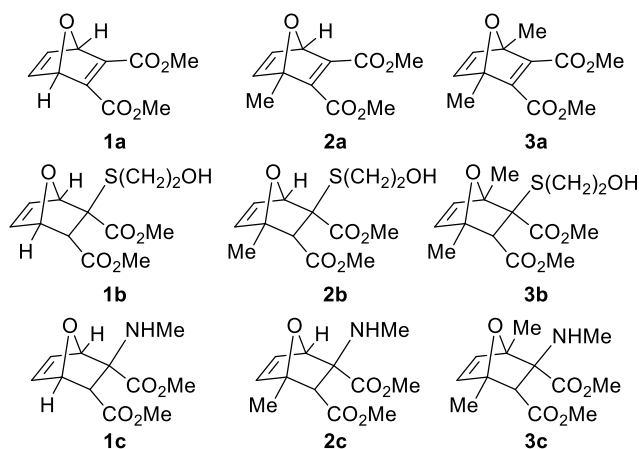


Figure 2.2. 7-Oxanorbornadienes (**1a-3a**) and the 7-oxanorbornene adducts after thiol (**1b-3b**) and amine (**1c-3c**) addition.

Figure 2.3 shows transition structures and product dienophiles for oxanorbornadiene (**1a** and **a**) and the thiol (**1b** and **b**) and amino (**1c** and **c**) oxanorbornene adducts. **TS-1a** is asynchronous; one of the ester substituents is conjugated with the π -bond participating in the retro-[4+2] cycloaddition, while the other methyl ester is orthogonal to the forming π -bond but conjugated to the pre-existing π -bond. We previously have found that available *p*-orbitals of dienophile substituents are aligned orthogonal in order to maximize the stabilization of developing partial negative charge in asynchronous transition structures.¹³ Both **TS-1b** and **TS-1c** have the same characteristics as the orthogonal substituent is at the more fully cleaved bond in the transition state. All three transition structures are concerted, but asynchronous; the newly-forming bond lengths differ by 0.34 Å, 0.62 Å and 0.42 Å, respectively. The degree of asynchronicity is related to the increased stabilization of a partial negative charge. The calculated charges on the forming dienophile fragments in the transition state are -0.3, -0.2 and -0.2 for fragments **1b**, **1c** and **1a**, respectively. The nitrogen and sulfur atoms inductively stabilize these partial charges, resulting in asynchronous transition states.

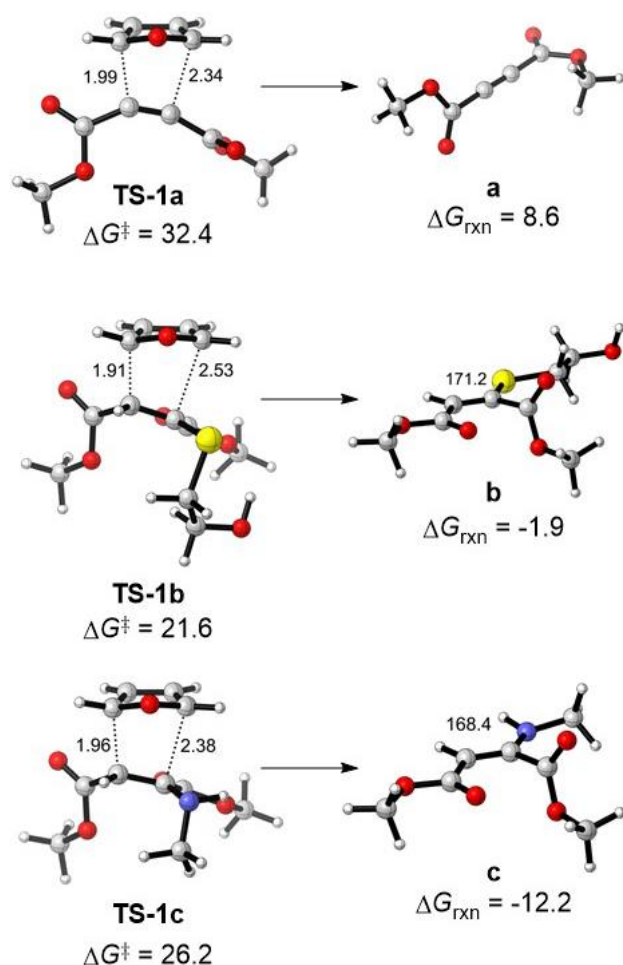


Figure 2.3. TS-1a, TS-1b, and TS-1c with respective alkyne (**a**) and alkene (**b** and **c**) products. Activation and reaction free energies are in kcal mol⁻¹. Breaking bond distances and C-X-C=C dihedral angles are reported in Ångstroms and degrees, respectively. ΔG^\ddagger for 1 ATM, 25 °C.

Fragmentations of 7-oxanorbornadienes typically require temperatures above 100 °C, but thiol- and amine-promoted fragmentations can take place *in vivo* at 37 °C.⁸ The computed activation free energies in Figure 2.3 are consistent with these experimental conditions. The activation free energies for **TS-1b** and **TS-1c** are 10.8 and 6.4 kcal mol⁻¹ lower than for **TS-1a**, respectively. The lone pairs on the sulfur and nitrogen atoms in **TS-1b** and **TS-1c** are orthogonal to the anti-bonding orbitals of the breaking C-C bond, contrary to expectation in Figure 2.1. We calculated the C-X-

C=C dihedral angle in **b** and **c** product alkenes to be 171° and 168°, respectively. The sulfur and nitrogen atoms in the product alkenes are fully conjugated with the π -bond and β -ester. The reaction thermodynamics also favors the formation of these polar alkenes that are push-pull stabilized; the fragmentation of **1b** and **1c** are exergonic ($\Delta G_{\text{rxn}} = -1.9$ and -12.2 kcal mol⁻¹, respectively), while the reaction of **1a** is endergonic ($\Delta G_{\text{rxn}} = +8.6$ kcal mol⁻¹). The formation of the two alkenes is kinetically and thermodynamically favored over alkynes.

Next, we explored how the retro-[4+2] reactivity depends on the bridgehead substitution pattern of the bicyclic intermediates. We performed calculations only on systems substituted with methyl groups to minimize the sampling of conformers. The retro-[4+2] transition structures of the thiol-oxanorbornene adducts are shown in Figure 2.4 with corresponding free energies of activation. Experimental activation free energies are listed for comparison, and were calculated from the experimental half-lives listed in Scheme 1 using the Eyring equation.

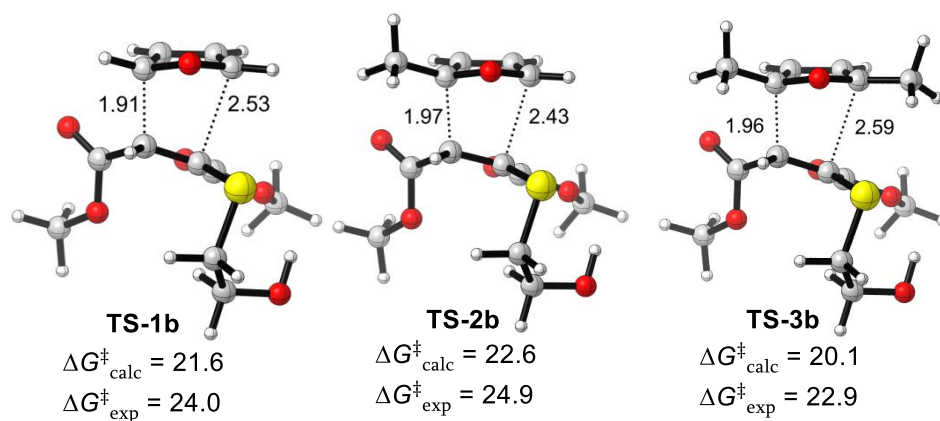


Figure 2.4. TS-1b, TS-2b and TS-3b, and computed and experimental activation free energies (kcal mol⁻¹). Breaking carbon-carbon bond distances are reported in Ångstroms. $\Delta G^\ddagger_{\text{exp}}$ are determined from rate constants at 37 °C using the Eyring equation; $\Delta G^\ddagger_{\text{calc}}$ were computed at 25 °C.

All three transition structures are concerted, but highly asynchronous. The carbon β to the thioether has a shorter breaking bond distance to C2 of the furan ($C\beta-C2$) than the carbon α to the thioether and C4 of the furan ($C\alpha-C4$). Along the reaction, the transition state shift to more product-like geometries (longer breaking bonds) opposite to the Hammond postulate but consistent with greater transition state stabilization.¹⁴

Our calculations predict the correct order of reactivity, and the computed free energies differ from experimental activation free energies by 2.3 - 2.4 kcal mol⁻¹. We utilize the Distortion/Interaction (D/I) or Activation Strain model to dissect the activation energies into distortion and interaction energies.¹⁵⁻¹⁹ The D/I model is used to analyze the activation energies of bimolecular reactions. The distortion term (ΔE_d^\ddagger) represents the energy required to distort the reactants into their respective transition state geometries without allowing the fragments to interact. The interaction energy (ΔE_i^\ddagger) is the difference between the activation energy and distortion energy, which represents energy gained from favorable orbital interactions. From the D/I model we will obtain the distortion and interaction energies from the [4+2] reaction of maleates and furans to produce the oxanorbornene adducts.

We performed D/I analysis on **TS-1b**, **TS-2b**, and **TS-3b**. Figure 2.5 shows these transition structures with corresponding ΔE^\ddagger , ΔE_d^\ddagger , and ΔE_i^\ddagger for the [4+2] reaction. The interaction energies become more negative with each bridgehead methyl substitution. Methyl substitution makes the forming diene fragment more electron-rich, which improves the orbital interaction with the electron-deficient dienophile. The HOMO energies of the furan increase along the series **1b**, **2b** and **3b** (-8.54, -8.20 and -7.88 eV). A methyl on the shorter forming bond (R_1) exerts a destabilizing steric effect, increasing the distortion energy from 33 to 35 kcal mol⁻¹. The second

methyl (R_2) is well separated from the diene and shows no steric effect. **TS-2b** and **TS-3b** have the same distortion energy.

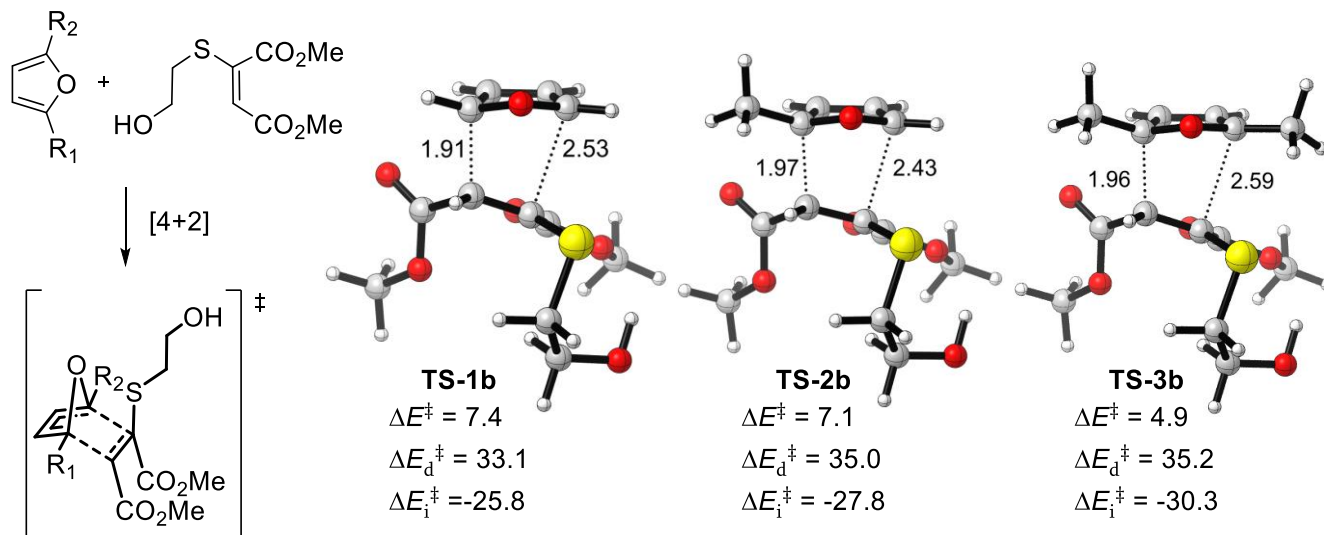


Figure 2.5. **TS-1b**, **TS-2b** and **TS-3b** with corresponding ΔE^\ddagger , ΔE_d^\ddagger , and ΔE_i^\ddagger for the [4+2] reaction. Energies and distances are reported in units of kcal mol⁻¹ and Ångstroms, respectively.

Frontier molecular orbital effects, manifested as ΔE_i^\ddagger , are responsible for the differences in reactivity based on the substitution pattern. With each addition of a methyl group the diene becomes more electron rich, increasing favorable interaction energy with the dienophile (thiomaleate, **a**). This favorable change in interaction energy is counteracted by an increase in unfavorable distortion energy by a single substituent from steric repulsion. Modulation of the furan electronic structure can be used to fine tune the retro-[4+2] reactivity to expand the utility of this chemistry in drug delivery applications.

The utility of the thiol and amine-activated retro-Diels-Alder reactions has been explained by theoretical analysis, and these principles can be used to fine tune the substrates to further the application of these reactions.

Acknowledgements

We would like to thank the National Science Foundation (CHE-1361104) for financial support of this research. We are grateful for the computational resources provided by UCLA Institute for Digital Research and Education and the National Science Foundation through XSEDE Science Gateways Program (TG-CHE040013N).

References

- (1) Diels, O.; Alder, K. *Justus Liebigs Ann. Chem.* **1928**, 460, 98.
- (2) Hong, V.; Kislukhin, A. A.; Finn, M. G. *J. Am. Chem. Soc.* **2009**, 131, 9986.
- (3) Kislukhin, A. A.; Higginson, C. J.; Hong, V. P.; Finn, M. G. *J. Am. Chem. Soc.* **2012**, 134, 6491.
- (4) Albert, S.; Soret, A.; Blanco, L.; Deloisy, S. *Tetrahedron* **2007**, 63, 2888.
- (5) Mahajna, M.; Quistad, G. B.; Casida, J. E. *Chem. Res. Toxicol.* **1996**, 9, 241.
- (6) Higginson, C. J.; Eno, M. R.; Khan, S.; Cameron, M. D.; Finn, M. G. *ACS Chem. Biol.* **2016**, 11, 2320.
- (7) Sanhueza, C. A.; Baksh, M.; Thuma, B.; Roy, M. D.; Dutta, S.; Préville, C.; Chrunk, B. A.; Beaumont, K.; Dullea, R.; Ammirati, M.; Liu, S.; Gebhard, D.; Finley, J. E.; Salatto, C. T.; King-Ahmad, A.; Stock, I.; Atkinson, K.; Reidich, B.; Lin, W.; Kumar, R.; Tu, M. H.; Menhaji-Klotz, E.; Price, D. A.; Liras, S.; Finn, M. G.; Mascitti, V. *J. Am. Chem. Soc.* **2017**, 139, 3528.
- (8) Higginson, C. J.; Kim, S. Y.; Peláez-Fernández, M.; Fernández-Nieves, A.; Finn, M. G. *J. Am. Chem. Soc.* **2015**, 137, 4984.
- (9) Frisch, M. J.; Trucks, G. W.; Schlegel, H. B.; Scuseria, G. E.; Robb, M. A.; Cheeseman, J. R.; Scalmani, G.; Barone, V.; Mennucci, B.; Petersson, G. A.; Nakatsuji, H.; Caricato, M.; Li, X.; Hratchian, H. P.; Izmaylov, A. F.; Bloino, J.; Zheng, G.; Sonnenberg, J. L.; Hada, M.; Ehara, M.; Toyota, K.; Fukuda, R.; Hasegawa, J.; Ishida, M.; Nakajima, T.; Honda, Y.; Kitao, O.; Nakai, H.; Vreven, T.; Montgomery, J. A.; Peralta, J. E.; Ogliaro, F.; Bearpark, M.; Heyd, J. J.; Brothers, E.; Kudin, K. N.; Staroverov, V. N.; Kobayashi, R.; Normand, J.; Raghavachari, K.; Rendell, A.; Burant, J. C.; Iyengar, S. S.; Tomasi, J.; Cossi, M.; Rega, N.; Millam, J. M.; Klene, M.; Knox, J. E.; Cross, J. B.; Bakken, V.; Adamo, C.; Jaramillo, J.; Gomperts, R.; Stratmann, R. E.; Yazyev, O.; Austin, A. J.; Cammi, R.; Pomelli, C.; Ochterski, J. W.; Martin, R. L.; Morokuma, K.; Zakrzewski, V. G.; Voth, G. A.; Salvador, P.; Dannenberg, J. J.; Dapprich, S.; Daniels, A. D.; Farkas; Foresman, J. B.; Ortiz, J. V.; Cioslowski, J.; Fox, D. J. Gaussian 09, Revision D.01, Gaussian Inc., Wallingford CT, **2009**.
- (10) Zhao, Y.; Truhlar, D. G. *Theor. Chem. Acc.* **2008**, 120, 215.
- (11) Lan, Y.; Zou, L.; Cao, Y.; Houk, K. N. *J. Phys. Chem. A* **2011**, 115, 13906.
- (12) Paton, R. S.; Mackey, J. L.; Kim, W. H.; Lee, J. H.; Danishefsky, S. J.; Houk, K. N. *J. Am. Chem. Soc.* **2010**, 132, 9335.
- (13) Dai, M.; Sarlah, D.; Yu, M.; Danishefsky, S. J.; Jones, G. O.; Houk, K. N. *J. Am. Chem. Soc.* **2007**, 129, 645.

- (14) Hammond, G. S. *J. Am. Chem. Soc.* **1955**, 77, 334. (15) Ess, D. H.; Houk, K. N. *J. Am. Chem. Soc.* **2007**, 129, 10646.
- (16) Ess, D. H.; Houk, K. N. *J. Am. Chem. Soc.* **2008**, 130, 10187.
- (17) van Zeist, W.-J.; Bickelhaupt, F. M. *Org. Biomol. Chem.* **2010**, 8, 3118.
- (18) Bickelhaupt, F. M. *J. Comput. Chem.* **1999**, 20, 114.
- (19) Fell, J. S.; Martin, B. N.; Houk, K. N. *J. Org. Chem.* **2017**, 82, 1912.

Chapter 3

New Class of Anion-Accelerated Amino-Cope Rearrangements as Gateway to Diverse Chiral Structures

Chogii, I.; Das, P.; Fell, J. S.; Scott, K. A.; Crawford, M. N.; Houk, K. N.; Njardarson, J. T. *J Am. Chem. Soc.* **2017**, *139*, 13141.

Abstract

We report useful new lithium-assisted asymmetric anion-accelerated amino-Cope rearrangement cascades. A strategic nitrogen atom chiral auxiliary serves three critical roles, by 1) enabling in situ assembly of the chiral 3-amino-1,5-diene precursor, 2) facilitating the rearrangement via a lithium enolate chelate, and 3) imparting its influence on consecutive inter- or intramolecular C-C or C-X bond-forming events via resulting chiral enamide intermediates or imine products. The mechanism of the amino Cope rearrangement was explored with density functional theory. A stepwise dissociation-recombination mechanism was found to be favored. The stereochemistry of the chiral auxiliary determines the stereochemistry of the Cope product by influencing the orientation of the lithium dienolate and sulfinyl imine fragments in the recombination step. These robust asymmetric anion-accelerated amino-Cope enabled cascades open the door for rapid and predictable assembly of complex chiral acyclic and cyclic nitrogen-containing motifs in one-pot.

Introduction

The oxy-Cope rearrangement¹ is an important transformation in organic chemistry whose applications and impact grew rapidly following the disclosure of an anion-accelerated variant by the David Evans group² in 1975.³ The corresponding 3-amino-Cope rearrangement has not received much attention in the last forty years⁴ despite the obvious opportunities for designing asymmetric variants and attractive bond-forming potential of the resulting enamine products (Figure 3.1).

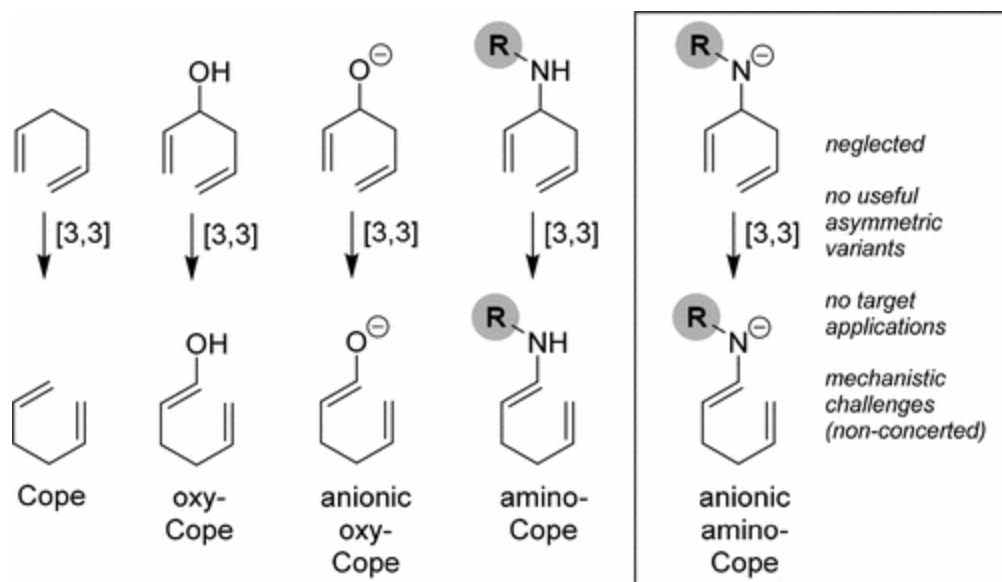
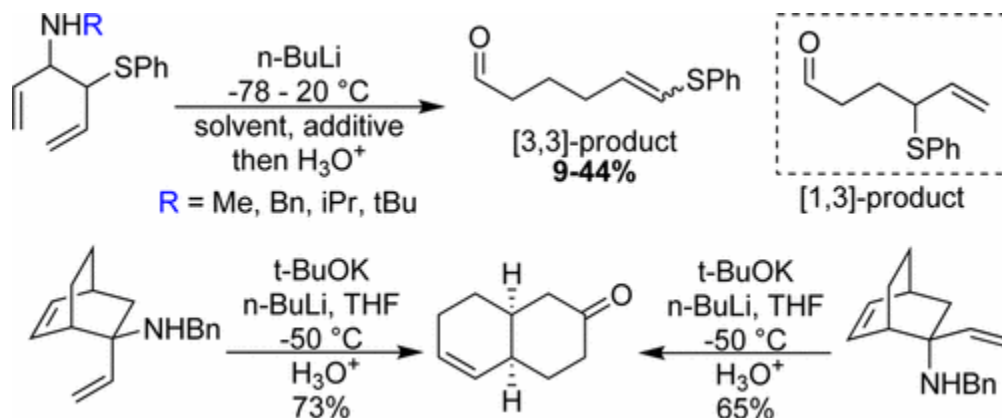


Figure 3.1. Anion-Accelerated Amino-Cope Rearrangement: A Neglected Class of Sigmatropic Rearrangements.

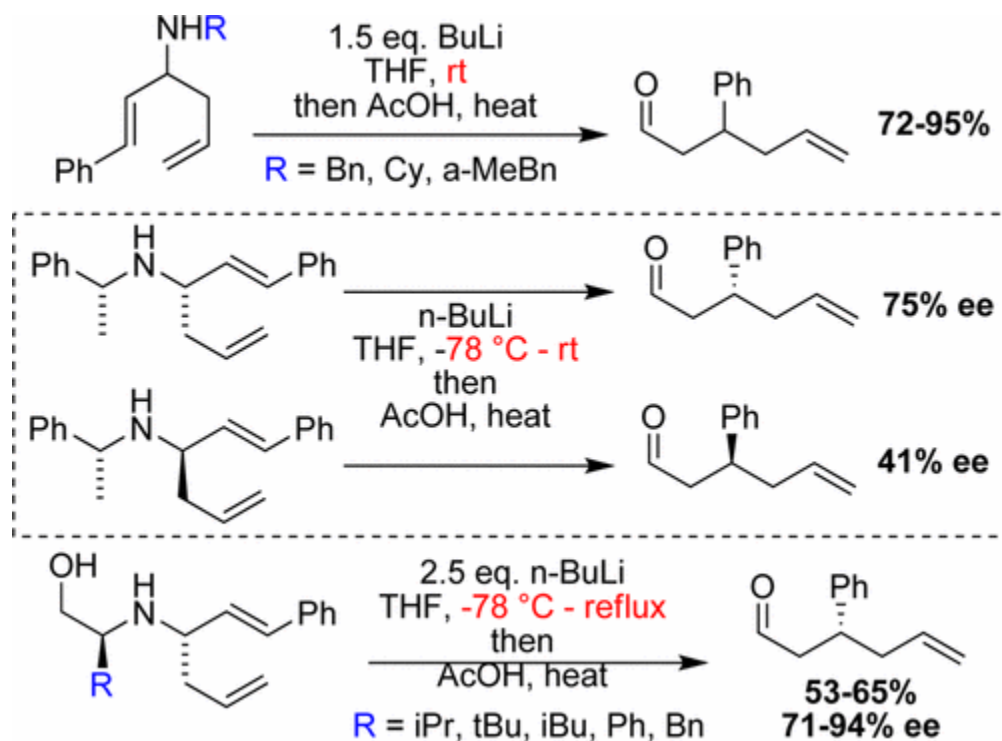
Three research groups have briefly investigated the anion-accelerated amino-Cope reaction, but as of yet these contributions have not captured the attention of the broader synthetic chemistry community. Insights from these early contributions help paint a picture of why adaptation of Evans' observations in regard to the 3-amino variant is not as straight forward as one might gather. The first report from a team of Merck-Frosst scientists demonstrated, for a specific series of N-alkyl-substituted substrates,⁵ the feasibility of this reaction and that it proceeded at far lower temperatures than the anionic-oxy Cope rearrangement. These low-yielding reactions (9-44%) were mainly plagued by a competing [1,3]-rearrangement, which strongly suggested a nonconcerted pathway (Scheme 3.1). Inspired by this study, Meyers and Houk evaluated the anionic rearrangement behavior of several 3-amino-Cope substrates.⁶ These substrates failed to rearrange; instead, they either did not react, decomposed, or deallylated. A rigorous computational investigation concluded that the anionic 3-amino-Cope rearrangement proceeds via a stepwise mechanism wherein the 3-amino-1,5-diene dissociates and then recombines.

Scheme 3.1. First Anion-Accelerated Amino-Cope Rearrangements Example (Merck-Frosst, 1993).⁵



Allin reported that a chiral auxiliary could be used for the anion-accelerated amino-Cope rearrangement (Scheme 3.2).⁷ Unfortunately, elevated temperatures were required and significant stereochemical erosion was observed when chiral N-benzyl substituents were employed. Optimizations revealed that amino-alcohol chiral auxiliaries could somewhat improve this erosion challenge, but this was accomplished at a cost of using excess n-butyl lithium and much higher (reflux) temperatures. Reaction outcomes varied greatly when substrate substituents were altered.⁸ Allin also concluded that the rearrangement proceeded through a nonconcerted pathway. Neither the Merck-Frosst group nor Allin attempted to harness the reactivity of the resulting enamide intermediate or imine product.

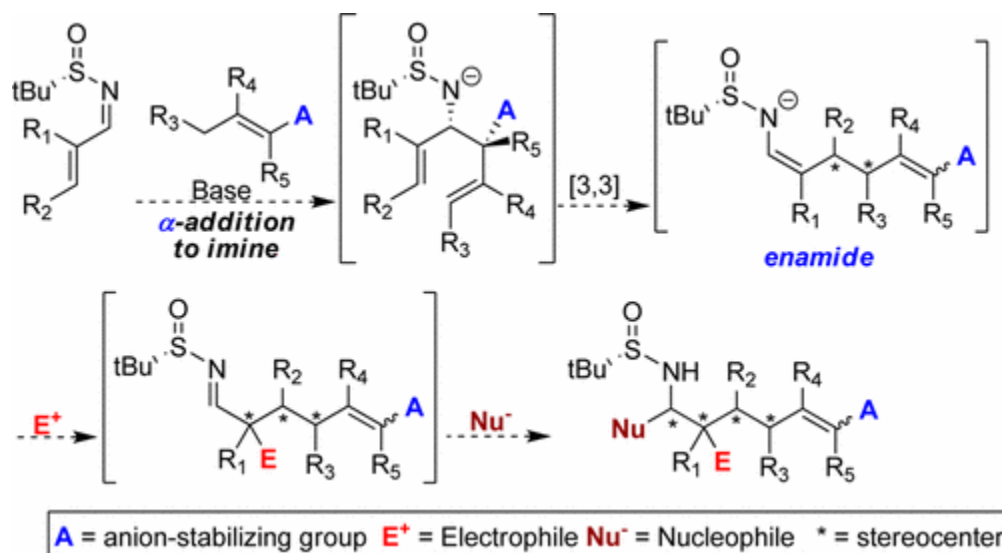
Scheme 3.2. Only Reported Asymmetric Anion-Accelerated Amino-Cope Rearrangement Studies (Professor Allin).⁷



It is evident that the anion-accelerated amino-Cope rearrangement can be realized, but multiple significant obstacles need to be addressed for it to be a useful synthetic tool. Perhaps the most challenging of these obstacles is highlighted by experimental and computational data that strongly suggest a nonconcerted mechanism, wherein the amino-diene undergoes a heterolytic cleavage followed by reunification in one of two ways (net [3,3]- or [1,3]-rearrangement) or fully dissociating. Arguably, the most impactful substituent for this reaction is the nitrogen atom substituent. To date, only a handful of alkyl substituents have been evaluated, none of which have proven to be a good match. We propose that judicious choice of the appropriate chiral *N*-substituent could not only address the aforementioned rearrangement challenges but also enable assembly of the chiral 1,5-amino-diene Cope precursor in situ. Inspired by the success of our recent one-pot asymmetric synthesis of 3-pyrrolines,⁹ we postulated that a chiral sulfinamide¹⁰ group might

represent a suitable nitrogen atom substituent. The auxiliaries used to form such imines are stable, inexpensive,¹¹ and readily available in both enantiomeric forms. We envisioned that anion-stabilized nucleophiles could selectively add to the chiral imine and that the resulting α -adduct would then undergo an anion-accelerated 3-amino-Cope rearrangement (Scheme 3.3). The resulting chiral enamide could then be trapped in the same pot by an electrophile in an inter- or intramolecular fashion. The chiral auxiliary could at this point be used to control a fourth consecutive step by treatment of the chiral imine with a nucleophile. In this proposed anionic cascade, the chiral auxiliary strategically directs all four steps (α -addition, rearrangement, enamide trapping, and imine addition) enabling access to a diverse array of complex chiral cyclic and acyclic products with multiple useful functional group handles.

Scheme 3.3. Anion-Accelerated Amino-Cope Rearrangement Cascade.



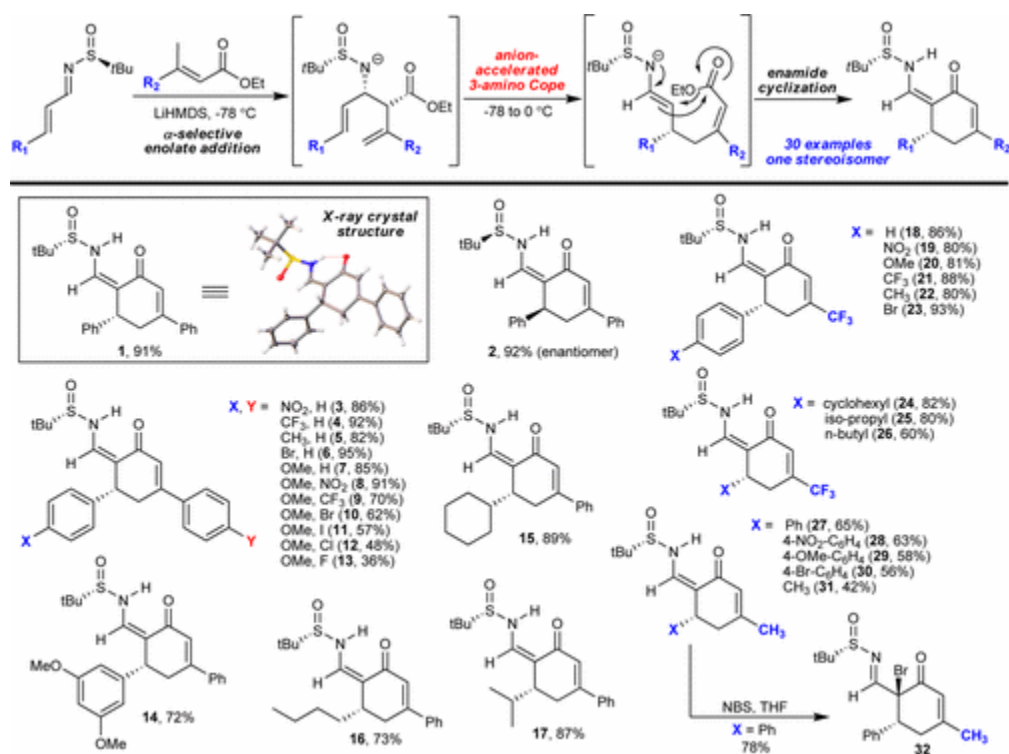
Results and Discussion

We have put the anion-accelerated amino-Cope rearrangement hypothesis to the test and are pleased to report that it has exceeded our most optimistic expectations (Scheme 3.4). When

conjugated chiral imines are treated with lithium bis-(trimethylsilyl)amide (LiHMDS) in the presence of ethyl β -methyl cinnamate, at low temperature, selective enolate α -addition takes place immediately followed by the proposed anion-accelerated amino-Cope rearrangement upon slight warming of the reaction mixture. Unexpectedly, the anionic cascade proceeded to cleanly undergo an intramolecular 6-*exo-trig* cyclization wherein the chiral enamide attacked a *Z*-enoate to form the six-membered ring products shown (Scheme 3.4) in excellent yields as single stereoisomers. Both aryl and alkyl imine substituents are tolerated. The nitrogen atom chiral auxiliary suppressed the previously deleterious competing [1,3]-rearrangement pathway, and regardless of the exact nature of the mechanism, the rearrangement proceeded without stereo-chemical erosion.¹² This new anion-accelerated amino-Cope rearrangement cascade affords complex chiral cyclohexanone products in high yields as single stereoisomers.¹³ An X-ray crystal structure of one of the cyclization products (**1**) unambiguously established the overall structure and the absolute configuration of the newly formed stereocenter. An attractive practical application of this anion-accelerated amino-Cope rearrangement is its ability to provide ready access to either enantiomeric series (**1** and **2**). These examples represent the first useful asymmetric anion-accelerated amino-Cope rearrangement reaction. This new anionic reaction cascade is not limited to cinnamate nucleophiles (**1-17**). For example, ethyl 3,3-dimethyl acrylate and its trifluoromethyl derivative are also well-matched. The fluorinated nucleophile performs particularly well, affording chiral cyclohexenone products (**18-26**) decorated with a trifluoromethyl group in 60-82% yields. The success of this particular nucleophile is noteworthy given the importance of trifluoromethyl groups in drug discovery as evident from our recent pharmaceutical structure analysis.¹⁴ Ethyl 3,3-dimethyl acrylate (**27-31**) also performs well, affording the chiral products in good to very good yields. When comparing the reactivity of the nucleophiles, we observe that the trifluoromethyl-

substituted nucleophile ($R_2 = CF_3$) affords the rearrangement products more rapidly, at lower temperature, and in uniformly high yields. Aryl-substituted nucleophiles perform well with the methyl-substituted nucleophile being the slowest. The product enamide moiety has the potential to react in a variety of useful ways. For example, treatment with *N*-bromo succinimide (NBS) stereo-selectively incorporates a bromine atom (**32**) in 78% yield.

Scheme 3.4. One-Pot Anion-Accelerated Amino-Cope Rearrangement Cascade.

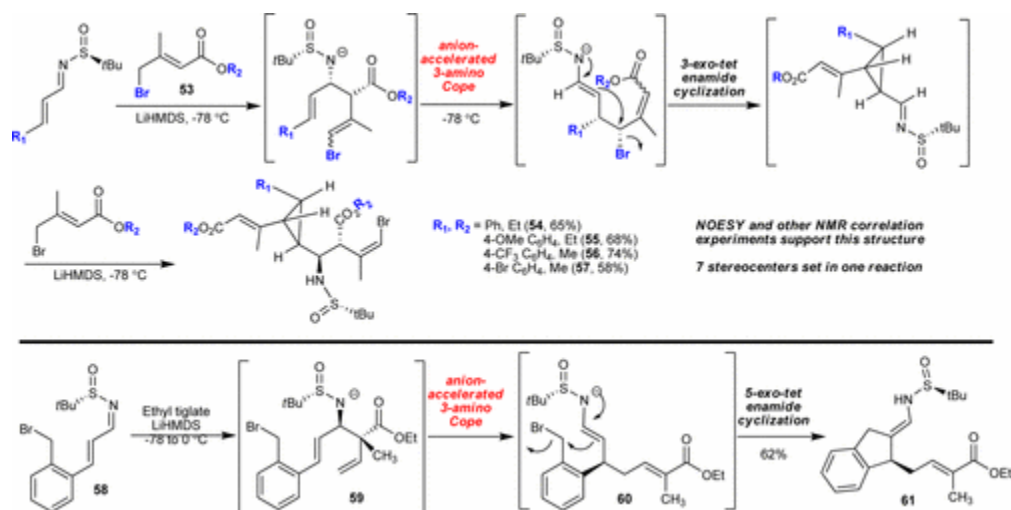


We postulated that if the acrylate nucleophile was substituted with an α -substituent the enamide cyclization scenarios observed for the β -substituted nucleophile (Scheme 3.4) could be suppressed, thus opening the door for diverting the rearrangement toward formation of chiral acyclic products. Toward that end, when ethyl tiglate (**34**, Scheme 3.5) is employed as nucleophile, the anion-accelerated amino-Cope rearrangement proceeds at $-78\text{ }^\circ\text{C}$ to afford a product (**37**) wherein the resulting enoate is of the *E*- instead of *Z*-configuration, which shuts down cyclohexenone

formation and affords an acyclic product instead. This promising reaction outcome creates opportunities for designing synthetic routes toward an incredible diversity of chiral acyclic products. Remarkably, we can isolate the intermediate enamine (**37**), which then readily converts to an imine (**38**). This has allowed us to confirm that both intermediate double bonds (enamine and enoate) are of *E*-configuration. The intermediate chiral enamide anion (**36**) can be trapped in situ with electrophiles. For example, exposure to allyl bromide results in exclusive N-allylation (**40**), while addition of an electrophilic bromide traps at carbon (**39**). Bromination affords exclusively an α,α -dibromo product. We have demonstrated this one-pot anionic cascade for nine *E*-conjugate imines (**38** and **41-48**), all of which afford chiral acyclic products¹⁵ as single stereoisomers in generally excellent yields. When a *Z*-conjugated imine (**49**) is employed, a single stereoisomer of a product (**50**) with opposite configuration at the newly created stereocenter (*R*) is obtained.¹⁶ In our original hypothesis (Scheme 3.3), we postulated that the anionic cascade could be pushed even further by adding a second nucleophile to the imine resulting from trapping of the intermediate enamide. This second in situ nucleophilic addition step would add another stereocenter, thus significantly increasing the complexity of the products. We have realized this reaction outcome as part of our efforts to unambiguously confirm the stereochemistry of the products presented in Scheme 3.5. Indium-mediated allylation of imine **42**¹⁷ and reduction of the resulting ester provided separable diastereomers of the amino alcohols (dr 3:1). Diene ring-closing metathesis reaction using second-generation Hoveyda-Grubbs (HG-II)¹⁸ catalyst afforded cycloheptenes **51** and **52**. Crystals of sufficient quality (**52**) enabled X-ray analysis, which surprisingly revealed that the absolute configuration of the newly formed stereocenter was opposite to that observed for β -substituted nucleophiles (Scheme 3.4).¹⁹ The most plausible

the products shown as single isomer (**54-57**).²¹ Incredibly, seven stereocenters were established in this one-pot amino-Cope-enabled anionic cascade. Finally, to further highlight the wide range of cyclization pathways the intermediate chiral enamide offers, we designed a substrate (**58**) with a strategic leaving group being part of the imine instead of the nucleophile. Treatment of this substrate with ethyl tiglate proceeded as expected with the anionic cascade being initiated with selective α -addition (**59**) followed by anion-accelerated amino-Cope rearrangement (**60**). We were excited to see that the enamide rearrangement product did indeed engage the benzylic bromide in a 5-*exo-tet* cyclization as proposed to afford a chiral indane product (**61**) in very good yield.

Scheme 3.6. Alternative Enamide Cyclizations (3- and 5-*exo-tet*).



Density functional theory (DFT) with the M06-2X functional and 6-311+G(d,p) basis set was employed to elucidate the mechanism of the amino-Cope rearrangement (Figure 3.2). The model includes a lithium counterion and two explicit THF solvent molecules as well as a polarizable continuum model for THF solvent.

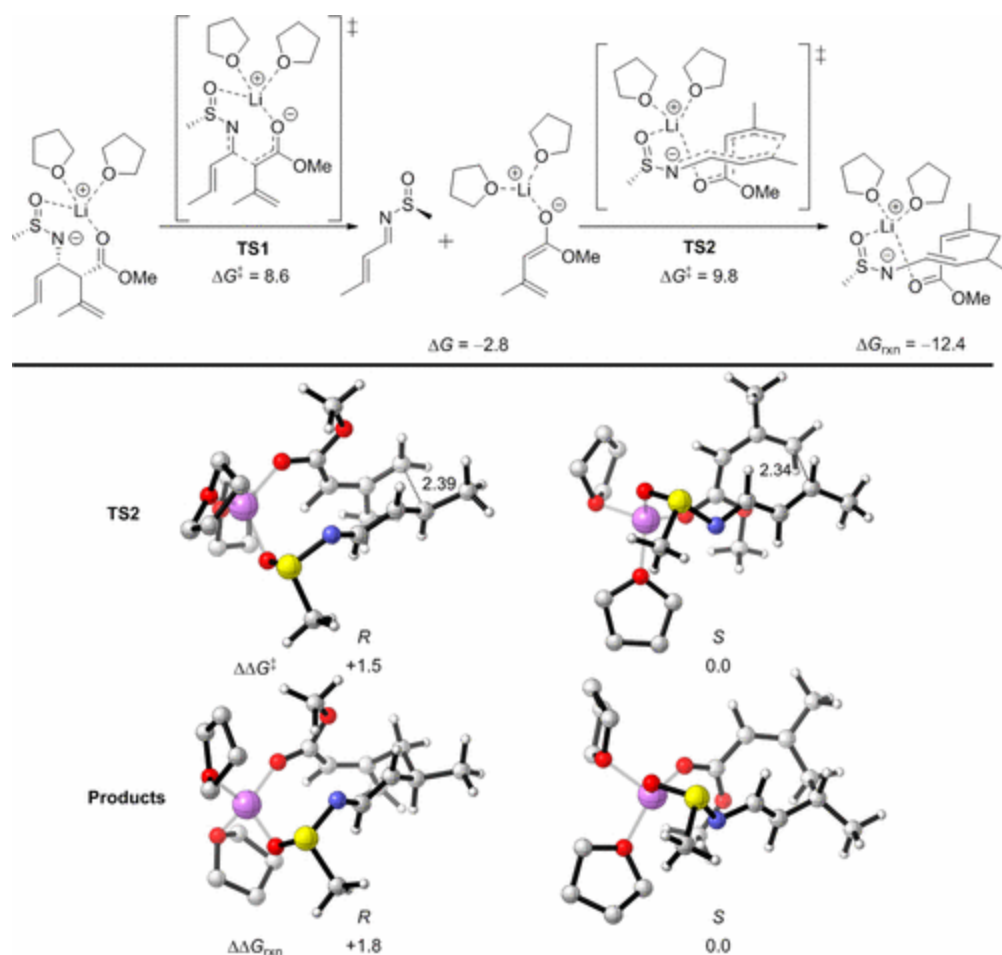


Figure 3.2. DFT-calculated mechanism of the anion-accelerated amino-Cope rearrangement. The structures of the recombination TS and the *R* and *S* products as shown. Distances and energies are given in units of Ångstroms and kcal mol⁻¹, respectively. Hydrogens on the THF solvent molecules were omitted for clarity.

The favored mechanism was found to be a stepwise dissociative mechanism. The first step (TS1) in the rearrangement mechanism is the cleavage of the C3-C4 to form a lithium dienolate and sulfinyl imine. The sulfinyl imine can be formed as the *E*- (shown in Figure 3.2) or *Z*-imine; the *E*-imine is more stable by 5.0 kcal mol⁻¹. These fragments recombine in a chair transition state (TS2) to form the new carbon-carbon bond, which we calculate to have a slightly higher energy than TS1 by 1.2 kcal mol⁻¹. Additionally, there is a 1.5 kcal mol⁻¹ preference for the transition

structure that forms the observed *S*-product. The reaction is calculated to be exergonic for the formation of both product isomers, with a 1.8 kcal mol⁻¹ (nearly 16:1 *S/R* product ratio) preference for the observed *S*-product. The origin of this preference arises from the conformation of the sulfinamide required to coordinate to the lithium counterion. In the *R* transition state, the sulfur and nitrogen atom lone pairs are *syn* to one another while in the *S* transition state they are *anti* to one another. The lone pair repulsion in the *R* transition state and product is also found in the corresponding conformers of the isolated imine (2.5 kcal mol⁻¹). A smaller lone pair repulsion on conformations has been observed in iminyl anions²³ and is well-known for peroxides and hydroxyl-amines. Our model shows that there is a kinetic and thermodynamic preference for the formation of the observed *S*-product due to the stereochemistry of the sulfinamide and the coordination geometry of the transition state (**TS2**).

Conclusions

In summary, we have developed useful new asymmetric anion-accelerated amino-Cope rearrangement reactions. A chiral sulfinamide nitrogen atom substituent ensures that the rearrangement is stereoselective and high yielding. This same chiral auxiliary enables assembly of the amino-Cope substrate *in situ* and imparts its influence on both the enamide rearrangement product and the resulting chiral imine. We have demonstrated that this amino-Cope enabled anionic cascade can be controlled to afford either chiral cyclic or acyclic products by use of appropriate nucleophiles and electrophiles. The possibilities for programming this fertile new anionic cascade for synthetic target purposes seem plentiful. Our efforts are currently focused on further deciphering the stepwise dissociation-recombination reaction mechanism as well as investigating and applying this new asymmetric anion-accelerated amino-Cope rearrangement cascade.

Acknowledgements

We thank the National Science Foundation (CHE-1266365 to J.T.N. and CHE-1361104 to K.N.H.) for financial support of this research. We are grateful for the computational resources provided by UCLA Institute for Digital Research and Education and the National Science Foundation through XSEDE Science Gateways Program (TG-CHE040013N).

References

- (1) (a) Berson, J. A.; Jones, M. J. *J. Am. Chem. Soc.* **1964**, *86*, 5019. (b) Wilson, S. R. *Org. React.* **1993**, *43*, 93.
- (2) (a) Evans, D. A.; Golob, A. M. *J. Am. Chem. Soc.* **1975**, *97*, 4765. (b) Evans, D. A.; Baillargeon, D. J.; Nelson, J. V. *J. Am. Chem. Soc.* **1978**, *100*, 2242. (c) Steigerwald, M. L.; Goddard, W. A., III; Evans, D.A. *J. Am. Chem. Soc.* **1979**, *101*, 1994.
- (3) (a) Paquette, L. A. *Tetrahedron* **1997**, *53*, 13971. (b) Paquette, L.A. *Angew. Chem., Int. Ed. Engl.* **1990**, *29*, 609. (c) Haffner, F.; Houk, K.N.; Reddy, Y. R.; Paquette, L. A. *J. Am. Chem. Soc.* **1999**, *121*, 11880.
- (4) (a) Stogryn, E. L.; Brois, S. J. *J. Org. Chem.* **1965**, *30*, 88. (b) Wender, P. A.; Schaus, J. M.; Torney, D. C. *Tetrahedron Lett.* **1979**, *20*, 2485. (c) Jemison, R. W.; Ollis, D. W.; Sutherland, I. O.; Tannock, J. *J. Chem. Soc., Perkin Trans. 1* **1980**, *7*, 1462. (d) Dollinger, M.; Henning, W.; Kirmse, W. *Chem. Ber.* **1982**, *115*, 2309.
- (5) (a) Sprules, T. J.; Galpin, J. D.; Macdonald, D. *Tetrahedron Lett.* **1993**, *34*, 247. (b) Dobson, H. K.; LeBlanc, R.; Perrier, H.; Stephenson, C.; Welch, T. R.; Macdonald, D. *Tetrahedron Lett.* **1999**, *40*, 3119. (6) (a) Yoo, H. Y.; Houk, K. N.; Lee, J. K.; Scialdone, M. A.; Meyers, A. I. *J. Am. Chem. Soc.* **1998**, *120*, 205. (b) Haeffner, F.; Houk, K. N.; Schulze, S. M.; Lee, J. K. *J. Org. Chem.* **2003**, *68*, 2310.
- (7) (a) Allin, S. M.; Button, M. A. C. *Tetrahedron Lett.* **1998**, *39*, 3345. (b) Allin, S. M.; Button, M. A. C.; Baird, R. D. Synlett 1998, 1117. (c) Allin, S. M.; Button, M. A. C. *Tetrahedron Lett.* 1999, 40, 3801. (d) Allin, S. M.; Baird, R. D.; Lins, R. J. *Tetrahedron Lett.* **2002**, *43*, 4195. (e) Allin, S. M.; Essat, M.; Horro-Pita, C. H.; Baird, R.D.; McKee, V.; Elsegood, M.; Edgar, M.; Andrews, D. M.; Shah, P.; Aspinall, I. *Org. Biomol. Chem.* **2005**, *3*, 809.
- (8) Allin, S. M.; Horro-Pita, C.; Essat, M.; Aspinall, I.; Shah, P. *Synth. Commun.* **2010**, *40*, 2696.
- (9) Chogii, I.; Njardarson, J. T. *Angew. Chem., Int. Ed.* **2015**, *54*, 13706.
- (10) Robak, M. T.; Herbage, M. A.; Ellman, J. A. *Chem. Rev.* **2010**, *110*, 3600.
- (11) Su, X.; Zhou, W.; Li, Y.; Zhang, J. *Angew. Chem., Int. Ed.* **2015**, *54*, 6874.
- (12) The initial α -enolate imine adducts can be isolated at low temperature and resubjected to alternative bases. Our preliminary investigations have revealed that Na and Li counterions (generated from treating the amino alcohol adduct with LiHMDS, NaH, BuLi, or NaHMDS) are critical for the success of the rearrangement while K is detrimental. This suggests that the Na and Li counterions are playing a key role, most likely by suppressing the dissociations that plagued earlier investigations.

- (13) Interestingly, when the imine is unsubstituted, two products are obtained in a 2:1 ratio in 86% yield. The minor product is the [3,3]-rearrangement product and major is the [1,3]-rearrangement product (2:1 dr).
- (14) Ilardi, E. A.; Vitaku, E.; Njardarson, J. T. *J. Med. Chem.* **2014**, *57*, 2832.
- (15) Protonation of the intermediate enamine results in *E/Z*-imine product mixtures, which result in a single compound when reduced with NaBH₄.
- (16) To further confirm this result, we have separately reduced the imines of **42** and **50** and then oxidized the chiral auxiliary of the resulting product to its Bus-substituted amine to afford products that are enantiomeric as evident from optical rotation.
- (17) Sun, X.-W.; Liu, M.; Xu, M.-H.; Lin, G.-Q. *Org. Lett.* **2008**, *10*, 1259.
- (18) (a) Hong, S. H.; Sanders, D. P.; Lee, C. W.; Grubbs, R. H. *J. Am. Chem. Soc.* **2005**, *127*, 17160. (b) Cho, J. H.; Kim, B. M. *Org. Lett.* **2003**, *5*, 531.
- (19) This stereochemical assignment has been further validated by subjecting a common chiral imine separately to the ethyl esters of β -methyl and α -methyl crotonate and then chemically converting the resulting amino-Cope rearrangement products to a common chiral structure. Chemical characterization revealed that these products were identical in all respects (NMR, IR, mass-spec) but had opposite optical rotation values.
- (20) The main competing pathway for this new class of anionic cascades is a retro-Mannich reaction (Davis, F. A.; Zhang, Y.; Qiu, H. *Org. Lett.* **2007**, *9*, 833). It is plausible that the α -substituted nucleophiles add from the same face as the nucleophiles in Scheme 4 but then fail to undergo the rearrangement and instead undergo a retro-Mannich reaction before then adding from the opposite face and rearranging.
- (21) Maintaining the reaction temperature at -78°C is critical for success.
- (22) Essafi, S.; Tomasi, S.; Aggarwal, V. K.; Harvey, J. N. *J. Org. Chem.* **2014**, *79*, 12148.
- (23) Zhang, H.; Wu, W.; Ahmed, B. M.; Mezei, G.; Mo, Y. *Chem. -Eur. J.* **2016**, *22*, 7415.

Chapter 4

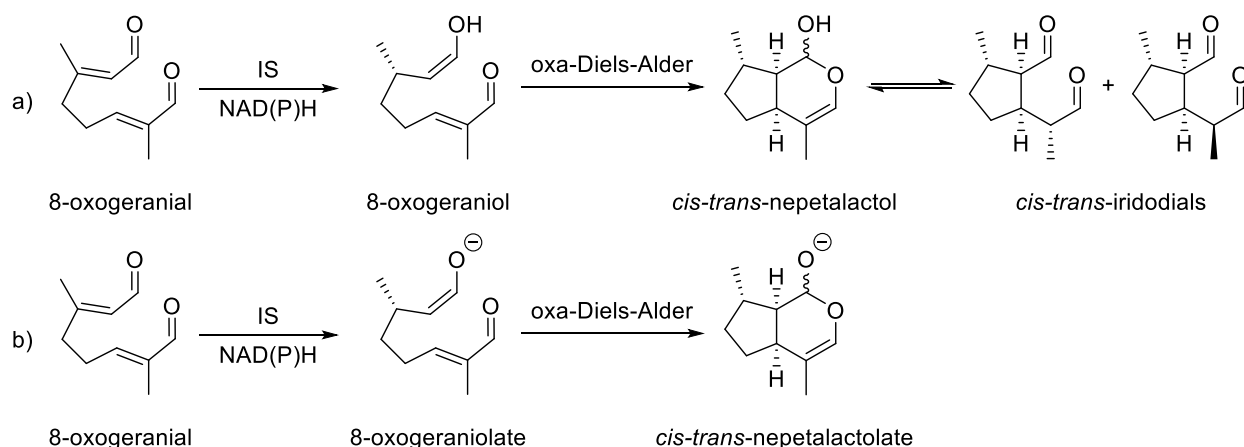
Computational Evaluation of the Mechanism of the Intramolecular Cyclization of 8-Oxogeranial

Fell, J. S.

The Diels-Alder (DA) reaction has enormous utility in synthetic organic chemistry.¹ First reported in 1928, the DA reaction results in the formation of an unsaturated six-membered ring and establishes up to four stereocenters. Consequently, many chemical methods for catalyzing the DA reaction have been developed, yet there are few examples of the DA reaction being involved in biosynthesis.^{2,3} Enzymes capable of catalyzing complex products via the DA reaction are called Diels-Alderase.⁴ While some headway has been made towards identifying and understanding Diels-Alderase, an understanding of the scope of enzymatic reactions of this type remains elusive.⁵ Liu *et al.* discovered the first Diels-Alderase directly responsible for the catalysis of a DA reaction in nature.⁶ We hope to identify new modes of catalysis for DA cycloadditions that inspire new catalysts by studying Diels-Alderase.

O'Connor *et al.* proposed that the enzyme iridoid synthase (IS) catalyzes the 1,4-reduction of 8-oxogeranial to 8-oxogeraniol in the presence of NAD(P)H.⁷ A subsequent cyclization reaction occurs that produces cis-trans-nepetalactol, a bicyclic intermediate which interconverts to cis-trans-iridoidals (Scheme 4.1a). The cyclization reaction likely occurs stereoselectively to form the cis-fused bicyclic intermediate, and may occur through a concerted (inverse electron demand oxa-DA) or stepwise pathway proceeding through a zwitterionic intermediate. No evidence classifying iridoid synthase as a hetero-Diels-Alderase is presently available, and there is little information available about hetero-Diels-Alderase.^{8,9}

Scheme 4.1. The reduction of 8-oxogeranial to either an enol (a) or enolate (b) that undergoes a cyclization to produce the bicyclic intermediate.



Further studies of IS by the O'Connor, Guo and Oldfield groups have produced crystal structures of the enzyme.^{10,11} These crystallization studies suggested that the reactive intermediate in the cyclization reaction is an enolate (8-oxogeraniolate, Scheme 4.1b). The enolate species would be stabilized by a hydrogen bond from a neighboring tyrosine residue in the IS active site. The enolate would be more reactive in cycloaddition reactions than the neutral enol.¹² Motivated by our interest in DA reactions in biology⁶ we have undertaken a computational study of the cyclization mechanism of 8-oxogeraniolate.

Quantum mechanical calculations were performed using Gaussian 09 Revision D.01.¹³ Stationary points were located using the M06-2X¹⁴ functional with the 6-311++G(d,p) basis set. Frequency calculations revealed a single negative frequency for transition states and no negative frequencies for minima. Water was used as a solvent to stabilize charges and to mimic biological conditions. Solvation was considered by using the integral equation formalism polarizable continuum model¹⁵ for both geometry and frequency calculations. Unscaled frequencies were then used to calculate zero-point energy and thermal corrections assuming a standard state of 1 atm and

298.15 K. All quantum mechanical calculations were performed using tight convergence criteria, and an “ultrafine” numerical integration grid, consisting of 99 radial shells and 590 angular points per shell. Truhlar’s quasiharmonic correction was applied to mitigate error in estimation of entropies arising from the treatment of low vibrational modes as harmonic oscillations by setting all frequencies less than 100 cm^{-1} to 100 cm^{-1} .^{16,17} Conformational searches were performed using the MMFF force field in Maestro 11.0.¹⁸ We utilized the Monte Carlo multiple minimum method with Oren-Spedicato variable metric minimization for optimized conformational sampling. Molecular structure images were produced with the CYLview program.¹⁹

The [4 + 2] cyclization of 8-oxogeraniolate involves the formation of a carbon-oxygen bond. This classifies the reaction as an oxa-DA reaction. The enolate acts as a dienophile and can assume the E and Z orientations which are nearly isoenergetic. Figure 4.1 shows the first transition structures for the eight possible stereoisomers. The nomenclature for each stereoisomer (**TS1-[(1)-(2)-(3)]**) is assigned by: **(1)** the relative orientation of the bicyclic ring fusion (*cis* or *trans*), **(2)** relative orientation of the five-membered ring to the C3 methyl group (*cis* or *trans*) and **(3)** the orientation of the alkoxide (*endo* or *exo*). Bond formation occurs by a stepwise mechanism, with the first transition state being the rate determining step.

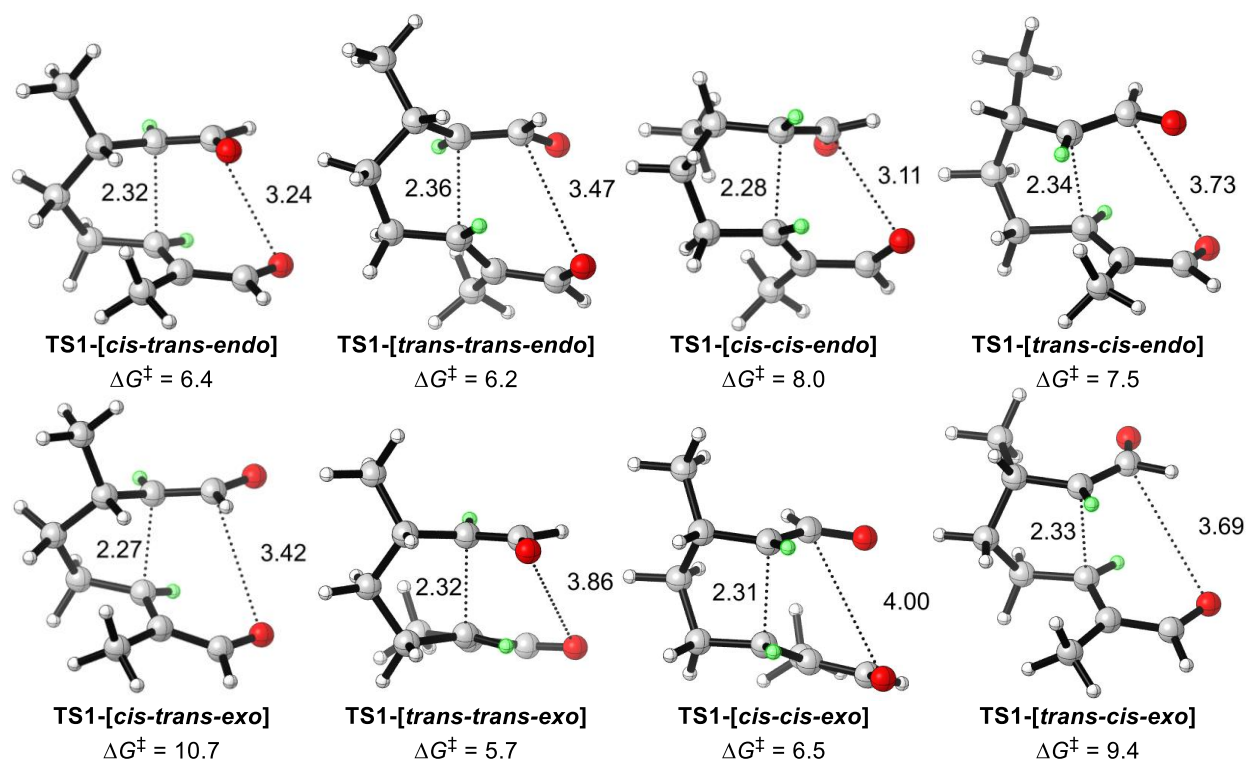


Figure 4.1. The first transition state of the stepwise oxa-DA reaction of 8-oxogeraniolate. Ring junction hydrogens are highlighted in green for clarity. Free energies and distances are reported in units of kcal mol⁻¹ and Ångstroms, respectively. Free energies are relative to 8-oxogeraniolate.

The stereochemistry of the fused rings is determined in the first transition state of the mechanism. The transition structures that form the observed product have *cis-trans* stereochemistry, the orientation of the alkoxide was not determined experimentally. The lowest energy transition structure is **TS1-[*trans-trans-exo*]**, which would lead to an unobserved *trans*-fused bicyclic intermediate. The two transition structures that would form the observed products are **TS1-[*cis-trans-endo*]** and **TS1-[*cis-trans-exo*]**, which are 0.7 and 5.0 kcal mol⁻¹ higher in energy than the lowest energy transition structure. The energy difference between the lowest energy transition structures would lead to an unobserved:observed product ratio of nearly 3:1. The background oxa-DA reaction is inherently non-stereoselective.

A low energy intermediate is formed after the first transition state, before the O₁₀–C₁ bond is formed. The subsequent intermediate, second transition state and product species that are formed for **TS1-[*cis-trans-endo*]** and **TS1-[*trans-trans-exo*]** are shown in Figure 4.2. The formation of the O₁₀–C₁ bond (TS2) is nearly barrierless relative to the energy of the intermediates. The energies of the bicyclic products that are formed are exergonic by 11.7 and 9.9 kcal mol⁻¹ for the *cis-trans-endo* and *trans-trans-exo* stereoisomers, respectively. Interestingly the free energy for the intermediate of the *trans-trans-exo* stereoisomer (**Int-[*trans-trans-exo*]**) is 2.2 kcal mol⁻¹ lower than that of the bicyclic product (**[*trans-trans-exo*]**). **Int-[*trans-trans-exo*]** will eventually become protonated and form an iridodial species that is not observed until later biosynthetic steps. For the *cis-trans-endo* isomer, the intermediate (**Int-[*cis-trans-endo*]**) is higher in energy than the bicyclic product (**[*cis-trans-endo*]**) by 1.6 kcal mol⁻¹. **[*cis-trans-endo*]** will become protonated to form *cis-trans*-nepetalactol. The two products from this reaction are predicted to be the **[*cis-trans-endo*]** bicyclic product and the **Int-[*trans-trans-exo*]** monocyclic product at a relative bicyclic:monocyclic product ratio of 1:1.8.

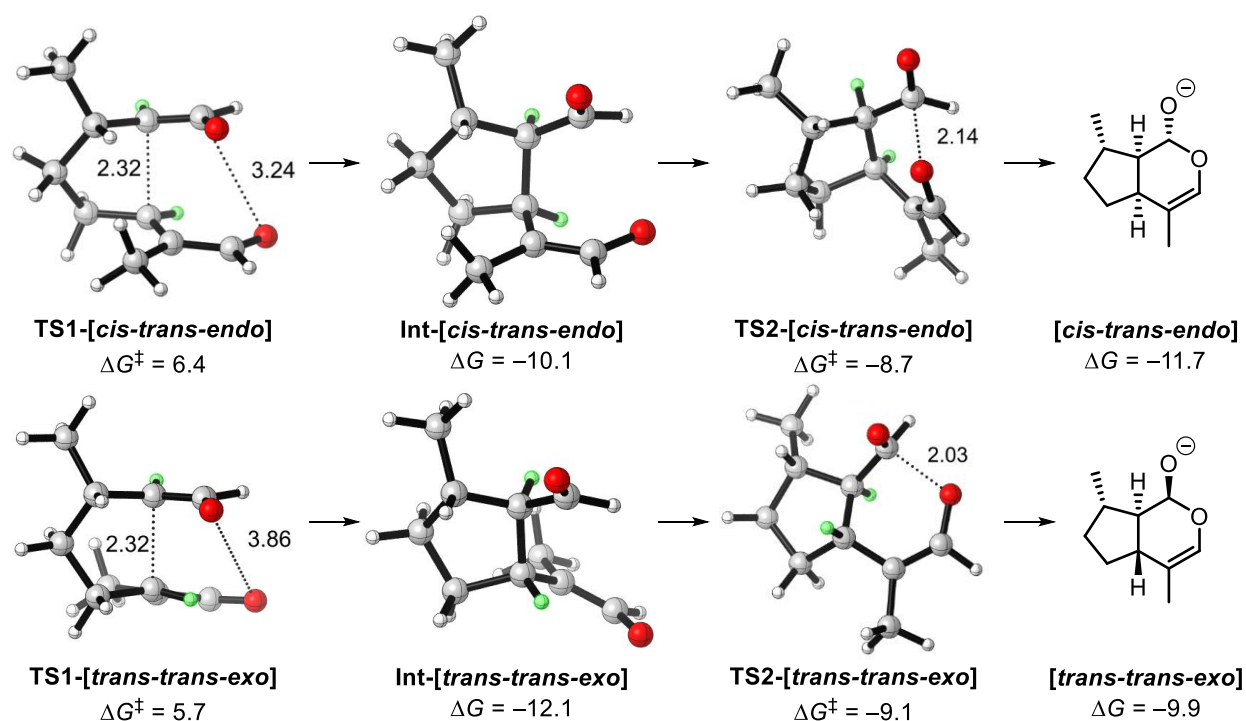


Figure 4.2. The subsequent low energy intermediates, second transition states and products that form from **TS1-[cis-trans-endo]** (top row) and **TS1-[trans-trans-exo]** (bottom row). Ring junction hydrogens are highlighted in green for clarity. Free energies and distances are reported in units of kcal mol⁻¹ and Ångstroms, respectively.

The background intramolecular reaction of 8-oxogeraniolate is a stepwise oxa-DA reaction of the enolate to the acrylaldehyde. The products of this intramolecular reaction would be monocyclic and bicyclic products that will become protonated to form *trans*-iridodials and *cis-trans*-nepetalactol.

REFERENCES

- (1) Diels, O.; Alder, K. *Justus Liebigs Ann. Chem.* **1928**, 460, 98.
- (2) Oikawa, H.; Katayama, K.; Suzuki, Y.; Ichihara, A. *J. Chem. Soc., Chem. Commun.* **1995**, 1321.
- (3) Kim, H. J.; Ruszczycky, M. W.; Choi, S.-h.; Liu, Y.-n.; Liu, H.-w. *Nature (London, U. K.)* **2011**, 473, 109.
- (4) Oikawa, H. *Bull. Chem. Soc. Jpn.* **2005**, 78, 537.
- (5) Stocking, E. M.; Williams, R. M. *Angew. Chem., Int. Ed.* **2003**, 42, 3078.
- (6) Kim, H. J.; Ruszczycky, M. W.; Liu, H.-w. *Curr. Opin. Chem. Biol.* **2012**, 16, 124.

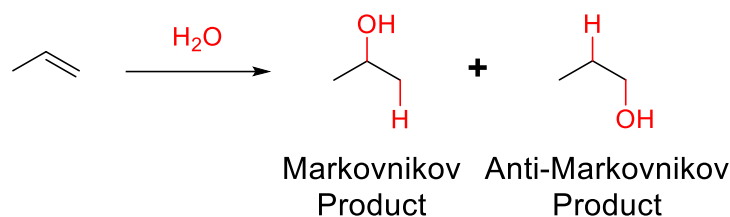
- (7) Geu-Flores, F.; Sherden, N. H.; Courdavault, V.; Burlat, V.; Glenn, W. S.; Wu, C.; Nims, E.; Cui, Y.; O'Connor, S. E. *Nature (London, U. K.)* **2012**, *492*, 138.
- (8) Gouverneur, V.; Reiter, M. *Chem. Eur. J.* **2005**, *11*, 5806.
- (9) Eschenbrenner-Lux, V.; Kumar, K.; Waldmann, H. *Angew. Chem., Int. Ed.* **2014**, *53*, 11146.
- (10) Kries, H.; Caputi, L.; Stevenson, C. E. M.; Kamileen, M. O.; Sherden, N. H.; Geu-Flores, F.; Lawson, D. M.; O'Connor, S. E. *Nat. Chem. Biol.* **2015**, *12*, 6.
- (11) Hu, Y. Liu, W.; Malwal, S.; Zheng, Y.; Feng, X.; Ko, T.; Chen, C.; Xu, Z.; Liu, M.; Han, X.; Gao, J.; Oldfield, E.; Guo, R. *Angew. Chem., Int. Ed.* **2012**, *492*, 138.
- (12) Qin, L.; Zhu, Y.; Ding, Z.; Zhang, X.; Ye, S.; Zhang, R. *J. Struct. Biol.* **2016**, *194*, 224.
- (13) Frisch, M. J.; Trucks, G. W.; Schlegel, H. B.; Scuseria, G. E.; Robb, M. A.; Cheeseman, J. R.; Scalmani, G.; Barone, V.; Mennucci, B.; Petersson, G. A.; Nakatsuji, H.; Caricato, M.; Li, X.; Hratchian, H. P.; Izmaylov, A. F.; Bloino, J.; Zheng, G.; Sonnenberg, J. L.; Hada, M.; Ehara, M.; Toyota, K.; Fukuda, R.; Hasegawa, J.; Ishida, M.; Nakajima, T.; Honda, Y.; Kitao, O.; Nakai, H.; Vreven, T.; Montgomery, J. A.; Peralta, J. E.; Ogliaro, F.; Bearpark, M.; Heyd, J. J.; Brothers, E.; Kudin, K. N.; Staroverov, V. N.; Kobayashi, R.; Normand, J.; Raghavachari, K.; Rendell, A.; Burant, J. C.; Iyengar, S. S.; Tomasi, J.; Cossi, M.; Rega, N.; Millam, J. M.; Klene, M.; Knox, J. E.; Cross, J. B.; Bakken, V.; Adamo, C.; Jaramillo, J.; Gomperts, R.; Stratmann, R. E.; Yazyev, O.; Austin, A. J.; Cammi, R.; Pomelli, C.; Ochterski, J. W.; Martin, R. L.; Morokuma, K.; Zakrzewski, V. G.; Voth, G. A.; Salvador, P.; Dannenberg, J. J.; Dapprich, S.; Daniels, A. D.; Farkas; Foresman, J. B.; Ortiz, J. V.; Cioslowski, J.; Fox, D. J. Gaussian 09, Revision D.01, Gaussian Inc., Wallingford CT, **2009**.
- (14) Zhao, Y.; Truhlar, D. G. *Theor. Chem. Acc.* **2008**, *120*, 215.
- (15) Cancès, E.; Mennucci, B.; Tomasi, J. *J. Chem. Phys.* **1997**, *107*, 3032.
- (16) Zhao, Y.; Truhlar, D. G. *Phys. Chem. Chem. Phys.* **2008**, *10*, 2813.
- (17) Ribeiro, R. F.; Marenich, A. V.; Cramer, C. J.; Truhlar, D. G. *J. Phys. Chem. B* **2011**, *115*, 14556.
- (18) Maestro, Schrödinger, LLC, New York, NY, 2017.
- (19) CYLview, 1.0b; Legault, C. Y., Université de Sherbrooke, 2009 (<http://www.cylview.org>).

Chapter 5

Computational investigation of anti-Markovnikov hydration of olefins by a di-Manganese catalyst

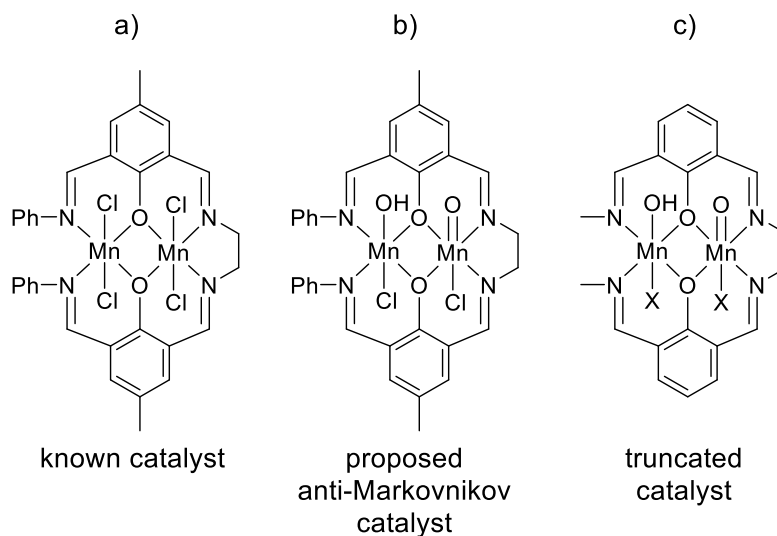
Chemical reactions that are addition across a carbon-carbon double bond occur through a mechanism that involves a carbocation intermediate. When addition occurs across an unsymmetrical double bond, the new group adds to the carbon atom with the most alkyl substituents, known as Markovnikov addition.¹ The formation of radical intermediates and the use of catalysts are required to reverse this selective addition, known as anti-Markovnikov addition.²⁻⁴ Scheme 5.1 shows the Markovnikov and anti-Markovnikov hydration of propene.

Scheme 5.1. Propene reacting with water to form the Markovnikov (2-propanol) and anti-Markovnikov (1-propanol) products.



Developments of catalysts that can perform anti-Markovnikov hydrations to alkenes can be useful in chemical synthesis. Previous di-Manganese catalysts have been successfully synthesized and characterized that can perform epoxidation reactions of stilbenes and styrenes (Scheme 5.2a).⁵ This catalyst can be altered to potentially catalyze the anti-Markovnikov hydration of olefins (Scheme 5.2b). In this study we have performed quantum mechanical calculations to determine the free energies of the anti-Markovnikov hydration of propene using a truncated version of the di-Manganese catalysts (Scheme 5.2c). The method used, B3LYP, is rather approximate for such systems, but our goal here was to screen potential catalysts to determine if barriers were low enough to make catalysis feasible, and to ensure that anti-Markovnikov hydration would be preferred. Our experimental collaborators, the Robert Grubbs group at Caltech, plan to test these predictions, and higher accuracy calculations would be performed once experimental data to compare are available.

Scheme 5.2. The previously synthesized di-Manganese catalyst (a), the proposed anti-Markovnikov catalyst (b), and the truncated catalyst used in this computational analysis (c).



Quantum mechanical calculations were performed using Gaussian 09 Revision D.01.⁶ Stationary points were located using the B3LYP⁷⁻¹⁰ functional with the 6-311G(d) basis set and the LANL2DZ pseudopotential¹¹. Energies were corrected with larger basis set single point calculations using the B3LYP function and the 6-311+G(d,p) basis set and the LANL2DZ pseudopotential. Frequency calculations revealed a single negative frequency for transition states and no negative frequencies for minima. Unscaled frequencies were then used to calculate zero point energy (ZPE) and thermal corrections assuming a standard state of 1 atm and 298.15 K. Truhlar's quasiharmonic correction was applied to mitigate error in estimation of entropies arising from the treatment of low vibrational modes as harmonic oscillations by setting all frequencies less than 100 cm⁻¹ to 100 cm⁻¹.^{12,13} Molecular structures representations were produced with the CYLview program.¹⁴

We initially calculated the enthalpies of the hydration reaction of propene and compared these enthalpies to the experimental heats of formation of 1- and 2-propanol, shown in Figure 5.1. Our

calculations underestimate the enthalpies by 3 kcal mol⁻¹, however we accurately predict the formation of 2-propanol is favored by nearly 4 kcal mol⁻¹.¹⁵⁻¹⁷

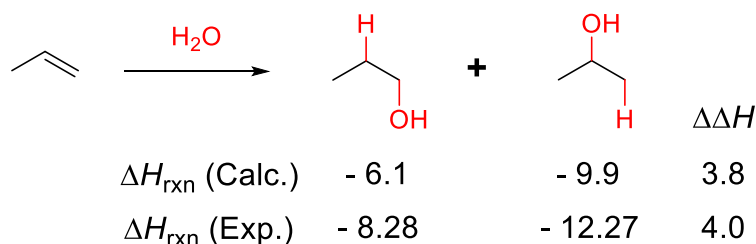
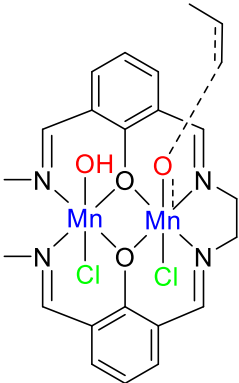
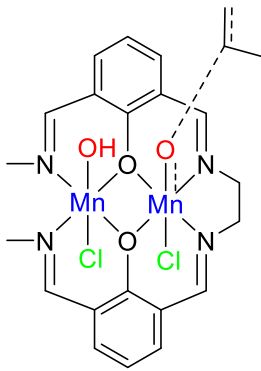


Figure 5.1. Comparison of calculated and experimental enthalpies of propene hydration.

Enthalpies are in units of kcal mol⁻¹.

With the truncated catalyst with chlorine axial ligands, the first transition structure for both Markovnikov and anti-Markovnikov addition to propene were calculated. The catalyst can be in two spin states: doublet and quartet. Each Markovnikov and anti-Markovnikov transition structure was calculated in both spin states. The free energies for these four transition structures are shown in Table 5.1. The calculated free energy differences between the two catalyst spin states is 0.2 kcal mol⁻¹ in favor of the quartet spin state, which we reason that the two spin states are respectively isoenergetic. The free energies of the doublet and quartet transition structures are respective to the doublet and quartet catalyst spin states. The catalyst in the quartet spin state is predicted to perform hydration reactions by nearly 10 kcal mol⁻¹ lower than the doublet spin state. In the quartet spin state, the rate of anti-Markovnikov hydration of propene is estimated to be 40 times greater than Markovnikov hydration.

Table 5.1. The Markovnikov and anti-Markovnikov transition structures for the doublet and quartet spin states with the truncated catalyst. Chlorine atoms are highlighted in green. Free energies are reported in units of kcal mol⁻¹.

		
	anti-Mark. TS1	Mark. TS1
Spin State:	ΔG^\ddagger	ΔG^\ddagger
Doublet	32.6	35.0
Quartet	20.7	23.0

With the catalyst in the quartet spin state, the remaining steps of the catalytic cycle of anti-Markovnikov hydration of propene were computationally investigated, which is shown in Figure 5.2 with the respective calculated free energies. The catalytic cycle begins with the catalyst (middle left) reacting with propene to produce the first low energy intermediate (**Int1**, top middle). This low energy intermediate then converts to a second low energy intermediate (**Int2**, middle right) through a hydrogen transfer from the hydroxyl ligand of the second manganese. This intermediate reacts with water to produce 1-propanol and the isocatalyst, which is overall endergonic. The isocatalyst tautomerizes back to the starting state with a very low barrier of 3.0 kcal mol⁻¹ and start the hydration cycle again.

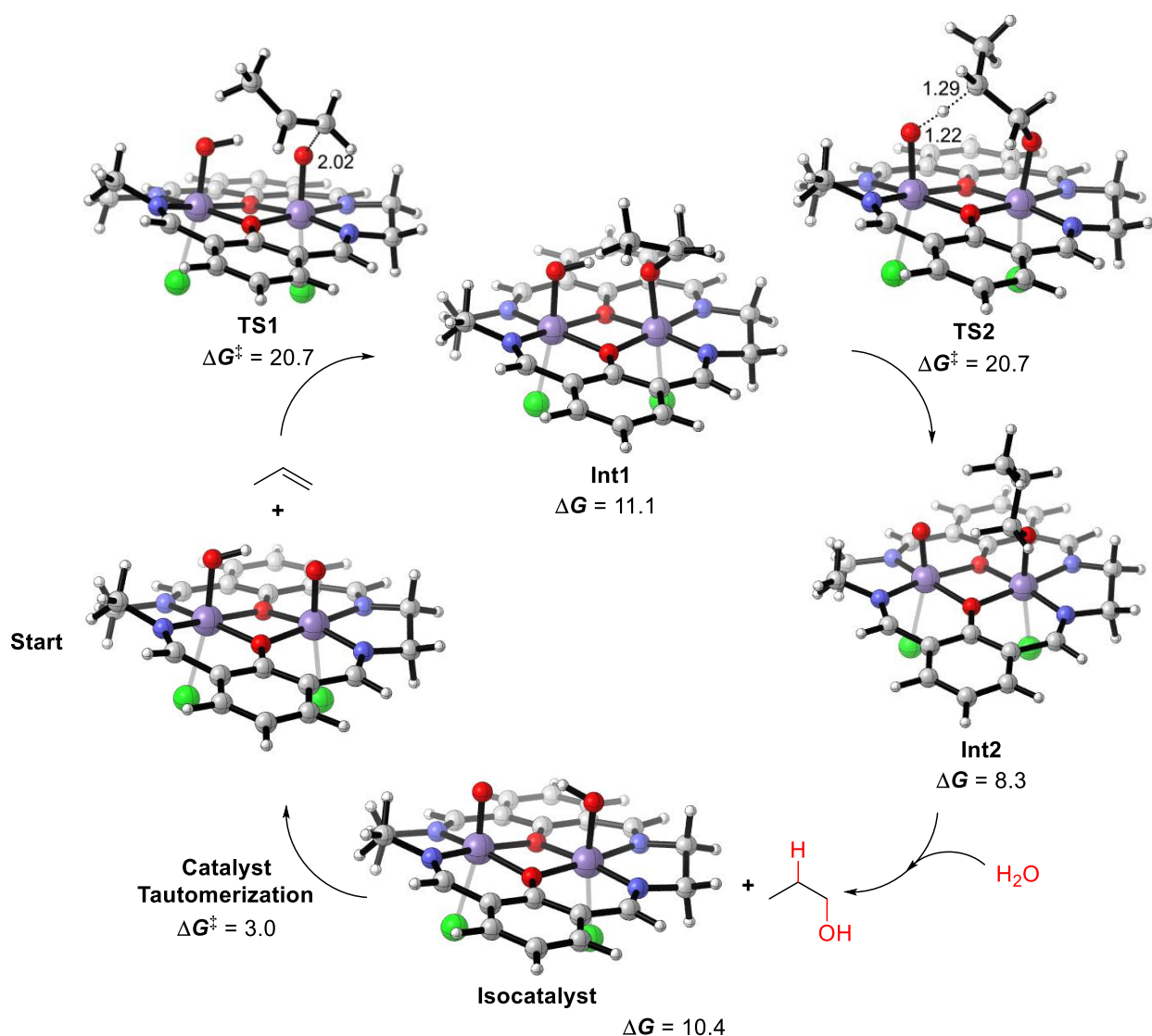


Figure 5.2. The catalytic cycle of anti-Markovnikov hydration of propene by the quartet state of the catalyst. Free energies are in units of kcal mol⁻¹.

The hydration mechanism was further investigated with axial bromine ligands and without any axial ligands, which would leave the catalyst as a cation. The latter calculation was performed to model the efficiency and regioselectivity that would be expected if ligands that coordinate more weakly than halogens were employed. The lowest anti-Markovnikov hydration free energy barriers are listed in table 5.2 with the relative free energy differences for Markovnikov hydrations. The catalyst with bromine axial ligands is calculated to perform hydrations of olefins

at nearly the same rate as the catalyst with chlorine ligands, but with a smaller ratio of anti-Markovnikov to Markovnikov products (12:1 compared to 40:1 with chlorine ligands). If the catalyst were to have no axial ligands the rate of hydration is predicted to be greatly increased with a greater ratio of anti-Markovnikov to Markovnikov products (nearly 171:1).

Table 5.2. The anti-Markovnikov hydration free energy barriers with respective free energy differences for Markovnikov hydration. Free energies are reported in units of kcal mol⁻¹.

Axial Ligand	anti-Markovnikov ΔG^\ddagger	Markovnikov $\Delta\Delta G^\ddagger$
Cl	20.7	+ 2.3
Br	20.7	+ 1.6
No Ligands	9.5	+ 3.2

Our computations predict that the proposed catalyst will perform preferential anti-Markovnikov hydration of olefins at room temperature. We predict that there would be an approximate 40:1 ratio of anti-Markovnikov/Markovnikov products with chlorine ligands, 12:1 with bromine ligands, and over 100:1 with no axial ligands. A cationic catalyst with no axial ligands is also predicted to perform hydrations at an increased rate compared to a catalyst with chlorine or bromine ligands. This suggests that a catalyst with a more poorly coordinating ligand would be the most effective catalyst.

Acknowledgements

This work was supported by the Office of Naval Research (N00014-14-1-0650). This work used computational resources for projects TG-CHE040013N and TG-CHE140139 in the Extreme Science and Engineering Discovery Environment (XSEDE), which is supported by National Science Foundation grant number ACI-1548562, and computational resources provided by the UCLA IDRE Hoffman2 cluster. All 3-dimensional images were made using CYLview.¹⁸

References

- (1) Markownikoff, W. *Justus Liebigs Annalen der Chemie* **1870**, 153, 228.
- (2) Hamilton, D. S.; Nicewicz, D. A. *J. Am. Chem. Soc.* **2012**, 134, 18577.
- (3) Labonne, A.; Kribber, T.; Hintermann, L. *Organic Letters* **2006**, 8, 5853.
- (4) Nishizawa, M.; Asai, Y.; Imagawa, H. *Organic Letters* **2006**, 8, 5793.
- (5) Das, D.; Pyeng Cheng, C. *Journal of the Chemical Society, Dalton Transactions* **2000**, 1081.
- (6) Frisch, M. J.; Trucks, G. W.; Schlegel, H. B.; Scuseria, G. E.; Robb, M. A.; Cheeseman, J. R.; Scalmani, G.; Barone, V.; Mennucci, B.; Petersson, G. A.; Nakatsuji, H.; Caricato, M.; Li, X.; Hratchian, H. P.; Izmaylov, A. F.; Bloino, J.; Zheng, G.; Sonnenberg, J. L.; Hada, M.; Ehara, M.; Toyota, K.; Fukuda, R.; Hasegawa, J.; Ishida, M.; Nakajima, T.; Honda, Y.; Kitao, O.; Nakai, H.; Vreven, T.; Montgomery, J. A.; Peralta, J. E.; Ogliaro, F.; Bearpark, M.; Heyd, J. J.; Brothers, E.; Kudin, K. N.; Staroverov, V. N.; Kobayashi, R.; Normand, J.; Raghavachari, K.; Rendell, A.; Burant, J. C.; Iyengar, S. S.; Tomasi, J.; Cossi, M.; Rega, N.; Millam, J. M.; Klene, M.; Knox, J. E.; Cross, J. B.; Bakken, V.; Adamo, C.; Jaramillo, J.; Gomperts, R.; Stratmann, R. E.; Yazyev, O.; Austin, A. J.; Cammi, R.; Pomelli, C.; Ochterski, J. W.; Martin, R. L.; Morokuma, K.; Zakrzewski, V. G.; Voth, G. A.; Salvador, P.; Dannenberg, J. J.; Dapprich, S.; Daniels, A. D.; Farkas; Foresman, J. B.; Ortiz, J. V.; Cioslowski, J.; Fox, D. J. Wallingford CT, 2009.
- (7) Becke, A. D. *J. Chem. Phys.* **1993**, 98, 5648.
- (8) Lee, C.; Yang, W.; Parr, R. G. *Phys. Rev. B: Condens. Matter* **1988**, 37, 785.
- (9) Vosko, S. H.; Wilk, L.; Nusair, M. *Can. J. Phys.* **1980**, 58, 1200.
- (10) Stephens, P. J.; Devlin, F. J.; Chabalowski, C. F.; Frisch, M. J. *J. Phys. Chem.* **1994**, 98, 11623.
- (11) Hay, P. J.; Wadt, W. R. *J. Chem. Phys.* **1985**, 82, 270.
- (12) Zhao, Y.; Truhlar, D. G. *Phys. Chem. Chem. Phys.* **2008**, 10, 2813.
- (13) Ribeiro, R. F.; Marenich, A. V.; Cramer, C. J.; Truhlar, D. G. *J. Phys. Chem. B* **2011**, 115, 14556.
- (14) Legault, C. Y.; 1.0b ed. Université de Sherbrooke, 2009.
- (15) Buckley, E.; Herington, E. F. G. *Transactions of the Faraday Society* **1965**, 61, 1618.
- (16) Lacher, J. R.; Walden, C. H.; Lea, K. R.; Park, J. D. *J. Am. Chem. Soc.* **1950**, 72, 331.
- (17) Chao, J.; Rossini, F. D. *Journal of Chemical & Engineering Data* **1965**, 10, 374.
- (18) Legault, C. Y.; 1.0b ed. Université de Sherbrooke, 2009.

Chapter 6

Theoretical Study of Diastereoselective NHC-Catalyzed Cross-Benzoin Reactions between Furfural and N Boc Protected α Amino Aldehydes

Abing Duan^{†,§}, Jason S. Fell^{†,§}, Peiyuan Yu[†], Yu-hong Lam[†], Michel Gravel^{‡,*} and K. N. Houk^{†*}

[†]Department of Chemistry and Biochemistry, University of California, Los Angeles, California
90095-1569, United States

[‡]Department of Chemistry, University of Saskatchewan, 110 Science Place, Saskatoon,
Saskatchewan S7N 5C9, Canada

§ These authors contributed equally.

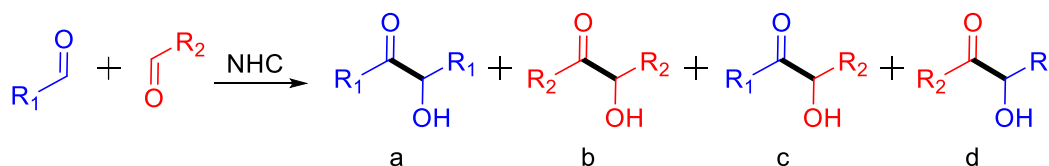
Abstract

The mechanism and origins of *syn*- and *anti*-selectivity of cross-benzoin reactions with furfural and α amino aldehydes were investigated using density functional theory. N-Boc- α -amino aldehydes were found to react with *anti*-selectivity, while N-Bn-N-Boc protected α amino aldehydes react with *syn*-selectivity. The change in selectivity is a result of an intramolecular hydrogen bond with the N-Boc- α amine and aldehyde, which induces a conformation of the α -carbon that places the α alkyl group *anti* to the incoming nucleophile. Switching to N Bn-N-Boc protected α amine removes the hydrogen bond, and induces a new conformation of the α carbon that places the amine *anti*-periplanar to the approaching nucleophile. These steric interactions are rationalized by a Felkin-Anh model.

Introduction

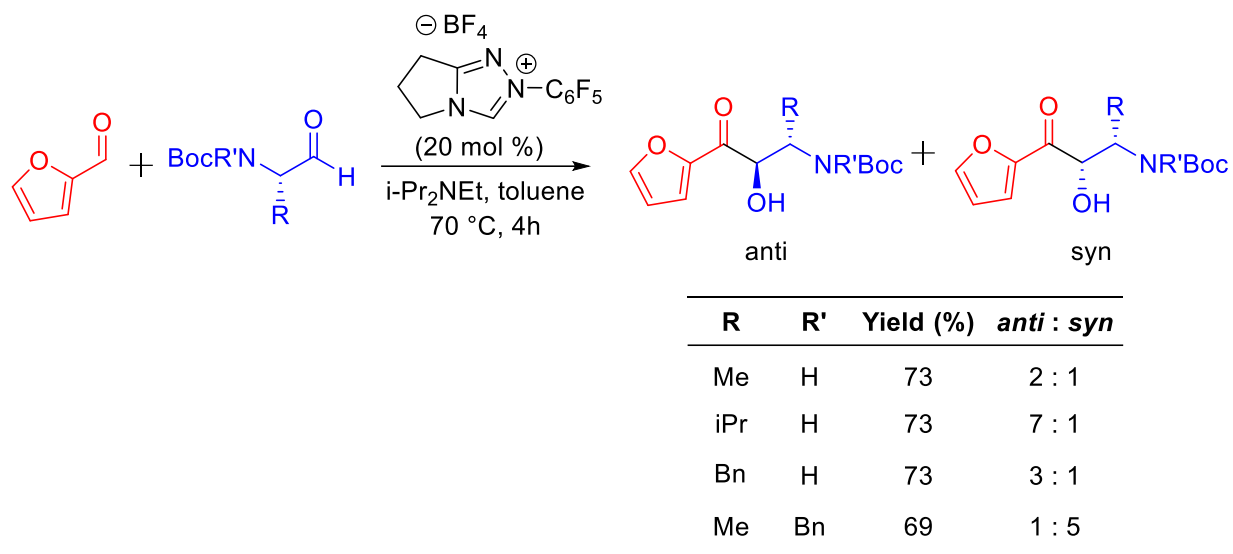
The benzoin reaction, first reported in 1832 by Wöhler and Liebig,¹ produces an acyloin from the coupling of two aldehydes. Ukai² and Breslow³ later reported the use of thiazolium salts in the presence of base as catalysts for the benzoin reaction. The use of *N*-heterocyclic carbenes (NHC) to catalyze benzoin reactions have been widely reported in recent years.⁴ The homocoupling of aldehydes with NHC's have had great success with impressive enantioselectives.⁵ However, heterocoupling between two different aldehydes in cross-benzoin reactions are substantially more challenging due to the lack of regioselectivity.⁶ The product mixture of cross-benzoin reactions will contain four total products: two homobenzoin (Scheme 6.1, a and b) and two cross-benzoin products (Scheme 6.1, c and d).

Scheme 6.1. General cross-benzoin reaction.



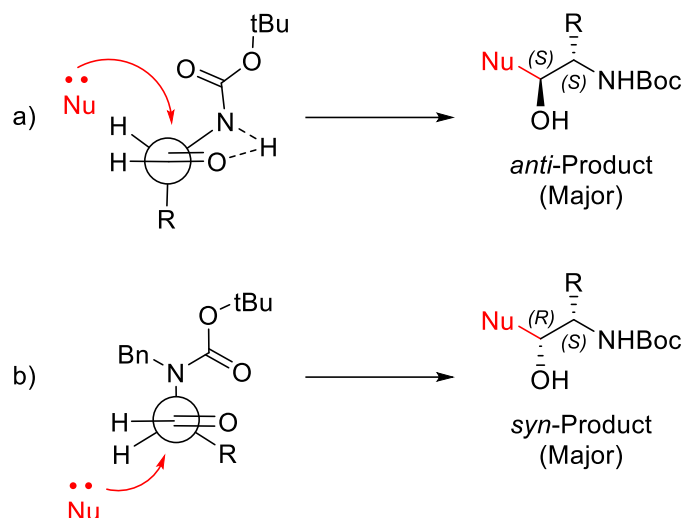
Recently the Gravel group has developed the first chemoselective cross-benzoin reactions between aromatic and aliphatic aldehydes catalyzed by triazolium based NHCs.⁷ Further experimental and computational studies performed by the Gravel group explored the kinetics and chemoselectivity of the preference for the formation of an NHC adduct (Breslow intermediate)³ with alkyl aldehydes.⁸ Previous studies performed by Connon, Zeitler and co-workers have demonstrated that the electron nature and steric bulk of the substrates greatly affects the chemoselectivity in cross acyloin-reactions.⁹ The Gravel group further demonstrated that installing bulky electron-withdrawing groups close to the reaction center can further influence chemoselectivity. *N*-Boc-protected α -amino aldehydes demonstrated to be excellent partners with either aliphatic or heteroaromatic aldehydes and are diastereoselective (Scheme 6.2, entries 1–3).¹⁰ Utilizing *N*-Bn-*N*-Boc- α -amino aldehydes (Scheme 6.2, entry 4) still affords high chemoselectivity, however the diastereoselectivity reverses.¹¹ Specifically, *N*-Boc-protected α -amino aldehydes mainly affords the *anti* product, while *N*-Bn-*N*-Boc-protected α -amino aldehydes lead to *syn* product.

Scheme 6.2. Diastereoselective NHC catalyzed cross-benzoin reactions.



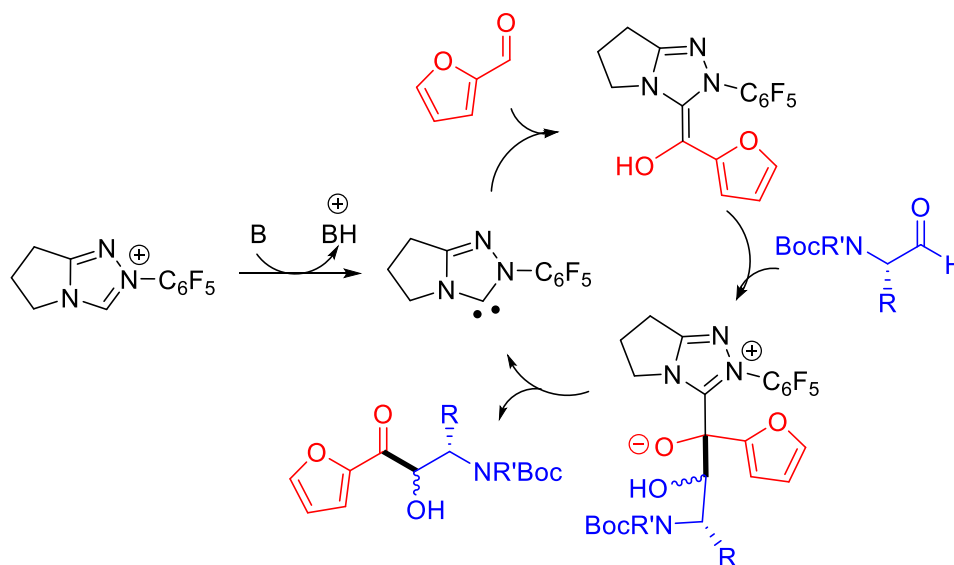
The reversal in diastereoselectivities for these α -amino aldehydes was rationalized by the presence of a hydrogen bond occurring between the *N*-Boc and aldehyde groups (Scheme 6.3a).¹¹ This hydrogen bond induces the groups on the α -carbon to be in a conformation that places the R group *anti* to the approaching nucleophile. When the amine group is replaced with *N*-Bn-*N*-Boc, this hydrogen bond is lost, and the α -carbon will rotate into a different conformation that will place the R group *syn* to the approaching nucleophile (Scheme 6.3b).

Scheme 6.3. The cross-benzoin reaction of *N*-Boc- α -amino aldehydes yields the *anti*-product as the major product due to a hydrogen bond between the amine and aldehyde (a). When the cross-benzoin reaction is performed with *N*-Bn-*N*-Boc- α -amino aldehydes the product selectivity changes to the *syn*-product from the loss of a hydrogen bond (b).



The mechanism for the NHC-catalyzed cross-benzoin reaction of 2-furaldehyde and protected α -amino aldehyde is shown in Scheme 6.4.^{3,12} Deprotonation of the triazolium precatalyst (**I**) generates the active NHC catalyst (**II**). This nucleophilic species attacks 2-furaldehyde to form the Breslow intermediate (**III**). The Breslow intermediate then attacks the α -amino aldehyde and undergoes a proton transfer (**IV**). Collapse of this intermediate (**IV**) releases the benzoin product (**V**) and regenerates the catalyst to repeat the cycle.⁷⁻⁸

Scheme 6.4. Proposed mechanism of NHC-catalyzed cross-benzoin reaction



Previous density functional theory (DFT) investigations into the benzoin reaction have focused primarily on non-NHC catalysts.¹³ Computational studies that have included NHC catalysts have primarily focused on the Stetter reaction.¹⁴ In 2004 Houk *et al.* published the first major study of benzoin reactions, focusing exclusively on the carbon–carbon bond formation step between the Breslow intermediate and second aldehyde.¹⁵ In order to firmly establish the origins of diastereoselectivity, there needs to be more thorough mechanistic studies. We have performed a DFT study to generate a detailed mechanism and to elucidate the diastereoselectivity of this reaction.

Computational Methods

All DFT calculations were performed using Gaussian 09 software package.¹⁶ Gas-phase ground state and transition state geometries were optimized with the B3LYP functional¹⁷ and the 6-31G(d) basis set. Geometry optimizations were followed by single-point calculations using the B3LYP function with Grimme's dispersion correction¹⁸ (B3LYP-D3(BJ)) and the def2-TZVPP¹⁹ basis set with toluene implicit solvent using the SMD²⁰ solvent model. These methods have been

shown to give good results in related stereoselectivity studies.²¹ Vibrational frequencies were computed to determine if the optimized structures are minima or saddle points on the potential energy surface corresponding to ground state and transition state geometries, respectively. Free energies were calculated for 1 atm at 298.15 K. Conformational searches were performed using the MMFF force field in Maestro 11.0.²² We utilized the Monte Carlo multiple minimum method with Oren-Spedicato variable metric minimization for optimized conformational sampling.²³ Molecular structures are displayed with CYLview.²⁴

Results and Discussion

Gravel *et al.* had previously reported the DFT computed mechanism of the homo- and cross-benzoin reactions of alkyl and aryl aldehydes.⁸ They had reported that the generation of the active carbene catalyst (**II**) is barrierless and the free energy of the carbene species is 1.4 kcal mol⁻¹ higher. Species **II** attacks furfural to generate the Breslow intermediate (**III**). Ensuing steps are reported using the lowest energy configuration of the Breslow intermediate, named (*E*)-*s-trans*. See the supporting information for full analysis of the major Breslow intermediate configurations.

We first investigated the mechanism of the cross-benzoin reaction between (*E*)-*s-trans* with *N*-**Boc-alaninal**, which is illustrated in Figure 6.1 with free energies relative to the separated reactants. Throughout this reaction there are four possible diastereomers for the carbon–carbon bond forming step (**TS1-a**), the succeeding intermediate (**Int-a**) and the release of the catalyst and cross-benzoin product (**TS2-a**). Each of these diastereomers is identified by the absolute stereochemistry of the carbons of the newly generated alcohol of the α -amino aldehyde and the alcohol/alkoxide of the Breslow intermediate. The removal of the catalyst results in the loss of a

stereocenter due to the formation of a ketone, which leaves two enantiomeric products that have the hydroxyl and methyl groups either *syn* or *anti* (***syn*-Prod-a** and ***anti*-Prod-a**, respectively).

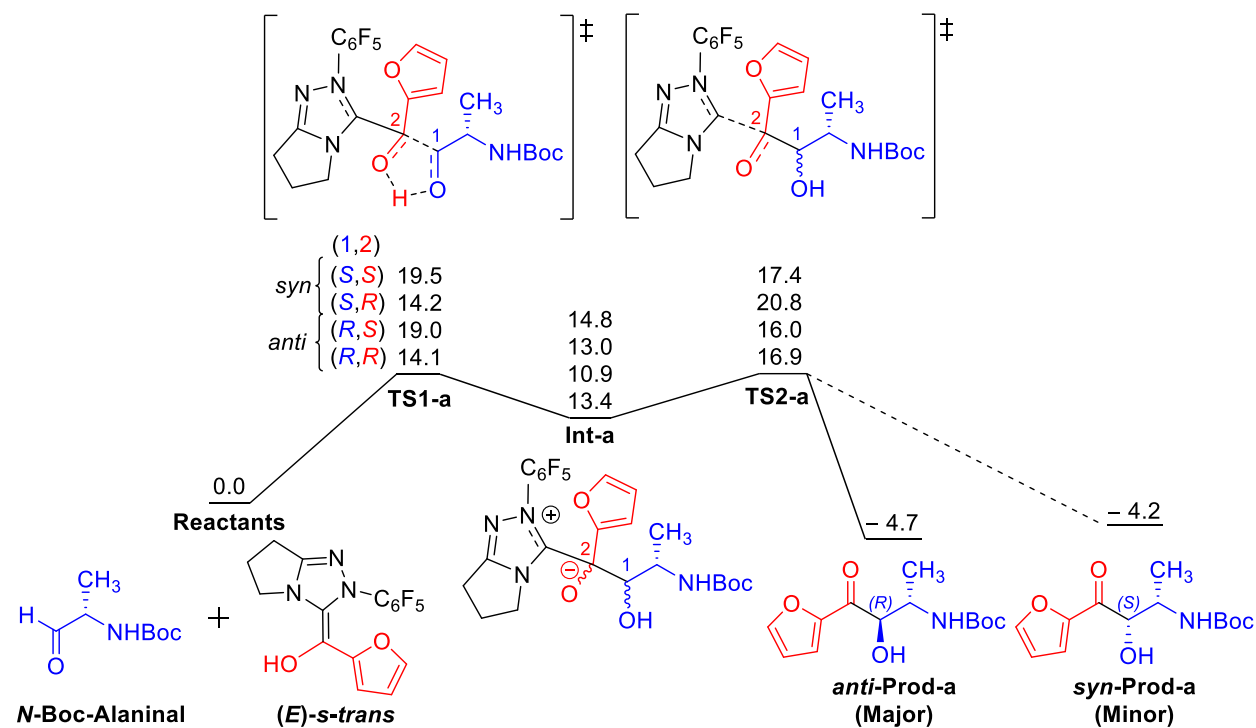


Figure 6.1. Free energy profile of the cross-benzoin reaction of (*E*)-*s-trans* with *N*-Boc-alaninal. The energies for each diastereomer is listed in order from top to bottom as (*S,S*), (*S,R*), (*R,S*) and (*R,R*). Energies are in units of kcal mol⁻¹.

The (*R,S*) and (*R,R*) diastereomers lead to the *anti* product (***anti*-Prod-a**), and the (*S,S*) and (*S,R*) diastereomers lead to the *syn* product (***syn*-Prod-a**). The formation of the cross-benzoin products are exergonic, with a preference for the *anti* product by 0.5 kcal mol⁻¹ which would give a 2:1 product ratio of *anti*:*syn*. The rate determining steps for forming the *anti* and *syn* products are **TS2-a**(*R,R*) and **TS1-a**(*S,S*) with free energies of 16.9 and 19.5 kcal mol⁻¹, respectively. The differences in our calculated free energies for the products and rate determining steps reveals both a kinetic and thermodynamic preference for the *anti* product (***anti*-Prod-a**), which is consistent with the experimental results shown in Scheme 6.1.

The nucleophilic attack of (*E*)-*s-trans* to *N*-Boc-alaninal during the first step in the mechanism is the rate determining step for producing the minor (*syn*) product. There is a 5.4 kcal mol⁻¹ energy difference between the transition structures that lead to the *anti* (TS1-a-(*R,R*)) and *syn* (TS1-a-(*S,S*)) products. These transition structures are shown as Newman projections along the α -carbon-aldehyde carbon bond of *N*-Boc-alaninal in Figure 6.2. The presence of a hydrogen bond (2.12 Å) in TS1-a-(*R,R*) induces a conformation of *N*-Boc-alaninal that places the methyl group *anti* to (*E*)-*s-trans*, with a measure dihedral angle of 153.7° (highlighted in green). In TS1-a-(*S,S*) there is a weak hydrogen bond (2.97 Å) which places the methyl group gauche to the approaching (*E*)-*s-trans*, with a calculated dihedral angle is 85.8°. The hydrogen bond induces a conformation that will place the methyl group *anti* in the transition state.

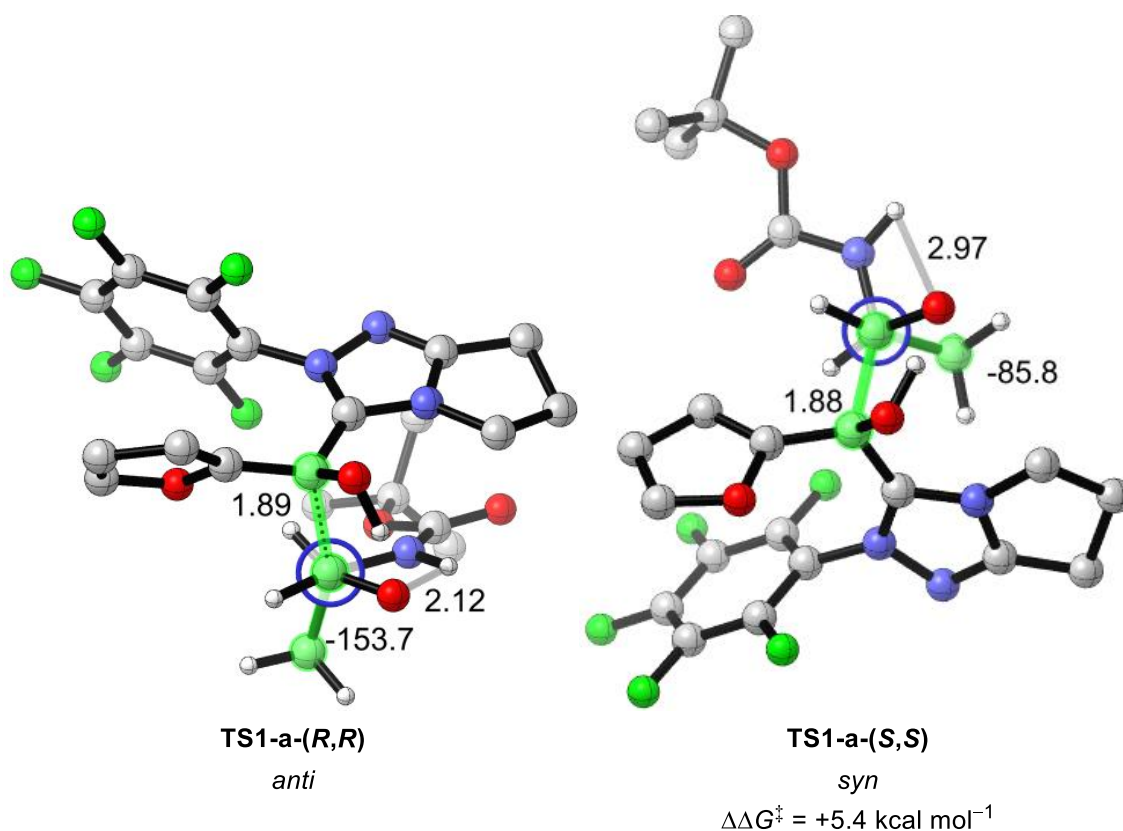


Figure 6.2. Newman projections of TS1-a-(*S,S*) and TS1-a-(*R,R*) for the cross-benzoin reaction of (*E*)-*s-trans* and *N*-Boc-alaninal are shown with free energies. Distances for the carbon-carbon formation and hydrogen bond are in units of Å. Atoms included in the calculated dihedral

angle are highlight in green. Hydrogen atoms on the Boc group and Breslow intermediate are hidden for clarity.

We then investigated the cross-benzoin reaction between *(E)*-*s-trans* with *N*-**Boc-valinal** and *N*-**Boc-phenylalaninal**. The relative energy differences between for the free energies of reaction and activation are listed in Table 1. The formation of the *anti* product is favored in the reaction of *(E)*-*s-trans* with both *N*-**Boc-valinal** and *N*-**Boc-phenylalaninal** by 2.3 and 0.7 kcal mol⁻¹, respectively. The predicted ratio of *anti:syn* for *N*-**Boc-alaninal** and *N*-**Boc-phenylalaninal** precisely match the experimental ratios. The rate determining step for the *syn* product is 0.3 kcal mol⁻¹ lower than the *anti* for the reaction involving *N*-**Boc-valinal**, however we predict that the thermodynamics control this specific reaction due to the large energy difference favoring the *anti* product (2.3 kcal mol⁻¹).

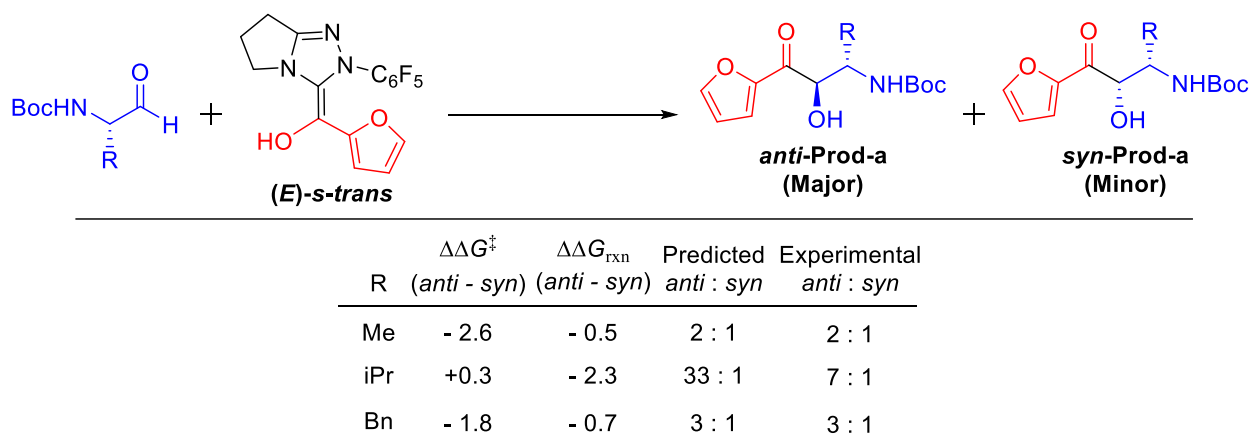


Table 6.1. Free energy profile of the cross-benzoin reaction of *(E)*-*s-trans* with *N*-**Boc-valinal** and *N*-**Boc-phneylalaninal**. Energies are in units of kcal mol⁻¹.

The *syn* and *anti* product preference for the cross-benzoin reaction of *N*-**Bn-N-Boc-alaninal** deviates from the previous aldehydes. The free energy profile for this reaction is illustrated in Figure 6.3. The major product in the cross-benzoin reaction of *N*-**Bn-N-Boc-alaninal** is the *syn* product, as opposed to the preference for the formation of the *syn* product for *N*-Boc-protected α -amino aldehydes. The mechanism is stepwise with the first step being the formation of a carbon-

carbon bond (**TS1-d**) between (*E*)-*s-trans* and *N*-Bn-*N*-Boc-alaninal to form the succeeding intermediate (**Int-d**). The NHC catalyst breaks from the intermediate (**TS2-d**) which leaves the products (*syn*-**Prod-d** and *anti*-**Prod-d**).

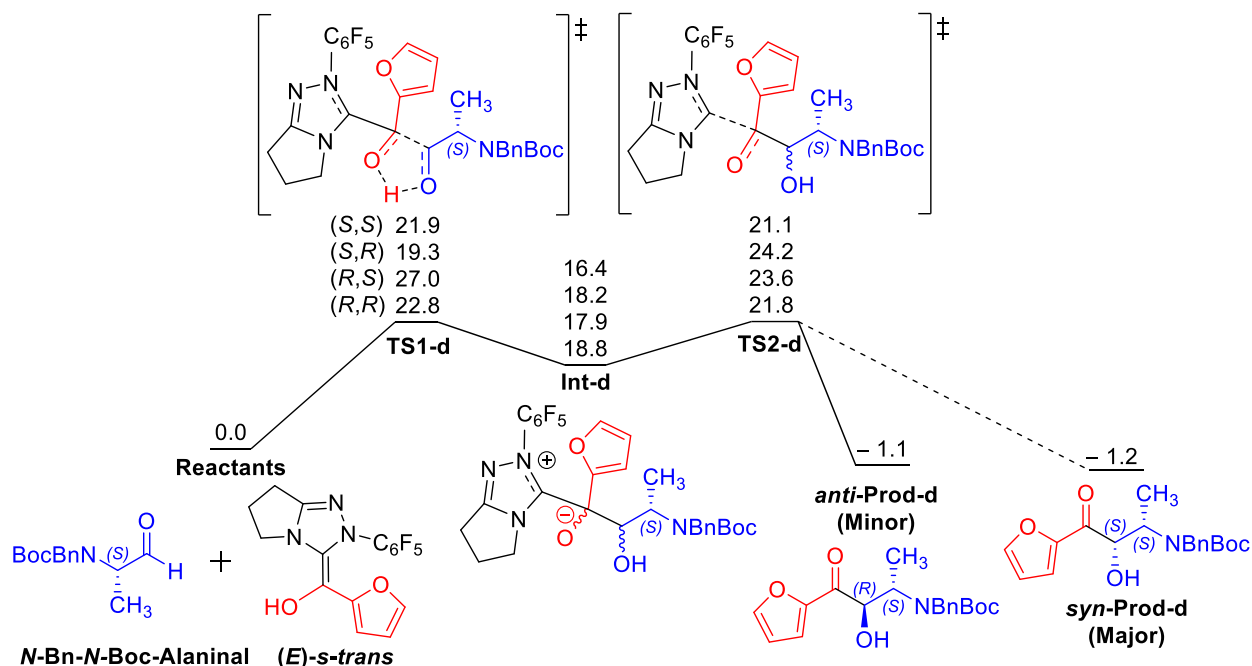


Figure 6.3. Free energy profile of the cross-benzoin reaction of (*E*)-*s-trans* with of *N*-Bn-*N*-Boc-alaninal. The energies for each diastereomer is listed in order from top to bottom as (*S,S*), (*S,R*), (*R,S*) and (*R,R*). Energies are in units of kcal mol⁻¹.

The free energies of formation for the *syn* and *anti* products are exergonic and are nearly isoenergetic ($\Delta\Delta G_{\text{rxn}} = 0.1$ kcal mol⁻¹). The rate determining step for the formation of the *anti* and *syn* products are **TS1-d**-(*R,R*) and **TS1-d**-(*S,S*) with free energies of 22.8 and 21.9 kcal mol⁻¹, respectively. Based upon the calculated free energy barriers the predicted ratio of observed *syn:anti* products is 4:1, which is in excellent agreement with experimental observations. These transition structures are shown as Newman projections along the α -carbon-aldehyde carbon bond of *N*-Bn-*N*-Boc-alaninal in Figure 6.4.

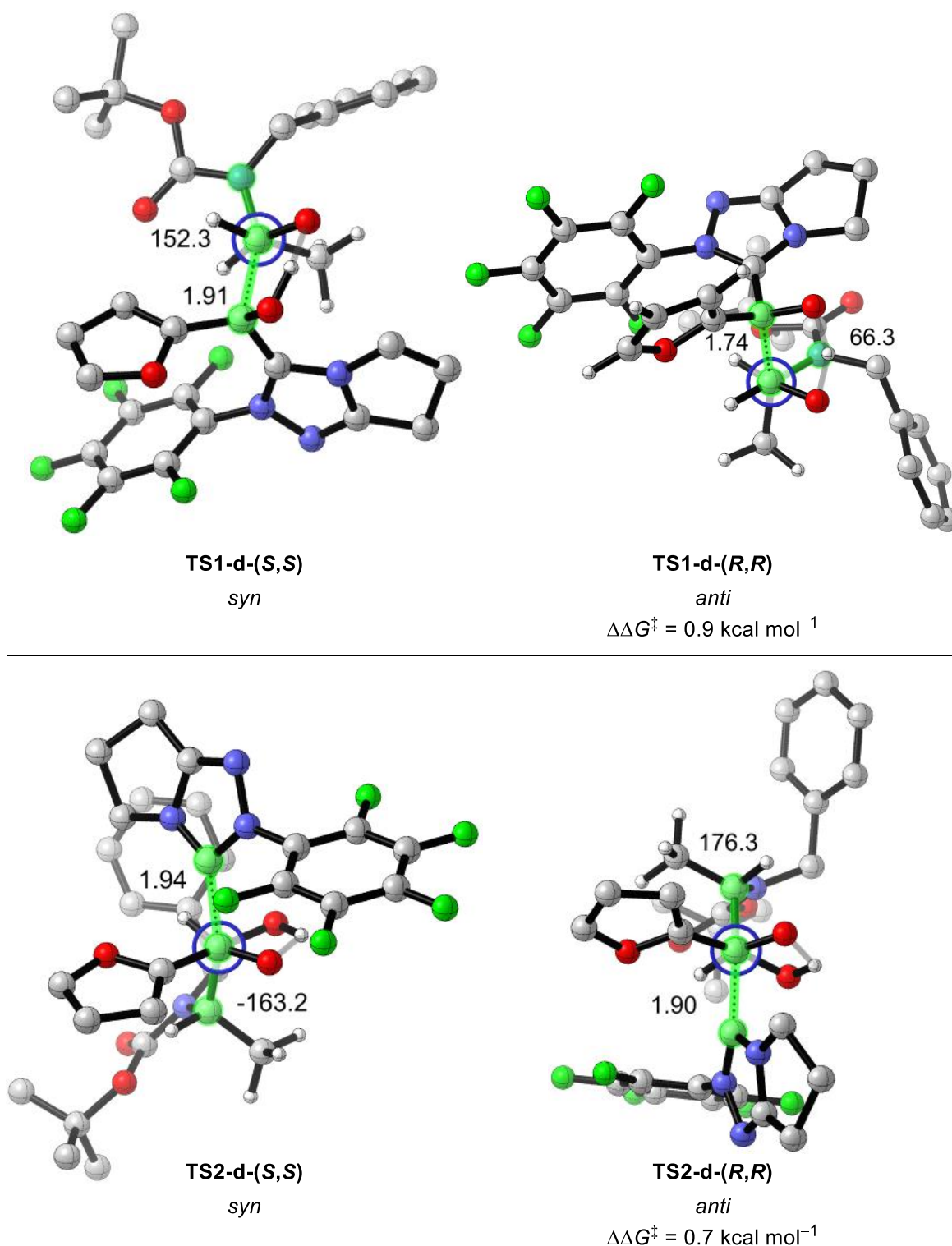


Figure 6.4. (top) Relative free energies (kcal mol^{-1}) and Newman projections of **TS1-d-(R,R)** and **TS1-d-(S,S)** along the C(aldehyde)-C(α) bond. (bottom) Relative free energies (kcal mol^{-1}) and Newman projections of **TS2-d-(R,R)** and **TS2-d-(S,S)** along the C(ketone)-C(α) bond. Distances are in units of Å. Dihedral angle is highlight in green. Hydrogens on the Boc, Bn and NHC moieties are omitted for clarity.

In the previous *N*-Boc-protected systems the alkyl substituent α to the aldehyde are placed *anti* to the nucleophile due to steric interactions and a stabilizing hydrogen bond. Without the stabilizing hydrogen bond the sterically largest group, the *N*-Boc-*N*-Bn amine, is *anti* to the nucleophile. For **TS1-d-(S,S)** the amine group on the α -carbon is nearly anti-periplanar to the approaching (*E*)-*s-trans*, with a calculated dihedral angle is 152.3° (highlighted in green). This conformation is maintained in **TS2-d-(S,S)** with the furfural moiety *anti* to the *N*-Boc-*N*-Bn amine. In **TS1-d-(R,R)**, the amine group is gauche to the approaching (*E*)-*s-trans*, with a calculated dihedral angle of 66.3°. This steric clash between (*E*)-*s-trans* and the *N*-Bn-*N*-Boc protected amine destabilizes the *anti* transition state, which impedes the formation of the *anti* product. In **TS2-d-(R,R)** the back carbon rotates the furfural moiety anti to the *N*-Boc-*N*-Bn amine, however this rotation results in a loss of enhanced gauche interactions. The switch in preference due to the lack of a hydrogen bond in the *N*-Boc-*N*-Bn protected amines.

Conclusion

We have explored the mechanism and diastereoselectivities of the cross-benzoin reactions of α -amino aldehydes and furfural catalyzed by NHC. The cross-benzoin reaction proceeds through a stepwise mechanism. Firstly, furfural reacts with the NHC catalyst to form a Breslow intermediate. The intermediate forms a new carbon-carbon bond with an α -amino aldehyde, which is then followed by the regeneration of the NHC. An intramolecular hydrogen bond influences the conformation of the groups on the α -carbon of the α -amino aldehyde, which places the alkyl group *anti* to the nucleophile. When the amine is replaced with an *N*-Bn-*N*-Boc protected amine there is a loss of the hydrogen bond, which induces a new conformation on the α -carbon based on the steric priorities of each group. The α -amine group becomes the sterically

larger than the α -alkyl substituent, which places the amine *anti* to the nucleophile. This reversal in steric priorities places the α -alkyl substituent *syn* to the newly formed hydroxyl group.

Acknowledgements

We are grateful to the National Science Foundation (CHE-1361104 and CHE-1464690) and China Scholarship Council (CSC) for financial support of this research. Calculations were performed on the Hoffman2 cluster at UCLA and the Extreme Science and Engineering Discovery Environment (XSEDE), which is supported by the NSF (OCI-1053575), and the cluster at HNU, which is supported by the Fundamental Research Funds for the Central Universities. We also want to thank Dr. Wanxiang Zhao (HNU) for helpful comments.

References

- (1) Wöhler, F.; Liebig, J. *Ann. Pharm.* **1832**, 3, 249.
- (2) Ukai, T.; Tanaka, R.; Dokawa, T. *J. Pharm. Soc. Jpn.* **1943**, 63, 296.
- (3) Breslow, R. *J. Am. Chem. Soc.* **1958**, 80, 3719.
- (4) (a) Bugaut, X.; Glorius, F. *Chem. Soc. Rev.* **2012**, 41, 3511; (b) Grossmann, A.; Enders, D. *Angew. Chem., Int. Ed.* **2012**, 51, 314; (c) Flanigan, D. M.; Romanov-Michailidis, F.; White, N. A.; Rovis, T. *Chem. Rev. (Washington, DC, U. S.)* **2015**, 115, 9307; (d) Izquierdo, J.; Hutson, G. E.; Cohen, D. T.; Scheidt, K. A. *Angew. Chem., Int. Ed.* **2012**, 51, 11686; (e) Vora, H. U.; Wheeler, P.; Rovis, T. *Adv. Synth. Catal.* **2012**, 354, 1617; (f) Bode, J. W. *Nature Chemistry* **2013**, 5, 813; (g) Ryan, S. J.; Candish, L.; Lupton, D. W. *Chem. Soc. Rev.* **2013**, 42, 4906; (h) Chen, X.-Y.; Ye, S. *Synlett* **2013**, 24, 1614; (i) Hopkinson, M. N.; Richter, C.; Schedler, M.; Glorius, F. *Nature* **2014**, 510, 485; (j) Menon, R. S.; Biju, A. T.; Nair, V. *Chem. Soc. Rev.* **2015**, 44, 5040.
- (5) (a) Moore, J. L.; Rovis, T. *Top. Curr. Chem.* **2010**, 291, 77; (b) Enders, D.; Kallfass, U. *Angew. Chem., Int. Ed.* **2002**, 41, 1743; (c) Ma, Y.; Wei, S.; Wu, J.; Yang, F.; Liu, B.; Lan, J.; Yang, S.; You, J. *Adv. Synth. Catal.* **2008**, 350, 2645; (d) Enders, D.; Han, J. *Tetrahedron: Asymmetry* **2008**, 19, 1367; (e) Baragwanath, L.; Rose, C. A.; Zeitler, K.; Connon, S. J. *J. Org. Chem.* **2009**, 74, 9214; (f) Soeta, T.; Tabatake, Y.; Inomata, K.; Ukaji, Y. *Tetrahedron* **2012**, 68, 894.
- (6) Bugaut, X.; Marek, I.; Knochel, P. *Comprehensive Organic Synthesis II*, 2014; Vol. 1.
- (7) Langdon, S. M.; Wilde, M. M. D.; Thai, K.; Gravel, M. J. *J. Am. Chem. Soc.* **2014**, 136, 7539.
- (8) Langdon, S. M.; Legault, C. Y.; Gravel, M. J. *J. Org. Chem.* **2015**, 80, 3597.
- (9) (a) Rose, C.; Gundala, S.; Connon, S.; Zeitler, K. *Synthesis* **2011**, 2011, 190; (b) O'Toole, S. E.; Rose, C. A.; Gundala, S.; Zeitler, K.; Connon, S. J. *J. Org. Chem.* **2011**, 76, 347.
- (10) Haghshenas, P.; Gravel, M. *Org. Lett.* **2016**, 18, 4518.
- (11) Haghshenas, P.; Quail, J. W.; Gravel, M. *J. Org. Chem.* **2016**, 81, 12075.

- (12) Lapworth, A. *J. Chem. Soc., Trans.* **1903**, 83, 995.
- (13) (a) Yamabe, S.; Yamazaki, S. *Org. Biomol. Chem.* **2009**, 7, 951; (b) He, Y.; Xue, Y. *J. Phys. Chem. A* **2010**, 114, 9222.
- (14) (a) Kuniyil, R.; Sunoj, R. B. *Org. Lett.* **2013**, 15, 5040; (b) Hawkes, K. J.; Yates, B. F. *European Journal of Organic Chemistry* **2008**, 2008, 5563; (c) Domingo, L. R.; Zaragoza, R. J.; Saéz, J. A.; Arnó, M. *Molecules* **2012**, 17, 1335; (d) Ajitha, M. J.; Suresh, C. H. *Tetrahedron Letters* **2013**, 54, 7144.
- (15) Dudding, T.; Houk, K. N. *Proc. Natl. Acad. Sci. U. S. A.* **2004**, 101, 5770.
- (16) Frisch, M. J.; Trucks, G. W.; Schlegel, H. B.; Scuseria, G. E.; Robb, M. A.; Cheeseman, J. R.; Scalmani, G.; Barone, V.; Mennucci, B.; Petersson, G. A.; Nakatsuji, H.; Caricato, M.; Li, X.; Hratchian, H. P.; Izmaylov, A. F.; Bloino, J.; Zheng, G.; Sonnenberg, J. L.; Hada, M.; Ehara, M.; Toyota, K.; Fukuda, R.; Hasegawa, J.; Ishida, M.; Nakajima, T.; Honda, Y.; Kitao, O.; Nakai, H.; Vreven, T.; Montgomery, J. A.; Peralta, J. E.; Ogliaro, F.; Bearpark, M.; Heyd, J. J.; Brothers, E.; Kudin, K. N.; Staroverov, V. N.; Kobayashi, R.; Normand, J.; Raghavachari, K.; Rendell, A.; Burant, J. C.; Iyengar, S. S.; Tomasi, J.; Cossi, M.; Rega, N.; Millam, J. M.; Klene, M.; Knox, J. E.; Cross, J. B.; Bakken, V.; Adamo, C.; Jaramillo, J.; Gomperts, R.; Stratmann, R. E.; Yazyev, O.; Austin, A. J.; Cammi, R.; Pomelli, C.; Ochterski, J. W.; Martin, R. L.; Morokuma, K.; Zakrzewski, V. G.; Voth, G. A.; Salvador, P.; Dannenberg, J. J.; Dapprich, S.; Daniels, A. D.; Farkas, Foresman, J. B.; Ortiz, J. V.; Cioslowski, J.; Fox, D. J. Wallingford CT, 2009.
- (17) (a) Becke, A. D. *J. Chem. Phys.* **1993**, 98, 5648; (b) Lee, C.; Yang, W.; Parr, R. G. *Phys. Rev. B: Condens. Matter* **1988**, 37, 785.
- (18) Grimme, S.; Ehrlich, S.; Goerigk, L. *J. Comput. Chem.* **2011**, 32, 1456.
- (19) (a) Weigend, F.; Ahlrichs, R. *Phys. Chem. Chem. Phys.* **2005**, 7, 3297; (b) Weigend, F. *Phys. Chem. Chem. Phys.* **2006**, 8, 1057.
- (20) (a) Marenich, A. V.; Cramer, C. J.; Truhlar, D. G. *J. Phys. Chem. B* **2009**, 113, 6378; (b) Ribeiro, R. F.; Marenich, A. V.; Cramer, C. J.; Truhlar, D. G. *J. Phys. Chem. B* **2011**, 115, 14556.
- (21) (a) Lam, Y.-h.; Grayson, M. N.; Holland, M. C.; Simon, A.; Houk, K. N. *Acc. Chem. Res.* **2016**, 49, 750; (b) Grayson, M. N.; Goodman, J. M. *J. Org. Chem.* **2013**, 78, 8796; (c) Grayson, M. N.; Goodman, J. M. *J. Org. Chem.* **2015**, 80, 2056; (d) Krenske, E. H.; Houk, K. N.; Harmata, M. *J. Org. Chem.* **2015**, 80, 744; (e) Lam, Y.-h.; Houk, K. N. *J. Am. Chem. Soc.* **2014**, 136, 9556; (f) Lam, Y.-h.; Houk, K. N. *J. Am. Chem. Soc.* **2015**, 137, 2116; (g) Simon, A.; Lam, Y.-h.; Houk, K. N. *J. Am. Chem. Soc.* **2016**, 138, 503; (h) Rodriguez, E.; Grayson, M. N.; Asensio, A.; Barrio, P.; Houk, K. N.; Fustero, S. *ACS Catal.* **2016**, 6, 2506; (i) Simon, L.; Goodman, J. M. *Org. Biomol. Chem.* **2011**, 9, 689.
- (22) In *Maestro*; 11.0 ed.; Schrödinger, LLC: New York, NY, 2017.
- (23) Banks, J. L.; Beard, H. S.; Cao, Y.; Cho, A. E.; Damm, W.; Farid, R.; Felts, A. K.; Halgren, T. A.; Mainz, D. T.; Maple, J. R.; Murphy, R.; Philipp, D. M.; Repasky, M. P.; Zhang, L. Y.; Berne, B. J.; Friesner, R. A.; Gallicchio, E.; Levy, R. M. *J. Comput. Chem.* **2005**, 26, 1752.
- (24) Legault, C. Y.; 1.0b ed. Université de Sherbrooke, 2009.